

# **Tsunami Vulnerability Assessment of the Canadian Pacific Coast**

**Isabelle Cheff**

Thesis submitted to the  
Faculty of Graduate and Postdoctoral Studies  
in partial fulfillment of the requirements for the degree of

**Master of Applied Science in Civil Engineering**

Under the auspices of the Ottawa-Carleton Institute for Civil Engineering

Academic advisor: Dr. Ioan Nistor and Dr. Dan Palermo



University of Ottawa  
Ottawa, Ontario, Canada  
September 2016

© Isabelle Cheff, Ottawa, Canada 2016

# Abstract

---

The North American Pacific coast, located within the Ring of Fire, is at risk of severe subduction tsunamis. This danger has pushed the United States to make a strong push in tsunami research. Recent advancement has resulted in the implementation of a new chapter in the ASCE 7-16 standards focusing on tsunami structural loads and effects. Within the scope of this new standard, the tsunami inundation hazard of the US West coast has been mapped. However, no such work has been completed in Canada, leaving the tsunami hazard and vulnerability for most of the Canadian West coast uncertain.

The life safety vulnerability from the most hazardous source, the Cascadia Subduction Zone, is evaluated in terms of pedestrian evacuation capabilities. Using a static distance-only model, the ability of individuals to evacuate to safety in natural high grounds is computed for all communities in British Columbia and compared by Tsunami Notification Zone. A new variable – the available time – for tsunamis life safety vulnerability assessment is proposed. This variable considers both tsunami arrival time and time to safety, resulting in a life safety threshold value of 0. Zone E has the largest surface area and population within the hazard zone, even though it has the smallest probable run-up range because of the large number of communities in this zone and the low-lying areas of the Lower Mainland. All communities within Zones A, B, D, and E have low life safety vulnerability at the maximum probable run-up of their respective zone, suggesting that pedestrian evacuation should be possible. Zone C has the highest vulnerability of all zones, as it has the lowest available times. With a 9 m run-up and over 25% of its communities lying within the moderate- or high-vulnerability categories, it has an available time of below 30 min and 15 min, respectively. Zone C also has the highest percentage of its surface area inundated at its maximum probable run-up (39.7%). The most vulnerable communities are identified, including 45 First Nation and 5 non-indigenous communities: Tofino, Winter Harbour, Ucluelet, Port Renfrew, and Bamfield. The life-safety threshold is surpassed in Barlett Island 32, Grassy Island 17, Hesquiat 1, and Tofino. Delta and Richmond, in Zone E, also have a minimum available time below the life safety threshold at run-ups between 5 and 7 m, at or above the probable run-up of their zone, as they have large low-lying areas. As the tsunami arrival time is very large here, the merits of vehicle evacuation should be evaluated. Additionally, they are likely to be more vulnerable to landslide tsunamis, as the tsunami arrival time would be much shorter than one from a Cascadia tsunami.

A more detailed vulnerability study using anisotropic path-distance modeling was performed in Tofino. This more complex model found lower available times than the distance-only model. Maximum differences ranging between 14.4 to 29.9 minutes were found for three pedestrian velocities. The minimum available time was found to be -29.0 minutes within the official

municipality boundary and -40.1 minutes within one of the beaches. Two vertical evacuation structures are required to reduce the time to safety below the tsunami arrival time of 28.1 minutes for run-ups between 13 and 19 m. Run-ups above 19 m required three vertical evacuation structures. No configuration could be found to sufficiently reduce the time to safety on Frank Island.

# Acknowledgements

---

First and foremost, I would like to express my deepest gratitude to my two academic advisors, Drs. Nistor and Palermo, for their mentorship and encouragement throughout this academic venture. I am grateful for the many opportunities they have provided me and for always being available for questions and discussions, no matter where they were around the globe.

I would also like to thank my colleagues at the University of Ottawa for their continuous support and friendship. I would like to specifically mention Steffanie Piché and Jacob Stolle for their guidance and motivation and for never hesitating to answer my sometimes-tireless questions.

I would like to thank my family and friends for their unfailing love and support throughout this journey, especially my parents for their continuous encouragement throughout all aspect of my life. A special thank you goes out to Aislynn, who never hesitated to provide me with her opposing skillset and help with this manuscript. Last but not least, the warmest of thanks goes to Phil, whose work ethic I strive for everyday and for his love and sacrifices and for continuously pushing me forward during this endeavor.

# Table of Contents

---

Abstract.....	ii
Acknowledgements .....	iv
Table of Contents .....	v
List of Figures.....	vii
List of Tables.....	xiii
List of Symbols and Acronyms .....	xiv
Chapter 1 . Introduction.....	1
1.1 Background and Motivation .....	1
1.2 Study Objectives and Scope .....	3
1.3 Contributions and Novelty of the Study .....	4
1.4 Publications .....	4
1.5 Outline of the Thesis .....	5
Chapter 2 . Literature Review .....	6
2.1 Tsunami Characteristics and Magnitude Determination .....	6
2.1.1 Run-Up .....	8
2.1.2 Tsunami Modeling.....	9
2.2 Canadian Tsunami Hazard .....	10
2.2.1 Historical Tsunamis from Local Sources .....	12
2.2.2 Historical Tsunamis from Distant Sources.....	15
2.2.3 Tsunami Modeling of Canadian Shores .....	17
2.3 Community Vulnerability Assessment.....	19
2.2.4 Static Evacuation Modeling .....	19
2.2.5 Dynamic Evacuation Modeling.....	21
2.3 Mitigation Techniques.....	22
2.4 Discussion.....	22
Chapter 3 . Study Area: Canadian West Coast.....	25
3.1 Tsunami Warnings Capabilities and Emergency Preparedness .....	25
3.1.1 Tsunami Detection.....	26
3.1.2 Tsunami Warning Communication .....	28
3.1.3 Tsunami Emergency Preparedness.....	29
3.2 Tsunami Warning Zones Overview.....	30
3.2.1 Planning Run-Up Level and Arrival Time .....	31
3.2.2 Population At-Risk .....	33
Chapter 4 . Methodology.....	37
4.1 Data Collection.....	37
4.1.1 Population Data .....	37
4.1.2 Geographical Data .....	38
4.2 Vulnerability Assessment Processes .....	40
4.2.1 Arrival Time .....	41
4.2.2 Time to Safety .....	46
4.2.3 Available Time .....	49
4.2.4 Run-Up Generalization Sensitivity Study .....	49
Chapter 5 . Tsunami Vulnerability of the West Coast.....	56

5.1	Run-Up Range .....	56
5.2	Arrival Time .....	58
5.3	Hazard Zone .....	61
5.4	Available Time .....	65
5.4.1	Available Time by Zone .....	65
5.4.2	Moderate and High Vulnerability Communities .....	70
5.4.3	Conclusion .....	88
Chapter 6	. Case Study: Tofino .....	90
6.1	Population .....	90
6.1.1	Population Estimation Methodology .....	90
6.1.1	Population Distribution .....	92
6.2	Pedestrian Evacuation Tool .....	93
6.3	Evacuation Capabilities .....	95
6.3.1	Available Time .....	96
6.3.2	Population At-Risk .....	98
6.4	Life Safety Mitigation Measures .....	100
6.4.1	Vertical Evacuation Structures .....	101
6.2	Conclusions .....	105
Chapter 7	. Conclusions and Recommendations for Future Work .....	107
7.1	Conclusions .....	107
7.2	Recommendations for Future Work .....	108
References	.....	109
Appendix A:	List of Suppressed Communities .....	120
A.1	Tsunami Notification Zones .....	121
A.2	Census Suppressed Communities .....	128
Appendix B:	Arrival Time Validation Data .....	130
Appendix C:	Example of Evacuation Maps .....	132

# List of Figures

---

Figure 1.1 Photograph of the damaged endured in Rikuzentakata, Japan following the 2011 Tohoku earthquake and tsunami (Hagen 2014).....	1
Figure 1.2 Tsunami sources from earthquake, volcanoes, landslides and other causes from 1410 B.C. to A.D. 2011, adapted from NOAA (2011).....	2
Figure 2.1 Tsunami wave characteristics at different water depth, adapted from Bryant (2014) ...	6
Figure 2.2 Idealized tsunami wave form with an exaggerated vertical dimension, adapted from Bryant (2014).....	7
Figure 2.3 Subduction faults in the Pacific Ocean creating the Ring of Fire or circum-Pacific belt (Clague, et al. 2003).....	11
Figure 2.4 Cascadia Subduction Zone (CSZ; Geological Survey of Canada 2011) .....	13
Figure 2.5 Location of geological evidence of past earthquake and tsunamis from the Cascadia Subduction Zone (Clague, et al. 2000) .....	14
Figure 2.6 Inundated area in Port Alberni from the 1700 Cascadia Subduction Zone tsunami (yellow and red) with a run-up of 16 m, and 1964 Great Alaska Earthquake and Tsunami (red) with a run-up of 10.3 m (Clague and Bobrosky 1999) .....	16
Figure 2.7 Modeled maximum tsunami wave height (m) along the outer coast of Vancouver Island from a North Cascadia Subduction Zone rupture adapted from (Hebenstreit and Murty 1989).....	17
Figure 2.8 Evacuation modeling approaches comparison as a function of cumulative percentage of grid cells to travel time to safety (Wood and Schmidlein 2012).....	20
Figure 3.1 Components of the tsunami warning system of British Columbia, adapted from Anderson (2016). .....	25
Figure 3.2 Locations of DART buoy stations across the Pacific and Indian Oceans (NOAA 2016c). .....	26
Figure 3.3 Tsunami Notification Zones of British Columbia (PreparedBC 2016). .....	27
Figure 3.4 BC tsunami alert level (PreparedBC 2016).....	28
Figure 3.5 First tsunami wave arrival time – values based on tsunami safety guidelines provided by the Province of British Columbia, adapted from BC Earthquake Alliance Society (2016) .....	32
Figure 3.6 Population distribution of non-indigenous communities considered in this study .....	34
Figure 3.7 Population distribution of First Nation communities considered in this study .....	35
Figure 4.1 Vulnerability Risk Assessment Workflow.....	40

Figure 4.2 Workflow for the first primary component: Tsunami Arrival Time. This section is separated into two components: the seamless bathymetry construction and the first tsunami wave arrival time.....	41
Figure 4.3 Bathymetry of grid 92E: (a) raw BAG data, (b) Natural Neighbour interpolation.....	42
Figure 4.4 Bathymetry limits of the Canadian (green) and American (blue) datasets within the Juan de Fuca Strait, South Vancouver Island .....	43
Figure 4.5 Tsunami propagation after: (a) 1:44:00; and (b) 1:57:00 inducing earthquake, within the Juan de Fuca Strait using the MOST3 model (adapted from Cherniawasky et al. 2007)	43
Figure 4.6 Water depth of the British Columbia coastal waters, calculated from the seamless bathymetry constructed.....	44
Figure 4.7 Cascadia subduction fault and full rupture zone along North American Pacific Coast, adapted from Cherniawasky, et al. (2007) .....	45
Figure 4.8 Buffer of 500 m radius (green) created around communities boundary (pink) used for the Zonal Statistic tool .....	46
Figure 4.9 Workflow for the time to safety and available time primary method component. The time to safety calculation is separated into three steps: the run-up generation, distance to safety, and time to safety. ....	47
Figure 4.10 Dry pockets created by the run-up generation method within the time to safety .....	48
Figure 4.11 Tsunami design zone for Hilo, Hawaii where dry pockets are also observed (Naito, et al. 2016) .....	50
Figure 4.12 Generalization process: (a) initial raster, (b) results of Expand process, and (c) results of Shrink following the Expand procedure.....	50
Figure 4.13 HZ computed with the generalization process E-S 1-4 and S-E 1-4 for a 7 m run-up in Laxgalts'ap, BC .....	53
Figure 4.14 (a) Cumulative total area within the hazard of the baseline and generalization cases E-S 1 and 2 for each run-up between 3-25 m, (b) Percent increase in the area compared to the baseline for E-S 1 and 2, (c) Area increase within the HZ compared to the baseline for E-S 1 and 2.....	54
Figure 4.15 (a) Cumulative sum of the maximum distance to safety of each community for the baseline and generalization cases E-S 1 and 2 at each run-up, (b) Percent increase in the sum of the maximum distance to safety between the baseline and cases E-S 1 and 2, (c) Difference in the maximum distance to safety increase from the baseline for E-S 1 and 2 ..	55
Figure 5.1 First tsunami wave arrival time ( $t_{arrival}$ ) in minutes for British Columbia, found using the arrival time process .....	58
Figure 5.2 Validation of tsunami arrival time with estimate values from BC Earthquake Alliance Society (2016): (a) Difference in arrival time between estimated and calculated values; (b)	

Error of the calculated arrival times values as a function of the site distance from the tsunami source .....	60
Figure 5.3 Cumulative surface area within the hazard zone (HZ) for run-ups between 3-25 m for each Tsunami Notification Zone (TNZ) .....	62
Figure 5.4 Cumulative percentage of the inundated area and resident population within the hazard zone (HZ) for run-ups between 3-25 m for each Tsunami Notification Zone (TNZ)	62
Figure 5.5 Cumulative resident population within the hazard zone (HZ) for run-ups between 3-25 m for each Tsunami Notification Zone (TNZ) .....	64
Figure 5.6 Available time vulnerability scale.....	65
Figure 5.7 Boxplot of the minimum available time of communities within Zone A for run-ups between 3 and 25 m .....	66
Figure 5.8 Boxplot of the minimum available time of communities within Zone B for run-ups between 3 and 25 m .....	67
Figure 5.9 Boxplot of the minimum available time of communities within Zone C for run-ups between 3 and 25 m .....	68
Figure 5.10 Boxplot of the minimum available time of communities within Zone D for run-ups between 3 and 25 m .....	69
Figure 5.11 Boxplot of the minimum available time of communities within Zone E for run-ups between 3 and 25 m .....	69
Figure 5.12 Location of non-indigenous communities with high and moderate vulnerability communities within Vancouver Island (Zone C).....	71
Figure 5.13 Minimum available time of Tofino using the model and BC EA tsunami arrival time for a range of run-ups between 3 and 25 m for three velocities: (a) Mobility impaired pedestrian ambulatory speed (MI); (b) Average adult ambulatory speed (AW); (c) Slow run (SR).....	72
Figure 5.14 Minimum available time of Ucluelet using the model and BC EA tsunami arrival time for a range of run-ups between 3 and 25 m for three velocities: (a) Mobility impaired pedestrian ambulatory speed (MI); (b) Average adult ambulatory speed (AW); (c) Slow run (SR).....	73
Figure 5.15 Minimum available time of Port Renfrew using the model and BC EA tsunami arrival time for a range of run-ups between 3 and 25 m for three velocities: (a) Mobility impaired pedestrian ambulatory speed (MI); (b) Average adult ambulatory speed (AW); (c) Slow run (SR) .....	74
Figure 5.16 Minimum available time of Winter Harbour using the model and BC EA tsunami arrival time for a range of run-ups between 3 and 25 m for three velocities: (a) Mobility impaired pedestrian ambulatory speed (MI); (b) Average adult ambulatory speed (AW); (c) Slow run (SR) .....	75

Figure 5.17 Minimum available time of Bamfield for a range of run-ups between 3 and 25 m for three velocities: (a) Mobility impaired pedestrian ambulatory speed (MI); (b) Average adult ambulatory speed (AW); (c) Slow run (SR) .....	76
Figure 5.18 Available time (min) of First Nation communities located within sub-region C-1 for the range of run-ups between 3 and 25 m for three velocities: (a) Mobility impaired pedestrian ambulatory speed (MI); (b) Average adult ambulatory speed (AW); (c) Slow run speed (SR) .....	77
Figure 5.19 Available time (min) of First Nation communities located within sub-region C-2 for the range of run-ups between 3 and 25 m for three velocities: (a) Mobility impaired pedestrian ambulatory speed (MI); (b) Average adult ambulatory speed (AW); (c) Slow run speed (SR) .....	78
Figure 5.20 Available time (min) of First Nation communities located within sub-region C-3 for the range of run-ups between 3 and 25 m for three velocities: (a) Mobility impaired pedestrian ambulatory speed (MI); (b) Average adult ambulatory speed (AW); (c) Slow run speed (SR) .....	79
Figure 5.21 Available time (min) of First Nation communities located within sub-region C-4 for the range of run-ups between 3 and 25 m for three velocities: (a) Mobility impaired pedestrian ambulatory speed (MI); (b) Average adult ambulatory speed (AW); (c) Slow run speed (SR) .....	80
Figure 5.22 Available time (min) of First Nation communities located within sub-region C-5 for the range of run-ups between 3 and 25 m for three velocities: (a) Mobility impaired pedestrian ambulatory speed (MI); (b) Average adult ambulatory speed (AW); (c) Slow run speed (SR) .....	81
Figure 5.23 Available time (min) of First Nation communities located within sub-region C-6 for the range of run-ups between 3 and 25 m for three velocities: (a) Mobility impaired pedestrian ambulatory speed (MI); (b) Average adult ambulatory speed (AW); (c) Slow run speed (SR) .....	82
Figure 5.24 Available time (min) of First Nation communities located within sub-region C-7 for the range of run-ups between 3 and 25 m for three velocities: (a) Mobility impaired pedestrian ambulatory speed (MI); (b) Average adult ambulatory speed (AW); (c) Slow run speed (SR) .....	83
Figure 5.25 Available time (min) of First Nation communities located within sub-region C-8 for the range of run-ups between 3 and 25 m for three velocities: (a) Mobility impaired pedestrian ambulatory speed (MI); (b) Average adult ambulatory speed (AW); (c) Slow run speed (SR) .....	84
Figure 5.26 Available time computed with model arrival time for Richmond and Delta for a 7 m run-up .....	85

Figure 5.27 Minimum available time of Delta using the model and BC EA tsunami arrival time for a range of run-ups between 3 and 25 m for three velocities: (a) Mobility impaired pedestrian ambulatory speed (MI); (b) Average adult ambulatory speed (AW); (c) Slow run (SR).....	86
Figure 5.28 Minimum available time of Richmond using the model and BC EA tsunami arrival time for a range of run-ups between 3 and 25 m for three velocities: (a) Mobility impaired pedestrian ambulatory speed (MI); (b) Average adult ambulatory speed (AW); (c) Slow run (SR).....	87
Figure 6.1 Structures distribution within the Tofino, mapped by type: commercial, industrial, park, institutional, residential, tourism and accommodation and short term rental.....	91
Figure 6.2 Tofino analysis zones.....	92
Figure 6.3 Population distribution for summer and winter night scenario: (a) resident population; (b) tourist population.....	93
Figure 6.4 Land cover of Tofino used in the Pedestrian Evacuation Analyst and associated speed conservation value (SCV) table .....	94
Figure 6.5 Tofino tsunami evacuation map, adapted from District of Tofino (2016).....	95
Figure 6.6 Tofino safe zones for run-ups between 7 m and 25 m.....	95
Figure 6.7 Minimum available time (min) by analysis zones for the municipality of Tofino found using the model tsunami arrival time at three evacuation velocities: (a) mobility impaired adult ambulatory speed (MI); (b) average adult ambulatory speed (AW) and, (c) slow run (SR).....	98
Figure 6.8 Cumulative resident and tourist population at-risk (located within the hazard zone) by analysis areas for the summer-night scenario .....	99
Figure 6.9 Buildings within the HZ for run-ups between 3 m and 25 m .....	100
Figure 6.10 Population within the hazard zone for a run-up of 17 m using no VEB, VEB 1, VEB 2 and VEB 3 for Chesterman Beach and Chesterman for a mobility impaired adult ambulatory speed (MI).....	102
Figure 6.11 Population within the hazard zone for a run-up of 19 m using no VEB and VEB 3 for a mobility impaired adult ambulatory speed (MI), (a) Chesterman Beach and Chesterman; (b) MacKenzie .....	103
Figure 6.12 Population within the hazard zone for a run-up of 25m using no VEB, VEB3 and VEB4 for a mobility impaired adult ambulatory speed (MI), (a) Chesterman Beach and Chesterman; (b) MacKenzie; (c) Cox Bay.....	104
Figure 6.13 Time to safety (min) using with 3 vertical evacuation structures in the VEB5 configuration.....	105
Figure A.1 Greater Masset evacuation map, Zone A (Village of Masset 2013).....	133

Figure A.2 Queen Charlotte tsunami evacuation map, Zone A (Village of Queen Charlotte 2012)  
..... 134

Figure A.3 Port Hardy tsunami evacuation zone, Zone C (District of Port Hardy 2016) ..... 135

# List of Tables

---

Table 3.1 Recommended planning tsunami run-up levels by tsunami notification zone (Anderson, et al. 2016).....	31
Table 4.1 Format, description, resolution and provider of the geographical data used.....	39
Table 4.2 Format, description, resolution and provider of the additional geographical data used in the Tofino case study .....	40
Table 4.3 Pedestrian travelling velocities considered for evacuation in model .....	49
Table 4.4 Cases considered for the run-up HZ generalization sensitivity analysis.....	51
Table 4.5 Number of dry pockets as a function of their size in cells for the baseline and test cases E-S 1 to 4 and S-E 1 to 4 for a 7 m run-up .....	52
Table 5.1 Summary of maximum wave amplitude and run-up within the Canadian West Coast from the literature review of historical and modelled tsunamis. Maximum run-up calculated as twice the maximum wave height at the shore.....	57
Table 6.1 Tofino resident and tourist population estimates for the winter and summer night scenario .....	92
Table 6.2 Minimum available time within the municipal boundary of Tofino found with the anisotropic path-distance (APD) model and distance-only (DO) model for run-ups between 3 m and 25 at three pedestrian evacuation velocities: mobility impaired adult ambulatory speed (MI), average adult ambulatory speed (AW) and slow run (SR).....	96
Table 6.3 Resident and tourist population within the hazard zone (HZ) with a travel time larger than the first wave tsunami arrival time of 28.1 min using a mobility impaired ambulatory speed (MI) for the summer and winter night scenario .....	102
Table A.1 List of communities where their population were suppressed by the census for confidentiality....	121
Table A.2 List of communities not included and alternative names in Zone C of the Tsunami Notification Zone...	123
Table A.3 List of communities not included and alternative names in Zone D of the Tsunami Notification Zone..	124
Table A.4 List of communities not included and alternative names in Zone E of the Tsunami Notification Zone...	125
Table A.5 List of communities where their population were suppressed by the census for confidentiality...	128
Table A.7 First tsunami wave arrival time result comparison: column [2] are the calculated values from the Arrival Time process and column [3] are the estimated values from BC Earthquake Alliance Society (2016). Calculated values greater than the estimated values are in red...	131

# List of Symbols and Acronyms

---

## Roman Numerals

A	Experimental constant of (0.5)
a	Roughness aperture [m]
d	Water depth [m]
f	Friction factor from Darcy's law
g	Gravitational constant (9.81 m/s <sup>2</sup> )
H	Tsunami peak-to-through amplitude [m]
H <sub>s</sub>	Tsunami wave height at the shoreline
H <sub>T</sub>	Tsunami wave height at 100 m depth
L	Tsunami wavelength [m]
L <sub>R</sub>	Tsunami inland horizontal inundation distance [m]
R	Run-up [m]
S <sub>0</sub>	Ground slope (°)
Y <sub>loss</sub>	Losses in the wave height [m]

## Greek Letter Symbols

η	Tsunami zero-to-peak amplitude, wave height
Φ	Slope of nearshore bathymetry (from 100 m depth to the high water elevation)

## Abbreviation

AANDC	Aboriginal Affairs and Northern Development Canada
APD	Anisotropic path-distance (model)
ASCE	American Society of Civil Engineers
BAG	Bathymetric Attributed Grid
BC	British Columbia
BC EA	British Columbia Earthquake Alliance Society
BPR	Bottom pressure recorder
CHS	Canadian Hydrographic Service
CSZ	Cascadia Subduction Zone
CY	City
DART	Deep-ocean Assessment and Reporting of Tsunami
DEM	Digital elevation model
DM	Distret municipality
EMBC	Emergency Management British Columbia
GIS	Geographic information system
HHW	Higher high water large tides
HZ	Hazard zone
ICO	Intergovernmental Oceanic Commission
IDG	Indian government district (referred to as First Nations community in this text)
IM	Island municipality
IPCC	Intergovernmental Panel on Climate Change
IRI	Indian Reserves (referred to as First Nations community in this text)
IST	Island trust

LLW	Lower low water low large tides
MOST	Method of Splitting Tsunami
NOAA	National Oceanic and Atmospheric Administration
NTWC	National Tsunami Warning Center
NVL	Nisga'a Land
ONSWG	Open Navigation Surface Working Group
PENS	Provincial Emergency Notification System
POPCT	Population centre
PTWC	Pacific Tsunami Warning Center
RAR	Resident population at-risk
SCV	Speed conservation value
SZ	Safe zone
T	Town
TAR	Tourist population at-risk
TNZ	Tsunami Notification Zone
UNESC	United Nations Education, Scientific and Cultural Organization
O	Unincorporated place
UNP	Universal Transverse Mercator
UTM	Vulnerability assessment
VA	Vertical evacuation building (or structure)
VEB	Village
VL	

# Chapter 1. Introduction

---

## 1.1 Background and Motivation

Tsunamis, from the Japanese word meaning “harbour waves”, are long-period gravity waves, rarely occurring alone. In fact, the second or third wave arriving onshore is usually the greatest. They are formed by a sudden disturbance in the water surface and can have many causes, such as subduction earthquakes, aerial and submarine landslides, volcanic eruptions and glaciers calving. Although known for being an ocean phenomenon, they can occur in lakes and rivers as well.

Tsunamis are one of the most devastating natural disasters, with potential to have severe impact on both loss of life and manmade structures. Images and videos of Japan’s coastal communities following the Tohoku 2011 earthquake surprised many across the world of the tsunamis widespread damage potential (Figure 1.1). The  $M_w$  9.0 earthquake caused waves as high as 40.5 m. This was the costliest natural disaster in history, causing over \$217 billion in damage and economic losses (Chock, et al. 2013) and causing 15,891 deaths. The Sumatra 2004 earthquake of  $M_w$  9.3, however initiated the deadliest tsunami, causing over 200,000 casualties across 13 countries in Indian Ocean. The most severe effects were observed in Sumatra, near the epicentre, Indonesia, India’s Andaman and Sri Lanka, but its deadly effects reached as far as Somalia (Grupta and Gahalaut 2013). It is estimated that on average 2 tsunamis occur every year that inflict damage near its source, and one every 15 years a causes wide-spread destruction (National Weather Service 2016).



Figure 1.1 Photograph of the damaged endured in Rikuzentakata, Japan following the 2011 Tohoku earthquake and tsunami (Hagen 2014)

Based on historical data, approximately 60% of tsunamis are generated and occur in the Pacific Ocean as demonstrated Figure 1.2 (NOAA 2011). The Pacific Ocean is a highly seismic region due to the active boundaries of the Pacific Plate, referred to as the Ring of Fire. The Great Alaska Earthquake of 1964 originated from this region, more precisely, from the subduction of Pacific Plate with the North America plate with its epicentre in Prince William Sound. The megathrust earthquake caused a tsunami that claimed 131 lives in Alaska. The tsunami continued southward and reached Canada, where it caused millions in damages in Port Alberni, Zeballos and Hot Spring Cove (Clague, et al. 2000). This is not the first tsunami to have occurred in Canada. A series of tsunamis occurs in the Kitimat inlet between 1952 and 1975, caused by submarine landslides due to unstable sediments. Peak waves were recorded as high as 8.2 m, and caused severe damage to wharf and boats within the inlet (Thomson 1981). The only deadly tsunami in Canada was also caused by landslides, which were triggered by the 1929 Grand Banks earthquake. The tsunami caused 28 deaths in Newfoundland. However, the greatest tsunami threat to Canada originates from the Cascadia Subduction Zone, off the western North America coast, extending from Vancouver Island to California (Clague, et al. 2003). Although it has not ruptured in recent time, the fault history has been reconstructed using geological evidence. Marine sediments have been found in Vancouver Island, Washington and Oregon that suggest large tsunamis following the fault rupture (Atwater, et al. 1995). The fault is estimated to have an average rupture interval of 500 years, with the last event occurring 300 years ago in 1700.

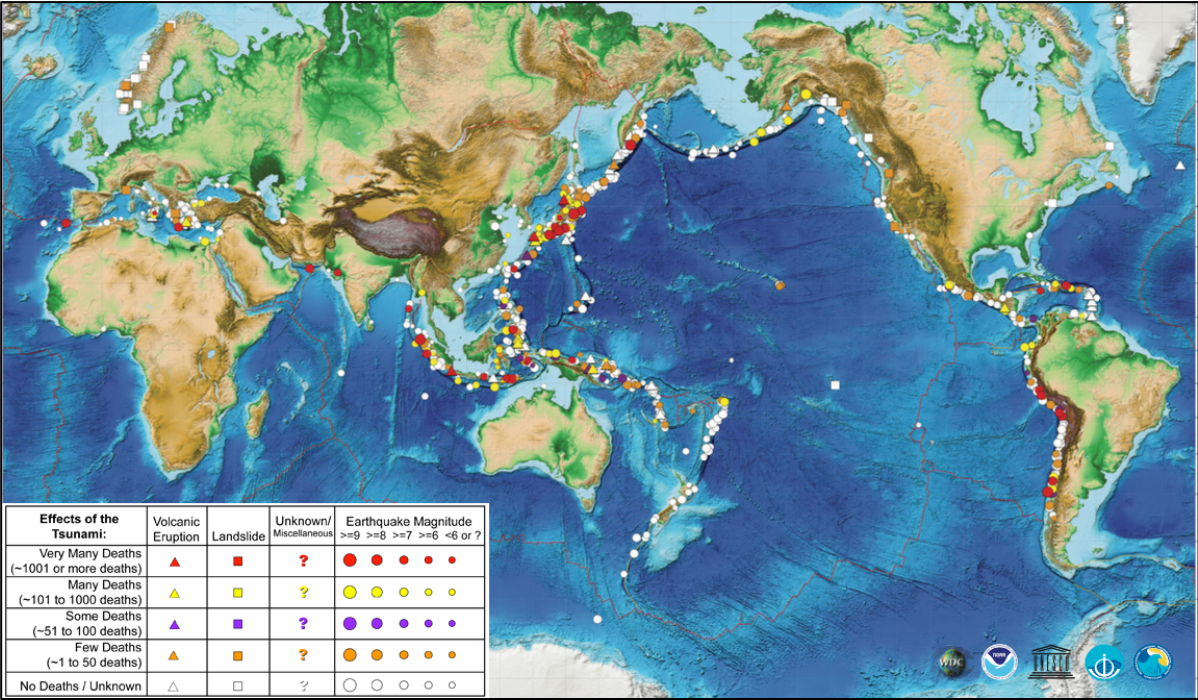


Figure 1.2 Tsunami sources from earthquake, volcanoes, landslides and other causes from 1410 B.C. to A.D. 2011, adapted from NOAA (2011)

Growing concerns for tsunami hazard from the Cascadia Subduction Zone in Washington, Oregon and California has prompted an increase in research on the subject in the United States with the formation of the National Tsunami Hazard Mitigation Program in 1995 (Folger 2015). Tsunami inundation hazard maps for communities on the West Coast of the United States and Hawaii have been developed in the scope of the new chapter “Tsunami Loads and Effects” of the American Society of Civil Engineers (ASCE) 2016 standard. The standard is the first to provide structural design procedures for tsunami resilience and modeling standards based on research and case studies that had previously been deficient. In Canada, no such effort has been initiated. Modeling of tsunamis has been focused on the Strait of Juan de Fuca and Georgia, where most of the population living on the Western Canada resides. Tsunami inundation modeling and has been initiated at a community level, once again limited to the Georgia Basin. However, the greatest threat from a Cascadia tsunami is evaluated to be on the West coast of Vancouver Island, and not in the Georgia Basin as the waves are attenuated once they have reached that region (Clague, et al. 2000). A great need for hazard determination in small communities in Western Canada currently exist.

## **1.2 Study Objectives and Scope**

First and foremost, the main objective of the study is to determine the vulnerability to loss of life of communities within the Canadian West Coast to a Pacific subduction tsunami. The study aims to evaluate the relative vulnerability of the five Tsunami Notification Zones established for warning capabilities in terms of the population and surface area within the tsunami hazard zone. Communities’ loss of life susceptibility, in terms of pedestrian evacuation capabilities, is evaluated using a quantitative variable, the available time. As the available time takes into account both the tsunami arrival time and the time to safety it provides an independent correlation, which can be used as a method of relating communities’ tsunami vulnerability, impartial to the tsunami hazard. The vulnerability is further assessed in terms of the tsunami hazard in each Tsunami Notification Zones in terms of probable run-up ranges assessed with the literature.

The works further aims at developing a simple methodology that can be applied using geographic information systems to determine areas of greatest tsunami risk and that may require more rigorous analysis. Such study is presented for the District Municipality of Tofino. Using a more complex model, the loss of life vulnerability is assessed. Tsunami mitigation methods are explored as optimal locations for vertical evacuation structures.

The study has the following limitations and constraints:

- The focus of the study is the potential loss of life only. The structural vulnerability and economical impact of a tsunami is not assessed.
- All communities located directly on the shoreline of the Canadian Pacific Coast or within a connecting inlet were evaluated. Both non-indigenous communities, listed in the 2011 census, and First Nations communities, listed by Aboriginal Affairs and Northern Development Canada, are included. The vulnerability was assessed only within the boundaries of the communities.
- Evacuation capabilities were considered only for pedestrian evacuation using a distance-only approach on a bear-earth elevation model for the Canadian West Coast vulnerability assessment. A detailed anisotropic path-distance modeling is used for the Tofino case study.

### **1.3 Contributions and Novelty of the Study**

Past investigation of tsunami impact in the Canadian Pacific have focused on Vancouver Island and the Georgia basin. These areas have been evaluated because they are the most populated region, encompassing the metropolitan area of Vancouver and Victoria. North Vancouver Island, the main coast and Haida Gwaii have been omitted as they are scarcely populated. The present study evaluates the tsunami susceptibility risk of the entire Canadian West Coast at a community level, including remote First Nations communities.

Additionally, the tsunami evacuation capabilities are described in past studies in terms of time to safety. This value cannot be used to compare the relative life safety risk in differing location, as the ability to evacuate to safety is also dependent on the tsunami arrival time, which varies by location. A new variable is proposed in this study, the available time, which is a function of both the tsunami arrival time and required time to safety. This variable enables direct comparison on the population abilities to evacuate. Additionally, the available time provides a scale where the life safety threshold is easily identifiable. Finally, anisotropic path-distance model is first applied to the municipality of Tofino.

### **1.4 Publications**

Cheff, Isabelle\*, Ioan Nistor and Dan Palermo. “Tsunami Vulnerability Assessment of the Canadian West Coast Communities Based On Evacuation Capability.” Natural Disaster Mitigation Specialty Conference, CSCE. London: CSCE, 2016.

(\*) – Indicates presenter of oral presentation.

## 1.5 Outline of the Thesis

**Chapter 1** as an introduction presents the objective, scope and contributions and novelty of this study to the thematic field of study.

**Chapter 2** first reviews the current literature regarding the Canadian tsunami hazard and current methods for determining the inland tsunami inundation with the goal of providing a range or probable run-ups for the Canadian Pacific Coast. Secondly, past community vulnerability assessment are reviewed in addition to different assessment model. Finally, lives saving tsunami mitigation systems are briefly reviewed.

**Chapter 3** presents an overview of the study area: the Canadian Pacific coast, encompassed within a single province, British Columbia. The current tsunami detection and warning capabilities in addition to emergency preparedness of the province are outline within this chapter. The population distribution of coastal communities within the pre-established Tsunami Notification Zone is described for permanent resident, First Nations and transient population. The hazards for each Tsunami Notification Zone from the current tsunami planning guidelines are reviewed in terms of potential run-up and first wave arrival time.

**Chapter 4** describes the methodology used for the vulnerability assessment, including a detailed descriptions of the geographical information systems (GIS) processes. As the run-ups are unknown for all locations within the Canadian Pacific coast, GIS process are used to assess the vulnerability in terms of the available time for a range of run-ups and various pedestrian evacuation speed. To find the available time, the first tsunami wave arrival time and time necessary to reach safety is calculated for the entire coast. The population and geographical data used are also listed within this chapter, including the data format, the provider and a short description.

**Chapter 5** examines the results of the vulnerability assessment. The impact of the generated run-ups within each Tsunami Notification Zone in assessed in terms of inundated surface area, population at-risk and percentage of the population at-risk. Next the vulnerability is assessed in terms of available time and categorized within three vulnerability classes: low, moderate and high. Communities with the high and moderate vulnerability are further evaluated.

**Chapter 6** presents a case study of the District of Tofino. In addition to a detailed vulnerability assessment conducted in terms of available time using a more precise anisotropic path-distance modeling, life saving mitigation solutions is explored in form of locations for vertical evacuation refuges.

**Chapter 7** presents the research conclusion recommendation for future work.

# Chapter 2. Literature Review

The following chapter reviews the past research relevant to the Canadian tsunami hazard and vulnerability assessment. First, the research of the inland tsunami propagation and existing numerical models are reviewed. Secondly, the Canadian hazard is assessed by reviewing past tsunami events and tsunami modeling of Canadian shores. Thirdly, the review will examine past research on community-scaled vulnerability and evacuation assessment methods. Finally, research on vertical evacuation structures as tsunami mitigation technique is reviewed.

The objective of this review is to: (i) present the Canadian tsunami hazard and current tsunami hazard assessment methods; (ii) provide a basis for the community-wide vulnerability assessment and; (iii) outline the gaps in knowledge relating to Canadian tsunami hazards and consequent research needs.

## 2.1 Tsunami Characteristics and Magnitude Determination

A tsunami is not a single wave but in fact a series of waves that can be separated by minutes or hours, and where the first wave is rarely the largest (Clague, et al. 2003, Bryant 2014). They can behave as a regular wave as they experience the same phenomenon: shoaling, refraction, reflection and diffraction (Murata 2009). Tsunami's characteristics can be described by their wavelength and their amplitude. The wavelength,  $L$ , is measured from two consecutive peaks and is typically between 10 and 500 km. The amplitude can be measured as either its zero-to-peak amplitude,  $\eta$ , also called wave height, or its peak-to-through amplitude,  $H$  (Figure 2.1). The tsunami wave heights are proportional to the magnitude of the earthquake (Thomson 1981).

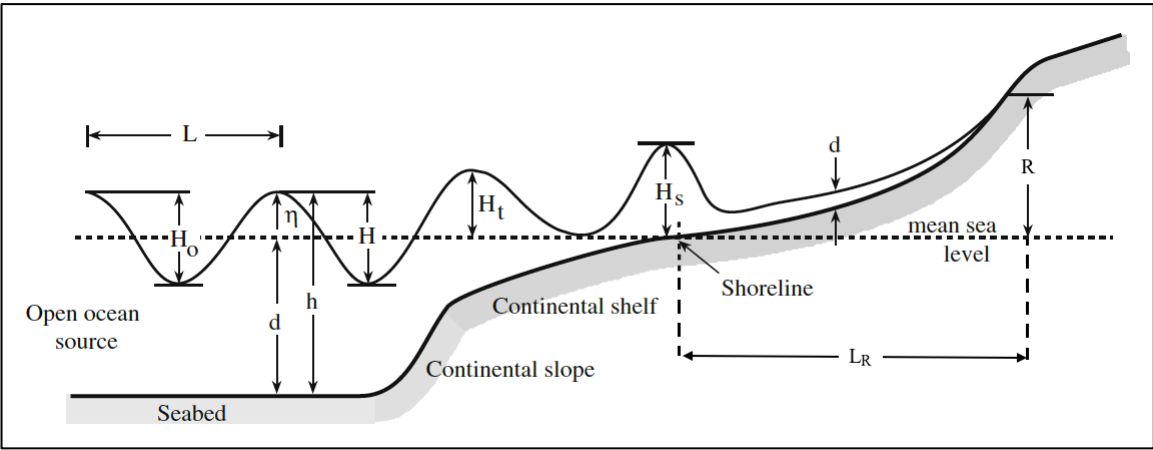


Figure 2.1 Tsunami wave characteristics at different water depth, adapted from Bryant (2014)

The wave can take different shapes depending on the water depth and its location in relation to shore (Geist 1998). In deep oceans, tsunami waves are approximated as sinusoidal (Figure 2.2) as they are considered a long wave: small height to length ratio ( $H/L$ ). They propagate linearly as shallow water waves, as per the Airy wave theory. It is considered shallow water when the water depth ( $d$ ) to wavelength ratio is less 0.5 (Titov 1997, Bryant 2014). The shallow water assumption holds true for a tsunami, as the ocean depth is rarely deeper than 5 km, which is half of the minimum typical tsunami wavelength, with an average depth of 3.7 km (NOAA 2015). As the wave approaches the continental shelf, the ocean bottom flattens out, causing the wave peak to get sharper and forming a nonlinear Stokes wave (Figure 2.2; Komar 1998, von Baeyer 1999). As the wave further approaches the shore, the wave takes the form of a solitary wave with a preceding trough, resembling an N-wave (Figure 2.1; Bryant 2014). The wave characteristics at the coastline depends on the steepness of the shore. Tsunamis are more likely to break on steeper slopes, but 75% of tsunamis do not break once they have reached the shore, and thus maintain most of their energy (Bryant 2014). On soft slopes, tsunamis are not likely to break but instead become turbulent onrushing surges, which can be very destructive (Clague, et al. 2003, Bryant 2014). Tsunami waves are also prone amplification within inlets and bays (Wigen and White 1964, Thomson 1981). The inland tsunami propagation can be measured by the length of the inundation area,  $L_R$ , or the topographic elevation at the maximum  $L_R$  called the run-up,  $R$  (Figure 2.1).

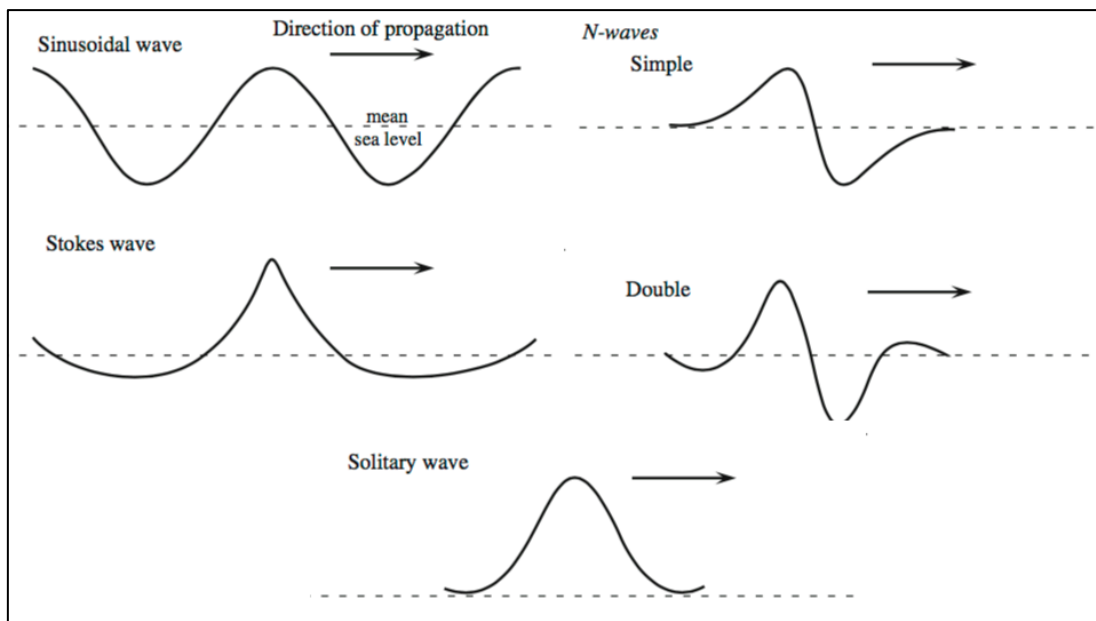


Figure 2.2 Idealized tsunami wave form with an exaggerated vertical dimension, adapted from Bryant (2014)

### 2.1.1 Run-Up

Tsunami hazards can be caused not only from the inundation but also from the erosive high velocity flows and debris impact. Additional hazards during the recovery can also be caused by the spread of combustible liquids creating fires or diseases from the spread of toxic liquids or waste (Clague, et al. 2003).

The tsunami hazard is typically evaluated by the run-up (Clague, et al. 2003, Leonard, et al. 2013). As the run-up represents the topographical elevation at the maximum inland inundation limit, the run-up is given as a height, but does not necessarily represent the inundation water depth. The run-up is used instead of the horizontal distance,  $L_R$ , as the latter is dependent on the local topography, and can be determined using the run-up. The local tsunami hazard is difficult to estimate as the run-up can differ drastically along the coastline as it is also dependent on the local topography and wave amplitude. Furthermore, the wave amplitude is dependent on the offshore bathymetry, shoreline orientation and shape of the coastline. For example, during the 1993 Hokkaido Nansei-Oki tsunami, the run-up ranged from 5 to 30 m along a 500 m portion of the coast in Okushiri Island, Japan (Satake and Tanioka 1995).

Run-ups of 0.5 m are reported to cause damage offshore, such as to boats and docks, and can be dangerous to swimmers (Whitmore, et al. 2008). Clague, et al. (2003) consider run-ups dangerous at 1 m, where as a value of 1.5 m is reported to cause inland damage by Whitmore, et al. (2008) and Leonard, et al. (2013). Run-ups of 3 m or greater are considered to have a potential for major damage (Leonard, et al. 2013). The probability of the Canadian Pacific coast enduring damaging run-ups ( $\geq 1.5$  m) has been evaluated at 40-80% in 50 years, compared to 10-30% in 50 years for major damage ( $\geq 3$  m; Leonard, et al. 2013). For comparison, the Canadian Atlantic coast's probability for damage and major damage is 1-15% and 1-5% respectively. The probabilities for damage on the Pacific coast exceed the current standard for seismic design in Canada of 10% per 50 years (NBCC 2015).

Calculating the run-up can be complex as the ground variability, such as the slope, built environment and roughness play an important role. Reese, et al. (2011) found that the run-up for the 2009 South Pacific tsunami was a negative logarithmic function of the ground slope. Tsunamis have also been found to act as a rapidly rising tide where the run-up is equal to wave peak-to-through amplitude, or twice the zero-to-peak amplitude (wave height) at the shoreline (Houston and Garcia 1978). Abe (1995) experimentally found that the run-up is equal to or less than the wave height at the shoreline for slopes less than 0.14, and as the slope increases so does the run-up. The run-up is calculated in New Zealand by doubling the maximum wave height at the shoreline and then decreasing maximum run-up by 1 m for every 200m the tsunami travels inland (Leonard, et al. 2009). However, the 1/200 ratio has been found to be overly conservative (Power 2013). Alternately, instead of finding the run-up, Bretschneider and Wybro (1977)

calculate the inland distance of the inundation,  $L_R$ , for flat coastal plains using the manning coefficient,  $n$ , and wave height at the shoreline,  $H_s$ :

$$L_R = 0.06H_s^{4/3}/n^2 \quad [2.1]$$

McSaveney and Rattenbury (2000) added a term for the slope,  $S_0$ , to Eq. 2.1 to find losses in the wave height per meter of inundation,  $Y_{loss}$ :

$$Y_{loss} = (167n^2/H_s^{1/3}) + 5\sin(S_0) \quad [2.2]$$

Smart, Crowley and Lane (2016) derived the Bernoulli equation assuming the tsunami wave has a depth averaged steady velocity onshore:

$$\frac{R}{S_0} = \frac{3a}{2} \ln\left(\frac{H_s}{aS_0} + 1\right) \quad [2.3]$$

Where  $a$  is the roughness aperture, which is the ratio of the distance between protrusions in the inundated area to the Darcy's friction factor,  $f$ . The roughness aperture is used instead of a friction factor, as such value is not easily obtained for the friction on obstructing elements in the inundation area such as buildings and tree trunks. The run-up is computed by the Army Corps of Engineers (Camfield 1980) using the following equation:

$$R/H_s = (1 + A)(1 + 2A)/(2A^2) \left(1 + (8gn^2/0.91A^2S_0H_s^{1/3})\right) \quad [2.4]$$

Where  $A$  is an experimental constant taken as 0.5, and  $g$  is the gravitational constant. Where tsunami inundation maps are not provided, the ASCE 7-16 is derived from numerical simulation and field observation (Synolakis 1986, Murata 2009, Li 2000, Li and Raichlen 2001, 2003) a ratio between the run-ups to the offshore tsunami amplitude at 100 m depth ( $H_T$ ):

$$\text{For } \cot\Phi < 10 \quad R/H_T = 4.0 \quad [2.5a]$$

$$\text{For } 10 \leq \cot\Phi < 40 \quad R/H_T = 4 - [(\cot\Phi - 10)/30] \quad [2.5b]$$

$$\text{For } \cot\Phi \geq 40 \quad R/H_T = 3.0 \quad [2.5c]$$

Where  $\Phi$  is the mean slope of the nearshore bathymetry, calculated from 100 m depth to the mean high water elevation.

The tsunami run-up can also be affected by the state of tide. High tides will therefore result in a higher run-up than a low tide (Ng, et al. 1990a, 1990b, Clague, et al. 2000)

### 2.1.2 Tsunami Modeling

Modeling of tsunamis is essential for real-time notifications and a useful tool to predict the tsunami arrival time and inundation area for use in evacuation planning and hazard mitigation. A

complete subduction earthquake tsunami scenario model includes three stages: tsunami generation, offshore propagation and inland inundation.

The tsunami generation is done with the assumption that the ocean water is incompressible and thus the sea floor displacement is the same as the sea surface deformation. The sea floor displacement for a subduction earthquake is simulated using the elastic deformation theory (Titov 1997, Titov and Synolakis 1998, Cherniawasky, et al. 2007).

Most numerical simulations use a finite-difference numerical model with shallow-water assumptions for the trans-oceanic propagation of the tsunami waves. Linear shallow-water models (Synolakis 1986, Synolakis 1987, Hebenstreit and Murty 1989, Tadepalli and Synolakis 1994, Kanoglu 1997, Satake, et al. 2003) fail to simulate more complex factors in the run-up and wave propagation such as the wave breaking, supercritical currents and complicated flows near the shoreline (Titov 1997). Nonlinear shallow-water models have also been developed (Ng, et al. 1990a,1990b). More recent nonlinear shallow-water models include the Method of Splitting Tsunami (MOST-3) model (Titov and Synolakis 1997, 1998, Titov, et al. 2005), which is used at the NOAA Center for Tsunami Research, the Alaska Tsunami Forecast Model (AFTM) (Kowalik and Whitmore 1991, Whitmore 1993), NEOWAVE (Cheung and Yamazaki 2012) and MIRONE. MIRONE integrates the SWAN code for trans-oceanic propagation (Nader 2004) with the tsunami N2 model (Professor Imamura of Tohoku University, Japan) for shoaling effects, coastal amplification and inland flooding. The open source Cornell Multi-Grid Coupled Tsunami Model (COMCOT) uses both linear and nonlinear assumptions (Liu and Seung-Buhm Woo 1998).

Fujima (1980) suggested a model for inland propagation using Euler's equations, but this model is limited because the viscosity and bottom friction forces are not included (Synolakis 1986, 1987). Henry and Murty (1972) studied the resonance of a tsunami wave within a complex series of inlet using 1D river-flow equations.

## **2.2 Canadian Tsunami Hazard**

Many tsunamis of various magnitudes affect the Canadian coastline every year, but few cause damages. Notably, the great Alaska earthquake in 1964 generated a tsunami that caused great damages in coastal communities located on the western front of Vancouver Island. On the other hand, the only deadly tsunami occurred in the Atlantic in 1929: the Grand Banks earthquake triggered a landslide that caused a tsunami, which claimed 27 lives in Newfoundland (Jones 1992).

Tsunamis can be produced by earthquakes, aerial or submarine landslides, submerged volcanic eruptions and explosions. For the Canadian Pacific coast, volcanic eruption hazard originates

from the Hawaiian Islands (McMurty, et al. 1999) while unstable glacio-marine clays located in most fiords in the Canadian Pacific coast create a landslides hazard. For instance, many submarine landslides occurred between 1952 and 1975 in the Kitimat inlet, causing tsunamis with a peak wave height of 8.2 m in 1975 (Murty and Brown 1975, Thomson 1981, Clague, et al. 2003). The Strait of Georgia is particularly at risk with sediments in the Fraser River Delta found to be unstable with its failure having the potential of causing 18 m waves (Mosher, et al. 2004, Rabinovich, et al. 2003).

However, most tsunamis are caused by subduction zone earthquakes (Atwater, et al. 1995, Clague, et al. 2003), which are the only source of tsunamis considered within the scope of this study. A subduction zone earthquake presents a great risk for the Canadian Pacific coast as it is located within the most active seismic region in the world, the circum-Pacific belt and often referred to as the Ring of Fire (Thomson 1981, Clague, et al. 2000, 2003). The Ring of Fire is a horseshoe shaped area of active subduction faults that lies on the Pacific Rim (Figure 2.3).

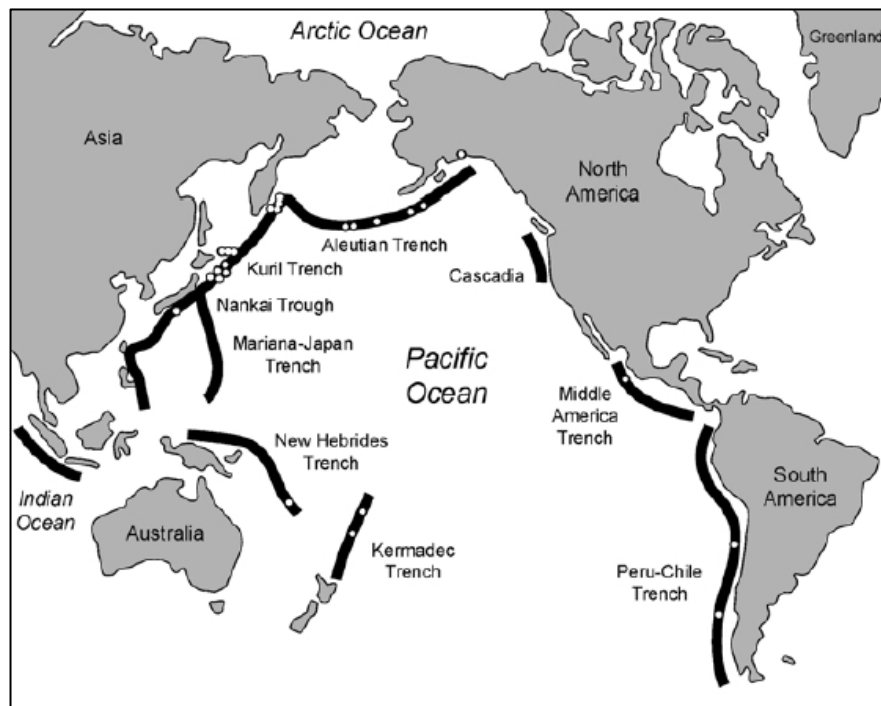


Figure 2.3 Subduction faults in the Pacific Ocean creating the Ring of Fire or circum-Pacific belt (Clague, et al. 2003)

Subduction earthquakes are typically caused by a sudden fault slip (McCaffrey and Goldfinger 1995). This occurs when the converging plate beneath the continental shelf exceeds the sliding stress, creating the elastic stress caused by the seaward edge of the plate being dragged down. The sudden release of elastic energy creates a springing action of the continental shelf edge that disturbs the water surface upward, creating a tsunami. Before the rupture, the additional mass of seaward edge underneath the continental shelf increases the ground surface elevation. A sudden

subsidence of these areas occurs following the seismic event. Once the earthquake has occurred, the plates lock once more and start accumulating strain energy (Thomson 1981, McCaffrey and Goldfinger 1995, Clague 1997).

Earthquake induced tsunamis affecting the Pacific coast of Canada can be further categorized by their source; distant, as generated beyond the continental shelf, or local, which are generated within the continental shelf. Distant tsunamis have longer periods and duration and affect a larger section of the coastline. In contrast, local tsunamis typically have a shorter period and duration and will affect a smaller section of the coastline than their counterpart (Clague, et al. 2003, Bryant 2014).

### **2.2.1 Historical Tsunamis from Local Sources**

The greatest tsunami threat to the Canadian West coast originates from a local source, the Cascadia Subduction Zone (CSZ; Clague, et al. 2000, Leonard, et al. 2013). The CSZ constitutes over a 1,000 km of eastward subduction from of the Juan de Fuca plate, and others, beneath North America (Atwater, et al. 1995, McCaffrey and Goldfinger 1995, Clague 1997) extending from Vancouver Island to California (Figure 2.4). Although the CSZ has not ruptured recently, its seismic history has been reconstructed from well documented geological evidence found in Oregon, Washington and Vancouver Island (Atwater 1987, Darienzo and Peterson 1990, Atwater and Yamaguchi 1992, Clague and Bobrowsky 1994, Atwater, et al. 1995, Clague 1997, Clague et al. 2000, Ollerhead, et al. 2001, Nelson, et al. 2002). Earthquake activity has been concluded from evidence of sudden subsidence in estuaries and intertidal marshes from buried forest soil and mud deposits found in areas previously above high tides. Sand sheets containing marine water evidence, such as marine fossils, were also found directly overlaying the intertidal mud and surrounding the tree trunks and leaves of herbaceous plants that were living within the subsided areas. This evidence suggests a tsunami occurred directly after the earthquake (Atwater 1987, Atwater and Yamaguchi 1992, Clague and Bobrowsky 1994, Atwater, et al. 1995, Clague 1997, Clague and Bobrosky 1999, Nelson, et al. 2002). The location of the geological evidence in sheltered areas, away from the coast in inlets, suggests that the sudden marine water inundation was caused by a tsunami and not a coastal storm. The location of the geological evidence found for prehistoric tsunamis in Vancouver Island is illustrated in Figure 2.5.

The CSZ is estimated to rupture at an approximate interval of 500 years, with a range between 300 and 2000 years, for events of  $M_w$  8 or higher (Atwater, et al. 1995, McCaffrey and Goldfinger 1995, Clague 1997, Clague, et al. 2000). The evidence of the seismic record dates back as far as 7,500 years in some areas (Ollerhead, et al. 2001). The evidence suggests that the latest events occurred approximately 300 years ago (Atwater, et al. 1995, Clague 1997, Clague, et al. 2000). This event is recorded in Japanese history, which cites a tsunami of remote origin, as no ground shaking was felt, in January 1700 A.D. (Satake, et al. 1996, 2003). This coincides

with the description in oral history of North American natives living on Vancouver Island, of a large shaking event and subsequent tsunami in the winter (McMillan and Hutchinson 2002). As no other evidence of an earthquake occurring in the Pacific around this time exists, these two events are believed to be one and the same. The geological evidence of the land subsidence suggests an event of  $M_w$  9 occurred (Atwater, et al. 1995, Clague 1997), supported by numerical simulations performed by Satake, Wang and Atwater (2003) of the elastic dislocation model of the fault and subsequent tsunami propagation. The authors found that the most likely event was an earthquake of  $M_w$  9.0 with a coseismic slip of 19 m (vertical displacement).

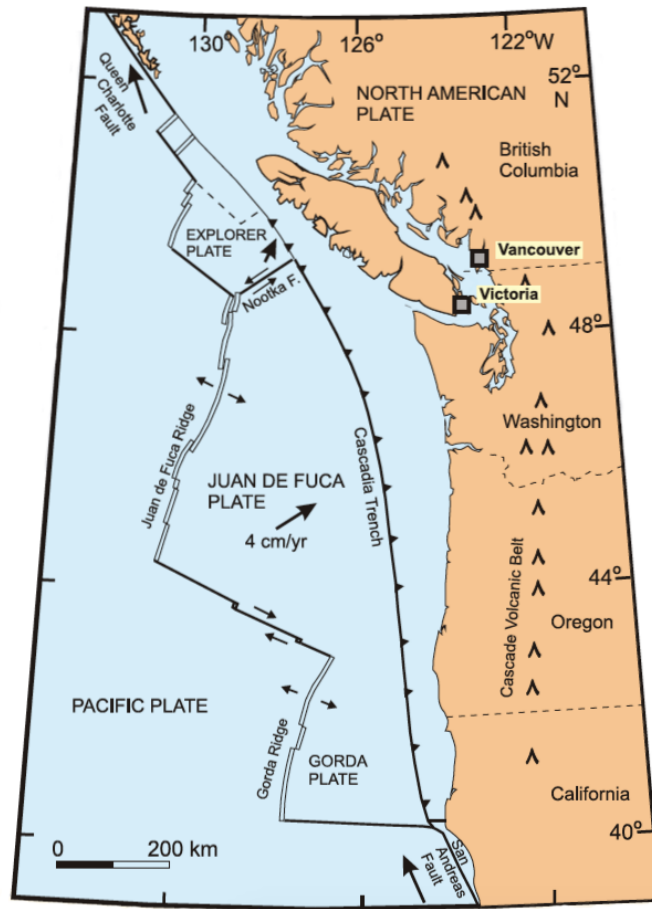


Figure 2.4 Cascadia Subduction Zone (CSZ; Geological Survey of Canada 2011)

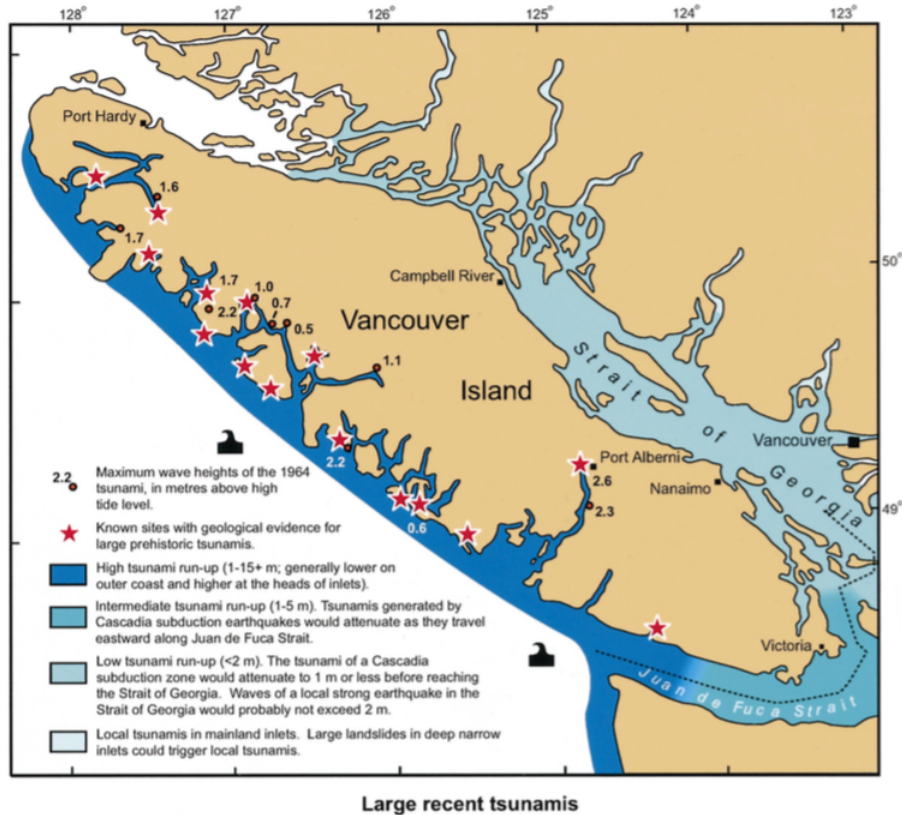


Figure 2.5 Location of geological evidence of past earthquake and tsunamis from the Cascadia Subduction Zone (Clague, et al. 2000)

The CSZ is estimated to rupture at an approximate interval of 500 years, with a range between 300 and 2000 years, for events of  $M_w$  8 or higher (Atwater, et al. 1995, McCaffrey and Goldfinger 1995, Clague 1997, Clague, et al. 2000). The evidence of the seismic record dates back as far as 7,500 years in some areas (Ollerhead, et al. 2001). The evidence suggests that the latest events occurred approximately 300 years ago (Atwater, et al. 1995, Clague 1997, Clague, et al. 2000). This event is recorded in Japanese history, which cites a tsunami of remote origin, as no ground shaking was felt, in January 1700 A.D. (Satake, et al. 1996, 2003). This coincides with the description in oral history of North American natives living on Vancouver Island, of a large shaking event and subsequent tsunami in the winter (McMillan and Hutchinson 2002). As no other evidence of an earthquake occurring in the Pacific around this time exists, these two events are believed to be one and the same. The geological evidence of the land subsidence suggests an event of  $M_w$  9 occurred (Atwater, et al. 1995, Clague 1997), supported by numerical simulations performed by Satake, Wang and Atwater (2003) of the elastic dislocation model of the fault and subsequent tsunami propagation. The authors found that the most likely event was an earthquake of  $M_w$  9.0 with a co-seismic slip of 19 m (vertical displacement).

From the geological evidence, the most vulnerable areas are on the outer coast and inlets of Vancouver Island (Clague, et al. 2000, Leonard, et al. 2013). More precisely, the outer coast is

estimated to have a potential run-up of 5 m and the bays and inlets have potential run-ups exceeding 15 m (Figure 2.5). Port Alberni, at the head of an inlet, is estimated to have run-ups exceeding 16 m (Ng, et al. 1990, Clague et al. 2000). A tsunami is expected to attenuate while passing through the Strait of Juan de Fuca, with estimated run-ups between 1 m and 5 m. The lowest hazard is in the Strait of Georgia, where run-ups are estimated to be below 2 m, but more likely around 1 m (Clague, et al. 2000). This is supported by the lack of geological evidence of tsunamis found in the low lands of Richmond and Delta, suggesting that the tsunami waves had a significantly lesser impact in this area (Clague, et al. 2005). This is further supported by the fact that native oral traditions of the area only include earthquake rites and not tsunami rites (McMillan and Hutchinson 2002).

Local earthquake tsunamis could also be generated from the Explorer-North America plate boundary or the Queen Charlotte faults, but these sources are currently poorly understood (Leonard, et al. 2013). Wave heights of 7.5 cm and 10.8 cm were recorded in Bamfield and Tofino in 2004 from a tsunami generated from a  $M_w$  6.6 earthquake originating from the Explorer-North America boundary (Rabinovich, et al. 2003). Additionally, three tsunamis have been recorded originating from the Queen Charlotte fault. The first was in 1949, which was the largest earthquake recorded in Canada, having a  $M_w$  of 8.1. Waves were recorded in Sitka, Alaska, with a height of 7.5 cm but are suspected to have been caused by landslides triggered by the earthquake, as the fault is primarily strike-slip – horizontal movement instead of vertical (Soloviev and Go 1984). In 2001 a smaller earthquake,  $M_w$  6.1, caused wave heights between 11.3 cm and 22.7 cm on the outer coast of Vancouver Island (Rabinovich et al. 2008). Finally, in 2012 a  $M_w$  7.7 subduction earthquake caused run-ups between 3 m and 13 m in Haida Gwaii (Leonard and Bednarski 2014). This was the first time a thrust movement was recorded in this fault, which is primarily strike-slip. Fortunately, the tsunami affected the unpopulated region to the West of Haida Gwaii.

Local crustal earthquakes could also produce a tsunami within inland waterways or fiords (Clague, et al. 2000, Leonard, et al. 2013). Such an earthquake occurred in 1946 of  $M_w$  7.3 in central Vancouver Island, which triggered landslides and submarine failures creating a tsunami with maximum wave height between 1 m and 2 m in the Strait of Georgia (Murty 1977, Hasegawa and Rogers 1978, Mosher, et al. 2004).

## **2.2.2 Historical Tsunamis from Distant Sources**

Far-field tsunamis are more frequent – 11 of 16 recorded tsunamis between 1964 and 2007 were far-field – but generally less damaging (Stephenson and Rabinovich 2009, Leonard, et al. 2013). Two earthquake tsunamis have originated from the Aleutian Trench in recent history. The first, in 1946, was produced by a  $M_w$  8.6 earthquake. The subsequent tsunami completely destroyed the Scotch Cap Lighthouse on Unimak Island in Alaska, but did not cause any damage in Canada

(Bodle 1946). The second, however, was the most damaging tsunami in Canada. The tsunami from the Great Alaska Earthquake of 1964 ( $M_w$  9.2) killed 139 individuals in Alaska. The tsunami reached the Canadian coast 4 hours later (Hensen, et al. 1966, Plafker 1969, Lander 1996, Wigen and White 1964, Clague, et al. 2000, Stephenson, et al. 2010). The tsunami had the greatest effect within inlets and not on the main coast. Port Alberni incurred the most damage with 260 damaged houses, including 60 extensively damaged and 2 were that were swept into the ocean (Ng, et al. 1990). The tsunami waves were amplified in Port Alberni due to the high tides and the combined effects of the topographic amplification in Barkley Sound, and the resonance magnification in the Alberni inlet (Wigen and White 1964, Thomson 1981, Clague, et al. 2000, Clague, et al. 2003). Ng, et al. (1990) found a magnification factor of 3 to 4 between the entrance of Barkley Sound and the head of the Alberni inlet. The maximum run-up in Port Alberni was 10.3 m (UMA Engineering LTD. 1992), approximately 6 m less than the estimated run-up from the 1700 event (Figure 2.6). The village of Hot Spring Cove was also destroyed and houses were swept out of their foundation in Zeballos. The total damage cost in Canada was \$10 million in 1964 dollars (Jones 1992). The highest wave heights were recorded in North Haida Gwaii of 8 m, and 2.4 m waves were recorded in Tofino.

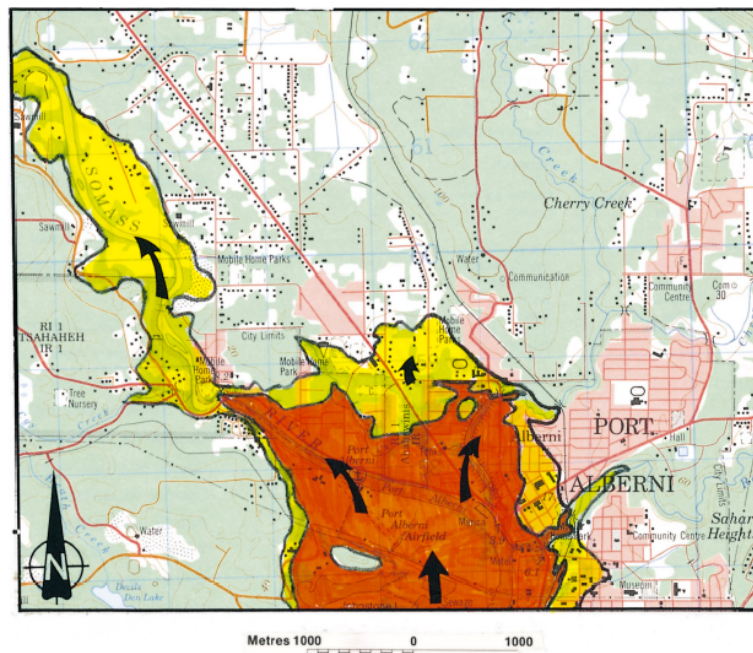


Figure 2.6 Inundated area in Port Alberni from the 1700 Cascadia Subduction Zone tsunami (yellow and red) with a run-up of 16 m, and 1964 Great Alaska Earthquake and Tsunami (red) with a run-up of 10.3 m (Clague and Bobrosky 1999)

A tsunami caused some damaged in Vancouver Island and in Haida Gwaii in 1960 from an  $M_w$  9.5 earthquake originating from Chile. Wave heights were recorded at 1.3 m in Tofino (Wigen 1960, Leonard, et al. 2013). The recorded wave heights were 1.1 m shorter than those of the

1964 tsunami because of the longer distance travelled and the angle of arrival. Distant tsunamis can also originate from Japan, Kuril Island, Mexico, Indonesia and Kamchatka (Leonard, et al. 2013).

### 2.2.3 Tsunami Modeling of Canadian Shores

Tsunami modeling of Canadian shores was first accomplished by Hebenstreit and Murty (1989) using linear shallow-water model and a CSZ north rupture scenario extending from Winter Harbour in North Vancouver Island to northern Washington state, with a sea floor displacement of 18 m. The rupture was further north by approximately 100 km than modern CSZ rupture scenarios used (Satake, et al. 2003, Cherniawasky, et al. 2007). Only the coastline of Vancouver Island was included, where wave heights were found between 2 m and 15 m (Figure 2.7).

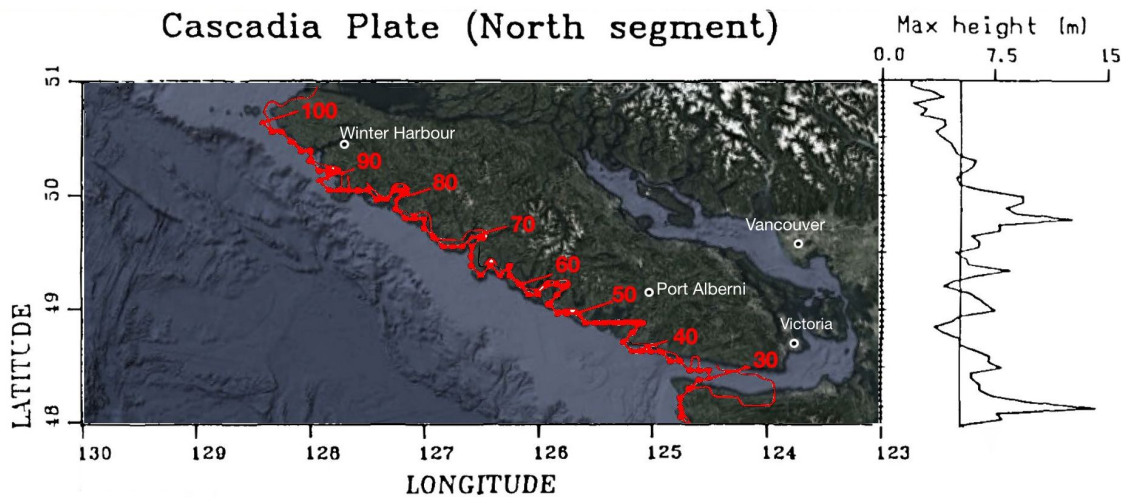


Figure 2.7 Modeled maximum tsunami wave height (m) along the outer coast of Vancouver Island from a North Cascadia Subduction Zone rupture adapted from (Hebenstreit and Murty 1989)

Ng, et al. (1990a) also modelled a CSZ north rupture of  $M_w$  8.2-8.5 using a non-linear shallow-water wave model. They found that the first waves would arrive in Victoria and Vancouver 2 hours and 4 hours after the earthquake respectively. Run-ups of 16 m were found for Port Alberni. The authors concluded that there is a significant loss of energy in the the Strait of Juan de Fuca and Georgia, which results in much smaller run-ups in Victoria (2 m). The tides were not considered, but the authors concluded that since they can vary as much as 5 m in some locations, superimposing them with the tsunami could have devastating effects. Further examination by the authors (Ng, et al. 1990b) found that waves can be amplified with a factor of 3 at the head of the Alberni Inlet compared to the Barkley Sound entrance. They found maximum wave amplitudes of 1 m in Vancouver and Queen Charlotte, 2 m in Tofino, and 7 m in Port Alberni. The outer coast of Vancouver Island was found to be the most affected.

Whitmore (1993), using the ATFM model, computed three CSZ earthquake of  $M_w$  between 7.8 and 8.8. The maximum wave amplitudes of 0.84 m and 1.41 m were found in Cape Scott and San Josef Bay in northern Vancouver Island, and 3.91 m in Tofino. The latter is 1.91 m larger than the result found from Ng, et al. (1990b).

Cherniawasky, et al. (2007), using MOST-3, simulated the long-narrow, short-north and short-south CSZ rupture scenarios described by Satake, et al. (2003). Only the offshore wave propagation was computed. The effects of tides and currents were not included. The model was limited to the South of Vancouver Island and the Strait of Juan de Fuca and Georgia. Nested grids with three resolution were used. The coarsest grid (1530 m by 1100 m) and medium grid (245 m by 185 m) was used in all experiments to propagate the tsunami waves trans-oceanically. Finer grids were used in Esquimalt and Victoria harbour (6.6 m by 10.1 m), and Uclulet Inlet (10.0 m by 10.3 m).

Peak-to-through wave amplitude of 6.0 m was found along Vancouver Island using the medium resolution grids. A localized maximum of 13.9 m was found to the West of the entrance of Barkley Sound, and 11.6 m near Tofino. Wave amplitudes of 6 to 10 m were found near Ucluelet, and decrease to less than 4 m and 3 m in the Juan de Fuca and Georgia Strait respectively.

Wave amplitudes between 6 m and 9 m were found on the Ucluth peninsula with the highest resolution grid. An isolated maximum of 15.7 m was observed in an adjacent bay. Currents in the Uclulet inlet varied between 1 m/s at the entrance to 10 m/s at the head. Maximum amplitudes of 4 m were observed in the Esquimalt and Victoria Harbours at the highest resolution. Maximum wave elevation in the harbours were smaller than on the West Coast of Vancouver Island by a factor of 2-3, and were 3-5 times larger inside the harbours than outside. Maximum currents of 15 m/s were found in narrow inlets.

Fine, et al. (2008) MOST-3 simulated two models to study the resonant characteristics in Barkley Sound and the Alberni inlet, which are suspected to have caused the large waves during the 1964 tsunami. First, an open boundary model with stationary autoregressive signal was used to simulate the background noise, and second a tsunami wave from a CSZ earthquake scenario of a southern rupture was simulated. The authors showed that wave amplification in the Alberni inlet is due to the frequency response of the area from the coupled oscillation in Barkley Sound-Alberni Inlet system and resonance magnification from the narrowing passage.

Finally, Xie, et al. (2012) computed the largest credible CSZ earthquake scenario with MIRONE. The earthquake had an  $M_w$  9.0 and a coseismic slip of 18 m, similarly to the 1700 event. Because of the high wave amplitude, with a maximum of 12 m, the authors concluded that there is a high

hazard for low-laying areas on Vancouver Island. The model did not consider diffraction near the shoreline, damping and energy dissipation from bottom friction.

## **2.1 Community Vulnerability Assessment**

Risk is defined as the product of the hazard with the vulnerability (Clague et al. 2003, IM-ELS 2006). The hazard is described by its inland inundation, using the run-up,  $R$ , or length of the inundation area,  $L_R$ . The vulnerability is the description of the potential societal loss that is threatened by a particular threat, such as be physical, social or economic. Wood and Schmidlein (2013) describes vulnerability assessment as:

[...] an attempt to quantify and qualify the conditions that create an environment in which the potential for societal losses is created or amplified. This information can be used to develop, target, and prioritize actions to reduce or manage these vulnerabilities [...]

A vulnerability assessment includes assessment of the evacuation capability, as individuals that do not have sufficient time to reach safety would then be exposed to the hazard and be at risk. Important factors in evacuation are the initiation time and mode of transportation of the evacuation. The public's reaction time to initiate evacuation will vary on the warning dissemination, and the public response. The latter is difficult to quantify as they are socially and psychologically dependent (Post, et al. 2009). Education, social and physical cues have been found to increase the evacuation response of individuals (Sorensen 2000).

Tsunami evacuation can be performed by vehicle or by foot. BC Earthquake Alliance Society (2016) and NOAA (2016d) recommends evacuating by car only if absolutely necessary. Roads may not be usable from subsidence, cracking, sand boils or downed power lines from the preceding earthquake (Wood and Schmidlein 2012, NOAA 2016d). Additionally, areas where the tsunami arrival time is small may not have enough time for vehicle evacuation as congestion is likely to occur due to the sudden influx of cars on the roads going in the same direction (Church and Sexton 2002). This was observed in Hawaii in 2012, where heavy traffic was caused by evacuees leaving by car and vehicle evacuation was deemed to be a non-viable option (Santos, et al. 2016). Additionally, pedestrian evacuation reduces the loads on the roads, leaving them open for emergency response. Evacuation capability can be by modelled static or dynamic approaches.

### **2.2.4 Static Evacuation Modeling**

Static models compute maps demonstrating vulnerability distribution or required time to safety using GIS. Simpler models compute the time to safety by finding the shortest distance of any point in the hazard zone to safety using approaches such as the Euclidean distance (Wood and Schmidlein 2012). Assuming that individuals will travel along roads, the shortest distance can

be computed by constraining the travel path to road networks by using network analysis tools (Cova and Church 1997, Wood and Schmidtlein 2012). These models omit the fact that land cover and slope can alter the speed at which individuals can evacuate (Laghi, et al. 2006).

Isotropic path-distance models account for the physical terrain thus computing the shortest path to safety in terms of time and energy expenditure (IM-ELS 2006, Laghi, et al. 2006, Post, et al. 2009, Wood and Schmidtlein 2012). The shortest path is computed by finding the difficulty of travelling on the terrain as a function of the ground type and slope, represented as a cost surface. The cost surface uses a speed conservation value, SCV (IM-ELS 2006, Laghi, et al. 2006), which is the percentage of the maximum travelling speed that would occur for the type of land cover and slope. The slope directionality is not considered, thus, the same value is assigned for both uphill and downhill travel. Optimal paths are then found by finding the least-costly path in terms of time by finding the product of the travel velocity, SCV and length of each cell within the model. The building density, population density, age and gender of the population and congestion factors based on the width of the roads can also be used in the SCV (Post, et al. 2009). Anisotropic path-distance models use a similar approach but the SCV considers the directionality of the slope. Such models have been used to compute accessibility to wilderness (Jobe and White 2009), pedestrian evacuation for wildfire hazard (Anguelova, et al. 2010) and for tsunami evacuation (Wood and Schmidtlein 2012, 2013).

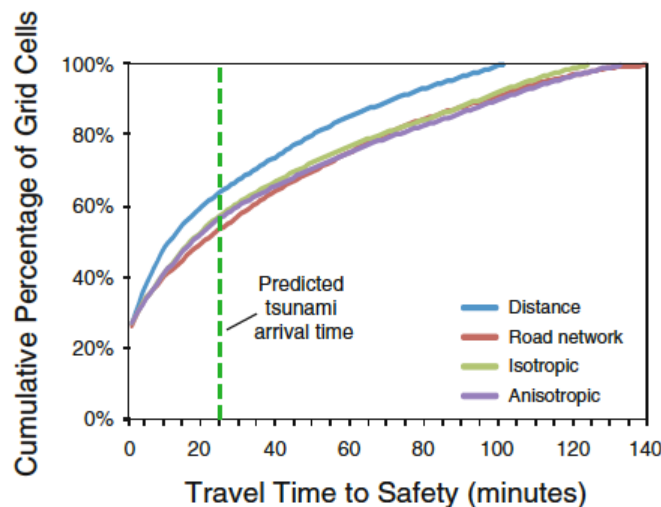


Figure 2.8 Evacuation modeling approaches comparison as a function of cumulative percentage of grid cells to travel time to safety (Wood and Schmidtlein 2012)

The time to safety computed with anisotropic path-distance modeling has been found to not be very sensitive to SCV used (Schmidtlein and Wood 2015). Wood and Schmidtlein (2012) also found that the resolution of the elevation data greatly impacts the travel time. Using an elevation model of 10 m resolution was found to underestimate the travel time by 35-100% from a 1 m resolution model. The same authors also found that the distance-only model and isotropic model

underestimate the average travel time by 30% and 4%, respectively, compared to the anisotropic model for a pedestrian evacuation scenario in Long Beach Peninsula, Washington (Figure 2.8). More precisely, the distance-only approach had no difference for 28% of the model, underestimated by 1 to 10 min for 32% and underestimated by 50 min or more for 1% of the study area. On the other hand, the same study found that the distance-only model using road network only overestimated the maximum time to safety by 5% (Figure 2.8). Overestimation is preferred over underestimation, as underestimated travel time could potentially represent areas at risk as safe and endanger the population.

### **2.2.5 Dynamic Evacuation Modeling**

Dynamic evacuation modeling can be achieved through agent-based models, such as BC Hydro (Johnstone and Lence 2009, 2012) or integrated simulators (Katada, et al. 2006). Agent-based models compute the movement of individuals in a scenario using “agents” that follow a set of preprogrammed rules to simulate social norms and choices they must make while evacuating, such as whether or not to evacuate, evacuate in-situ (move to higher storeys) or change route if congestion is met along the way. Agent-based models can integrate static modeling results to dictate the shortest or optimal routes (Leon et March 2016). Vehicle and pedestrian movement are simulated through traffic streams models (Johnstone and Lence 2009, 2012). Dynamic costs, such as route capacity, velocity decrease from crowding, fatigue and road congestion can be implemented (Leon and March 2016). Some models integrate tsunami hazard modeling and model structural loss and casualties by comparing the strength of objects and individuals with the hazard forces using inundation depth, depth velocity product and force from entrained debris (Jonkman, et al. 2002, Kelman and Spence 2004, Johnstone and Lence 2009, 2012)

Agent-based models are best for specific tsunami scenarios, as they require an in-depth knowledge of the variables implemented. The population distribution must be precisely estimated to dictate the locations of the agents. Dynamic models evaluate the evacuation capacity with the effects of the season or time of day, failure in the transport system due to a preceding earthquake, structural failure and vulnerable population (Katada, et al. 2006, Leonard and Bednarski 2014, Leon and March 2016).

Agent-based modeling was performed for the community of Ucluelet in Vancouver Island (Johnstone and Lence 2012). The tsunami propagation was implemented within the evacuation model to simulate the temporal inland hazard. Multiple run-ups were found within the community, ranging from 10 m to 20 m. The population was estimated using both residents and tourists. Four population distribution scenarios were used: winter-night, winter-day, summer-night and summer-day. The projected casualties range from 237 (winter-night) to 1149 (summer-day), representing 15.7% to 21.8% of the total population.

## 2.3 Mitigation Techniques

Tsunamis cannot be prevented, but using mitigation techniques can reduce societal and economic impacts. Non-structural mitigation techniques can include restricting land-use, to limiting the number of buildings and individuals within the potential hazard zone using zoning and relocation of home owners by property acquisition (Clague, et al. 2003, Johnstone and Lence 2012). Preventive urban planning can also play an important role by limiting high-density neighbourhoods in the hazard area, and planning for larger roads to act as efficient evacuation routes (Leon et March 2016). Mitigation can also be done in terms of increasing the emergency preparedness with educational and training programs (Clague, et al. 2003, FEMA P-646). External features like signage – indicating tsunami hazard zones and evacuation routes – and outdoor sirens can increase hazard awareness and evacuation efficiency (Wood and Schmidlein 2013).

Structural mitigation can also be used to lessen or prevent the tsunami inundation using dykes, breakwaters and seawalls (Burcharth and Hughes 2003, Mikami, et al. 2015). Barriers need to be built high enough to prevent overtopping waves. They can be very expensive and thus only economically feasible in areas with large populations. Barriers can also lessen the tsunami energy by reflecting part of the waves but typically offer limited protection (Clague, et al. 2003). It is also important that these structures are able to withstand the preceding earthquake (FEMA P-646, ASCE 7-16). For example, many barriers against tsunamis in Japan during the 2011 Tohoku tsunami were severely damaged and did not prevent inundation (Mikami, et al. 2015).

Vertical evacuation shelters can be implemented to provide additional safe areas within the inundation zone where individuals are at-risk due to insufficient time to travel to safety. Vertical shelters can take the form of engineered earthen mounds, and single- or multi-purpose tsunami resistant facilities (Clague, et al. 2003, FEMA P-646). Structures need to elevate evacuees above the inundation levels. Additionally, they need to resist strong earthquake effects with a low level of damage to be able to resist the subsequent tsunami forces (ASCE 7-16). Some residential apartment buildings are used in Japan as multi-purpose vertical evacuation structures by using the roof as evacuation space (FEMA P-646). The first vertical evacuation structure in the United States is the Ocosta Elementary School near Newport, Washington. The roof of the gym structure has a capacity of thousands of people and is a refuge site for both the school children and other evacuees from the community (Gonzales, et al. 2013).

## 2.4 Discussion

The literature review had three primary goals. First to determine the Canadian Pacific coast tsunami hazard and to review methods of quantitatively determine inland tsunami hazard.

Second, to provide a basis and methods for vulnerability assessment on a community level. Finally, to outline the gaps in knowledge in the Canadian tsunami hazard and consequent research needs.

The following points are of important consideration for the tsunami hazard:

- Tsunami waves propagate in deep ocean as linear shallow-water waves. Amplification can play an important role in increasing the wave heights, mostly in inlets and bays. The tsunami inland hazard is measured with the run-up,  $R$ , which is the vertical elevation at the maximum horizontal distance of the inundation. The run-up can vary drastically along the coast, as it is dependent on the local physical on and offshore characteristics.
- The run-up can be empirically computed using many relationships derived from tsunami wave amplitude, the onshore and offshore slopes, roughness or friction coefficients. The run-up can also be estimated as twice the tsunami wave height at the shoreline.
- The probability of damaging tsunamis on the Canadian West coast with run-up  $\geq 1.5$  m is 40-80% in 50 years, and the probability of tsunamis with significant damage potential with run-ups  $\geq 3.0$  m is 10-30%.
- The greatest tsunami threat to the Canadian Pacific coast is from a local source: the CSZ. This fault's seismic history has been reconstructed using geological evidence found throughout Vancouver Island, Oregon and Washington. It has an average rupture interval of 500 years, with the latest occurrence in 1700. Potential run-ups from faults range from over 15 m on the outer coast of Vancouver Island to 1 m in the Strait of Georgia.
- Local earthquake tsunamis could also originate from the Explorer-North America boundary or the Queen Charlotte fault, but these sources are still misunderstood.
- A distant tsunami from the Aleutian trench in 1964 was the most damaging in Canada. The tsunami had a maximum run-up of 10.3 m in Port Alberni. Maximum wave heights were recorded as 8 m and 2.4 m in North Haida Gwaii and Tofino respectively. Distant tsunamis can originate from around the Pacific Ocean, but are typically less damaging than those from local sources.
- Numerical models agree with the geological evidence of CSZ tsunamis that the greatest risk is to the outer coast of Vancouver Island and that waves attenuate in the Strait of Juan de Fuca and Georgia. Models predict a wave height between 1 m and 3 m in the Strait of Georgia, 1 m to 4 m in the Strait of Juan de Fuca and between 2 m and 15 m on the outer coast of Vancouver Island.
- Significant amplification occurs in Barkley Sound and Alberni inlet, making Port Alberni particularly at risk from tsunamis.

The following points are of important consideration for the vulnerability assessment on a community level:

- Evacuation capability can be modelled using static or dynamic approaches. Static modeling uses GIS to evaluate the time required to reach safety from all locations within the hazard zone using approaches such as distance-only (Euclidean distance or road networks) and isotropic or anisotropic path-distance.
- The distance-only model and isotropic path-distance models were found to underestimate the travel to safety time from the anisotropic path-distance modeling by 30% and 4%, respectively. Using an elevation model with a resolution of 10 m instead of 1 m was also found to drastically underestimate the time to safety by 35-100%.
- Agent-based models can be used to dynamically model the evacuation capabilities and can be integrated with tsunami hazard models to compute structural and life losses. Such models require precise inputs of the population distribution and built environment.
- Mitigation techniques can take the form of non-structural solutions such as restricted land-use in inundation zones, increased emergency preparedness with educational programs, or external evacuation features like outdoor sirens and signage.
- Vertical evacuation structures can be implemented to reduce potential loss of life in areas where there is insufficient time to reach safety. The ASCE 7-16 standard provides new design guidelines for the construction of such structures.

From the literature review the following gaps in knowledge are outlined:

- Numerical models have focused their studies on the outer coast of Vancouver Island the Juan de Fuca and Georgia Strait. Thus, the wave amplitude North of Vancouver Island on the main coast and in Haida Gwaii is uncertain.
- As recent studies using better resolution grids have focused on the wave propagation, the inland propagation of tsunami waves is unknown outside of the Juan de Fuca and Georgia Strait.
- No vulnerability assessment of evacuation capabilities has been performed outside of Ucluelet.

# Chapter 3. Study Area: Canadian West Coast

The Canadian coast is the longest in the world with over 200,000 km, and vast stretches which are sparsely inhabited. Surrounded by three oceans, the Atlantic, the Arctic and the Pacific, coastline characteristics vary drastically by location and includes sandy or gravel beaches, fjords and deltas. The Pacific Ocean borders entirely Canada’s west coast, bordering only a single province, British Columbia (BC).

The tsunami risk in this province, in terms of its exposure vulnerability and susceptibility to loss of life, is presented in the following sections. Tsunami warning capabilities and emergency preparedness are explored to better understand the exposure vulnerability while the population distribution within the province is investigated to assess the susceptibility of loss of life in the case of an extreme tsunami event.

## 3.1 Tsunami Warnings Capabilities and Emergency Preparedness

Earthquakes and tsunamis cannot be predicted. Depending on the source of the tsunami – whether it is local or distant – the first wave’s arrival time may range from minutes to hours. Such short warning times make an effective warning system crucial, particularly as “it is the trigger for all of the subsequent activities that will occur during the emergency period, including response, rescue, relief and recovery.” (Anderson, et al. 2016)

Tsunami warning systems and early detection in North America were put in place following the devastating 1964 Alaskan earthquake and tsunami. No casualties occurred in Port Alberni, which was the most affected city by this event in Canada, because residents took it upon themselves to warn fellow neighbours and evacuate to higher ground following the first wave, which arrived near midnight (Alerni Valley Museum 2016). The current tsunami warning system in British Columbia has 3 main stages (Figure 3.1): detection, emergency management, and the public response. These procedures involve a variety of partners, ranging from international, federal, and provincial agencies, as well as a well-informed public.

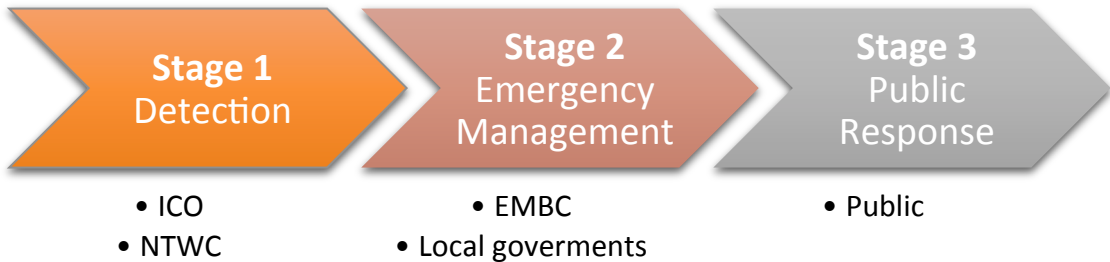


Figure 3.1 Components of the tsunami warning system of British Columbia, adapted from Anderson (2016).

### 3.1.1 Tsunami Detection

Early detection of tsunami events in the Pacific Ocean is internationally coordinated through the Intergovernmental Oceanographic Commission (IOC) of UNESCO, led by the National Oceanic and Atmospheric Administration (NOAA) in the United States. There are two tsunami warning centers, each with a specific area of responsibility: the National Tsunami Warning Center (NTWC) in Palmer, Alaska, monitors the US west coast, Alaska, Puerto Rico, the US Virgin Islands, and Canada, while the Pacific Tsunami Warning Center (PTWC) in Honolulu, Hawaii, services Hawaii, most Pacific nations and Island States, countries in the Caribbean Sea, and some in the Indian Ocean.

Earthquakes and subsequent tsunamis are detected and the ensuing inundation is predicted using seismic and sea level data. Seismic data is the first to be collected, as wave-travelling velocity is nearly 100 times greater than a tsunami wave: seismic waves travel with a velocity of 14,000 km/h compared to the average celerity of a tsunami of 500-1,000 km/h in deep water conditions. The seismic parameters (epicenter location and magnitude) of the triggering earthquake event are used to estimate the initial ground floor vertical displacement and, thus, the initial sea surface displacement.

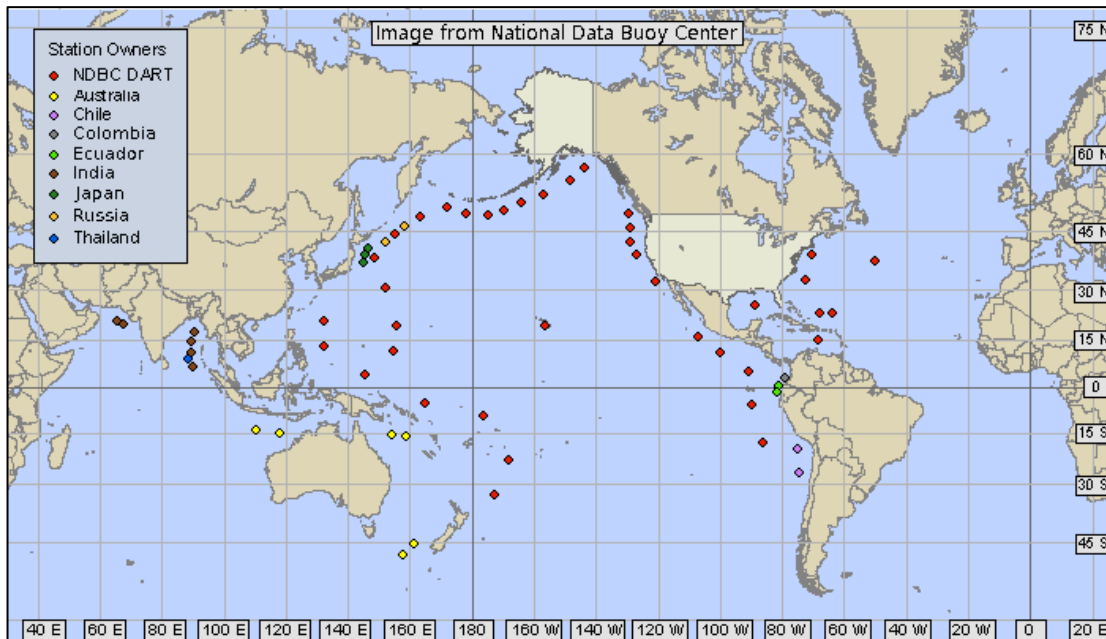


Figure 3.2 Locations of DART buoy stations across the Pacific and Indian Oceans (NOAA 2016c).

Coastal boundaries likely to be affected by the tsunami inundation are predicted using pre-computed scenarios with similar parameters in NOAA's forecast database, which were computed using the MOST (Method of Splitting Tsunami) model (Titov and Gonzalez 1997). Sea level data from tidal gauges and buoys are then used to confirm the occurrence of a tsunami event and

refine the initial tsunami parameters. NOAA currently has 39 buoys relaying sea level information in real-time as part of their Deep-ocean Assessment and Reporting of Tsunami (DART) program. These buoys are located throughout the world in areas that have previously been affected by destructive tsunamis (Figure 3.2). Sea level heights are transmitted to the PTWC and NTWC via satellite from moored surface buoys, which are acoustically linked to the seafloor bottom pressure recorder (BPR). The NTWC's goal is to issue tsunami warnings within 5 minutes of an earthquake occurring, with its average response time being 3 minutes (Anderson, et al. 2016).



Figure 3.3 Tsunami Notification Zones of British Columbia (PreparedBC 2016).

Canadian and BC officials receive alert levels, earthquake parameters, predicted inundated areas, and forecasted and observed tsunami parameters from the NTWC based on three predefined locations: the Alaskan and BC border, the north tip of Vancouver Island, and the BC and Washington State border, indicated as the white square text window in Figure 3.3. Emergency Management British Columbia (EMBC), under the auspice of the provincial Ministry of Justice,

is responsible for coordination and tsunami message dissemination in the province. It reassesses the tsunami information provided by NOAA to ascertain the danger for the BC coastline specifically, based on 5 distinct Tsunami Notification Zones (TNZ) (Figure 3.3). These zones have been geographically devised to take into account the different risk levels associated with their location for different tsunami hazards (local and distant). For example, the Juan de Fuca and Georgia straits are partly sheltered and have therefore a lower risk factor than the exposed coast on Vancouver Island for a tsunami event generated in the Pacific Ocean.

### 3.1.2 Tsunami Warning Communication

The Provincial Emergency Notification System (PENS) is used to broadcast the NTWC and BC-specific alerts to individuals within the province. This system disseminates the information using direct phone calls and interactive calls, email, fax, television, text messages, social media, weather radio, and outdoor sirens. Social media platforms communicate in real time and are the quickest method of dispensing information. PENS primary social media platform is Twitter, under the following handles: EMBC (@EmergencyInfoBC) and NTWC (@NWS\_NTWC).

The tsunami message broadcast typically includes a brief description of the seismic event (location and magnitude), whether a tsunami has been generated, the TNZs affected with an associated alert level (Figure 3.4), and the recommended actions. As new information is received and assessed, the broadcast messages may change, including a change in the alert level. Evacuation is only suggested at the “warning” alert level.






		<i>ACTION</i>
 <b>WARNING</b>	FLOOD WAVE POSSIBLE	FULL EVACUATION SUGGESTED
 <b>ADVISORY</b>	STRONG CURRENTS LIKELY	STAY AWAY FROM THE SHORE
 <b>WATCH</b>	DANGER LEVEL NOT YET KNOWN	STAY ALERT FOR MORE INFORMATION
 <b>INFORMATION STATEMENT</b>	MINOR WAVES AT MOST	NO ACTION SUGGESTED
 <b>CANCELLATION</b>	TIDAL GAUGES SHOW NO WAVE ACTIVITY	CONFIRM SAFETY OF LOCAL AREAS

Figure 3.4 BC tsunami alert level (PreparedBC 2016).

Local government, including local authorities and First Nations communities, are responsible for their jurisdiction’s emergency planning, which includes ensuring that key emergency responders (fire department, first responders, police department, etc.) are notified and that the general and local tsunami information reaches their residents. Additional local information might include

evacuation orders, evacuation procedures, and safe reception locations. Because tsunami waves may arrive before without warning, local authorities in high-risk areas may activate their tsunami plans before being contacted by EMBC in the event of strong ground shaking. The federal ministry of Aboriginal Affairs and Northern Development Canada (AANDC) is an important liaison between the EMBC and BC's First Nations communities.

Outdoor warning systems, such as sirens, are a useful and quick method of alerting those in outdoor and isolated locations such as beaches and parks. They are loud enough to wake resident at night, they do not discriminate amongst recipients, and they can be used to diffuse a wide range of messages. The following BC communities currently use sirens: Port Alberni, Tofino, Tseshah First Nation, Zeballos, Gitga'at First Nation, Bella Bella, Bamfield, and the Village of Queen Charlotte. No uniform standard currently exists in Canada to regulate tsunami sirens and inconsistencies between communities may exist.

### **3.1.3 Tsunami Emergency Preparedness**

BC's Emergency Program Act of 1996 dictates the roles and responsibilities of the province's various levels of government in managing disasters and emergencies. Local authorities are responsible at all times for the direction and control of local emergency responses, with a local authority being defined as the municipal council for a municipality, an electoral area for regional districts, or the superintendent in a national park. Communities at-risk should include in their tsunami emergency plans an identifiable tsunami hazard zone (with in-situ delineator marks and map), a detailed evacuation route, and community safe zones at elevations above any possible run-ups. A survey of 86 communities revealed that only 52% and 61% had in tsunami action plans and emergency communication plans, respectively, in place (Anderson 2016).

In the event of a strong ground motion, the primary directive to individuals from EMBC and federal emergency authorities is to "drop, cover and hold on" (PreparedBC 2016). In coastal areas prone to tsunamis, there is an additional directive of "then move to higher ground". Pedestrian evacuation is primarily recommended unless impossible. This leaves the roads clear for emergency personnel and for individuals with severe mobility impairment that may not be able to evacuate my foot (PreparedBC 2016). Individuals and families should also have household emergency plans and a grab-and-go bag (or 72-hour emergency kit), which should contain enough water, food, clothing, and other emergency supplies to be self-sufficient for three days and be located in an easy to grab location within the household.

Disaster education has been effective in increasing population readiness responses to a disaster (Tanaka 2005; Faupel, Kelley and Petee 1992). Education should be an integral part of any community's disaster planning. The Great British Columbia Shake Out is a new province-wide yearly earthquake drill. Residents, organizations, businesses, and governmental agencies can

voluntarily participate. The event encourages community-wide participation to build neighbourhood resilience. In addition to the drill, educational booths and activities are organized to increase the reach of public education efforts. The exercise also promotes and practices inter-agency emergency response co-operation, as well as providing tsunami readiness guidance and drills for coastal communities. Finally, many communities organize educational events during the first week of May, also designated as the federal Emergency Preparedness (EP) week. While schools are recommended to hold a minimum of three earthquake drills during the school year (Ministry of Education 2015), no specific recommendations are made for tsunami drills.

Tsunami signage indicating hazard zones and evacuation routes are present in some communities, such as Tofino, Port Alberni, Port Renfrew, and Ucluelet; however, these signs have caused displeasure from some residents, believing they lower property values (Moneo 2007).

### **3.2 Tsunami Warning Zones Overview**

An area's risk level is determined by hazard and vulnerability. Tsunami vulnerability is assessed by exposure level, such as the run-up and tsunami arrival time, and susceptibility of loss, such as the at-risk population. The BC coast is separated in 5 distinct TNZs (Figure 3.3) representing different risks based on the maximum expected run-up level and arrival. Each zone includes all islands and inlets within its boundary.

- Zone A is the northern-most and includes the Haida Gwaii archipelago, which is directly adjacent of the Queen Charlotte fault. This zone also includes a small portion of the mainland coast, from the Alaska border to the southern tip of Banks Islands.
- Zone B continues south from the southern tip of Zone A on the mainland coast, with its limit at the convergence point of Tsitika River and the Johnstone Strait. Also included is the eastern portion of Vancouver Island directly facing Zone B, with its western limit at Shushartie Bay.
- Zone C encompasses the remainder of the north coast of Vancouver Island and the outer west coast to Port Renfrew.
- Zone D encompasses the south of Vancouver Island in the Juan de Fuca Strait, starting at Port Renfrew to the north of the Saanich Peninsula, but excludes the Saanich Inlet. It also includes Victoria and the capital region.
- Zone E includes the Saanich Inlet and the remainder of Vancouver Island, circling back to the Johnstone Strait, and all Islands within the Georgia Basin. The mainland facing Vancouver Island is also part of Zone E, including the greater Vancouver region.

### 3.2.1 Planning Run-Up Level and Arrival Time

Run-up values are provided to emergency managers for guidance by the Provincial Emergency Program (PEP) and EMBC to determine evacuation areas, evacuations routes, and safe areas for their tsunami emergency plans (Table 3.1). The planning levels are based on the most accurate scientific data as of 2006 for the maximum expected wave height and represent the worst-case scenario for either a distant or local tsunami. The levels are measured for the normal highest tide and calculated as the run-up equal to twice the wave height times the safety factor. This method is not typically used to calculate run-up, as this can vary drastically based on the local nearshore bathymetry and inland topography. A value of 1 m is added to Zone C for the expected subsidence of the area due to a CSZ earthquake.

Table 3.1 Recommended planning tsunami run-up levels by tsunami notification zone (Anderson, et al. 2016)

Zone	Wave height [m]	Run-up (x2.0) [m]	Safety factor (x1.5) [m]	Subsidence [m]	Planning level [m]
A	2.0	4.0	6.0		6
B	2.0	4.0	6.0		6
C	3.0	6.0	9.0	1.0	10
D	1.3	2.7	4.1		4
E	0.5	1.0	1.5		2

Importantly, these planning levels are not a maximum for locations that may suffer from wave amplification due to local bathymetry features or because they are located at the head of inlets, such as Port Alberni in Zone C.

Preliminary estimates of the tsunami first wave arrival time from the BC Earthquake Alliance for south Vancouver Island is presented in Figure 3.5. The lowest arrival time is on the outer west coast of Vancouver Island near Tofino and Ucluelet with values of 20 and 25 minutes, respectively. The arrival time is significantly larger within the Georgia Basin and at Port Alberni, as the wave needs to travel through narrower and shallower passages of the Juan de Fuca Strait and Alberni Inlet. Fortunately, the majority of BC's population resides in the Victoria and Vancouver region, with a minimal tsunami wave arrival time of 70 minutes.

Haida Gwaii and Prince Rupert in Zone A have arrival times of 55 and 170 minutes, respectively, and Bella Bella, located in Zone B, of 40 minutes (BC Earthquake Alliance Society 2016).

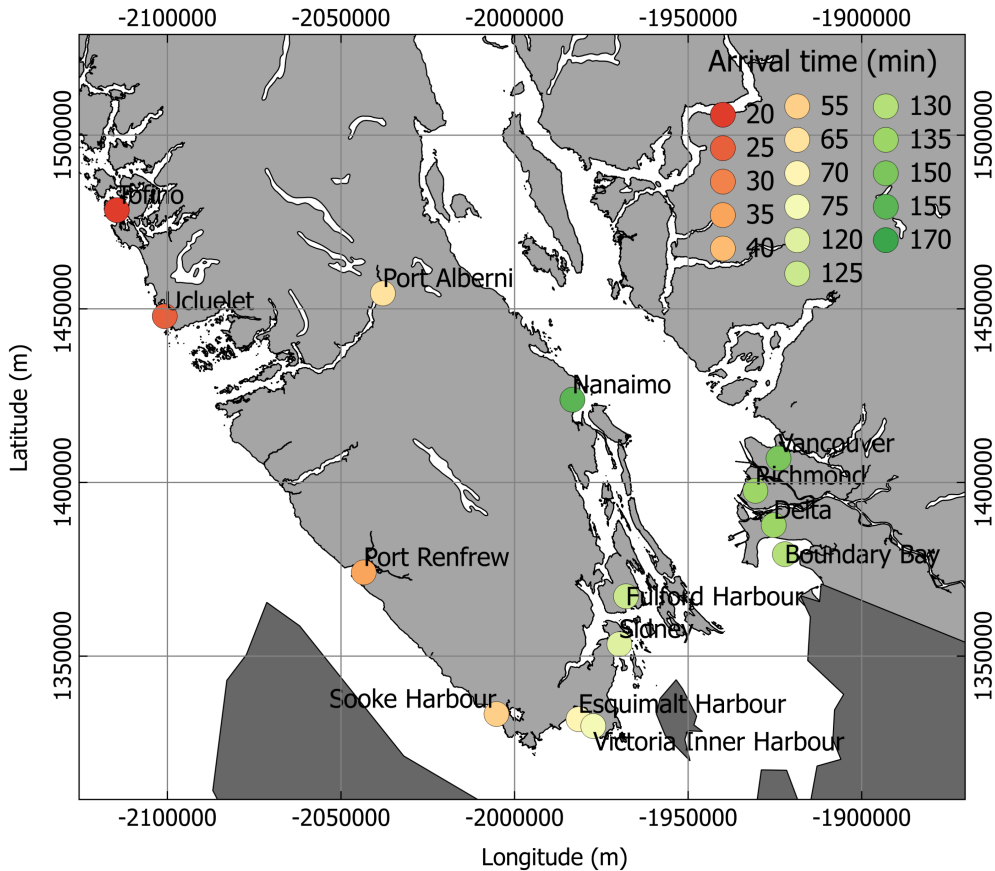


Figure 3.5 First tsunami wave arrival time – values based on tsunami safety guidelines provided by the Province of British Columbia, adapted from BC Earthquake Alliance Society (2016)

### *Sea Level Rise Due to Climate Change*

Anthropogenic global warming due to the accumulation of greenhouse gases within the atmosphere is assumed to result in sea level rise, global temperature rise, warming of the oceans, shrinking ice sheets, and ocean acidification (IPCC 2007). Sea level rise present a particular danger for coastal communities. The sea level rise along the coast of BC is due to a combination of global effects, such as melting glaciers and ice caps due to global warming, and local effects, such as the vertical movement of land (The Arlington Group Planning + Architecture Inc., et al. 2013)

Local effects differ by location. In the Fraser River estuary, particularly affecting the municipalities of Delta, Richmond, Queensborough, and New Westminster Quay, subsidence of the alluvial soil is causing the area to sink at a rate of 1-3 mm/year. This is aggravated by human interaction through large construction projects and diversion of sediments into deeper water (Thomson, et al. 2008). Meanwhile, the subduction of the Juan de Fuca tectonic plate beneath the North American plate creates the opposite effects on the western front of Vancouver Island, uplifting the land at a rate of 2-3 mm/year (Thomson, et al. 2008). A comparable uplift rate is

also observed in Haida Gwaii, caused by shifting of the Queen Charlotte fault. However, the uplift effects on the western coast of Vancouver Island could be inverted during the next CSZ earthquake. The last rupture, which occurred in 1700, caused an instantaneous subsidence of 500 to 2,000 mm (Leonard, et al. 2003). Minimal additional uplift also occurs due to post-glacial rebound at an estimated rate of less than 0.5 mm/year (Clague and James 2002). The combination of these effects causes varying sea level rise throughout BC.

The Intergovernmental Panel on Climate Change's projected global sea level rise by 2100 has been revised from their 2007 prediction of 0.18-0.59 m to 0.47-1.9 m (IPCC 2012). BC's current recommendation is a sea level rise planning level of 0.5 m for 2050, 1.0 m for 2100, and 2.0 m for 2200 (Ausenco Sandwell 2011). These levels are higher than the original IPCC report in 2007, but are more in line with the 2012 report and are in line with US and European recommendations.

### **3.2.2 Population At-Risk**

An integral part of an area's vulnerability is the population within the hazard zone. BC's population is 4,400,047 (2011 census), which represents 13.14% of the Canadian population. Increasingly diverse, up to 16% of new immigrants to Canada choose to reside in this province. British Columbia also has a large First Nation population, roughly 5% of the Canadian total.

In this study, the coastal communities considered to be in the tsunami hazard zone are those adjacent to the western, outer Pacific coast and all adjacent inlets. A total of 745 communities are considered, including 583 First Nations communities. The next section discusses BC's population distribution by major subgroups: permanent residents, First Nations and transient population.

#### *Permanent Resident*

Permanent residents are defined here as those people included in the following federal 2011 census subdivisions: city (CY), population centre (POPCT), district municipality (DM), island municipality (IM), island trust (IST), town (T), unincorporated place (UNP), or village (VL), and herein described as non-indigenous communities. The total coastal permanent resident population is 3,008,719. The majority of the population living near or on the coast resides in the Georgia Basin (Figure 3.6), which encompasses the Straits of Georgia and Juan de Fuca; indeed, the two largest urban centres, Vancouver (Zone E) and Victoria (Zone D), are in this region. In fact, Zone E is by far the most populated zone, with 2,662,458 residents, representing 88.5% of those considered permanent residents. The majority of cities and population centres are also located in this zone (20 out of 24). Zone D is the second most populated zone, having a total of 282,717 residents (9.4%).

Compared to Zones D and E, Zones A, B, and C have a very low population, 16,580, 17,061, and 29,903, respectively, each of which represents less than 1% of total residents. Zones A, B, and C are mostly comprised of low-density DMs, UNPs, and VLs, with 74% of these having a population of less than 1000.

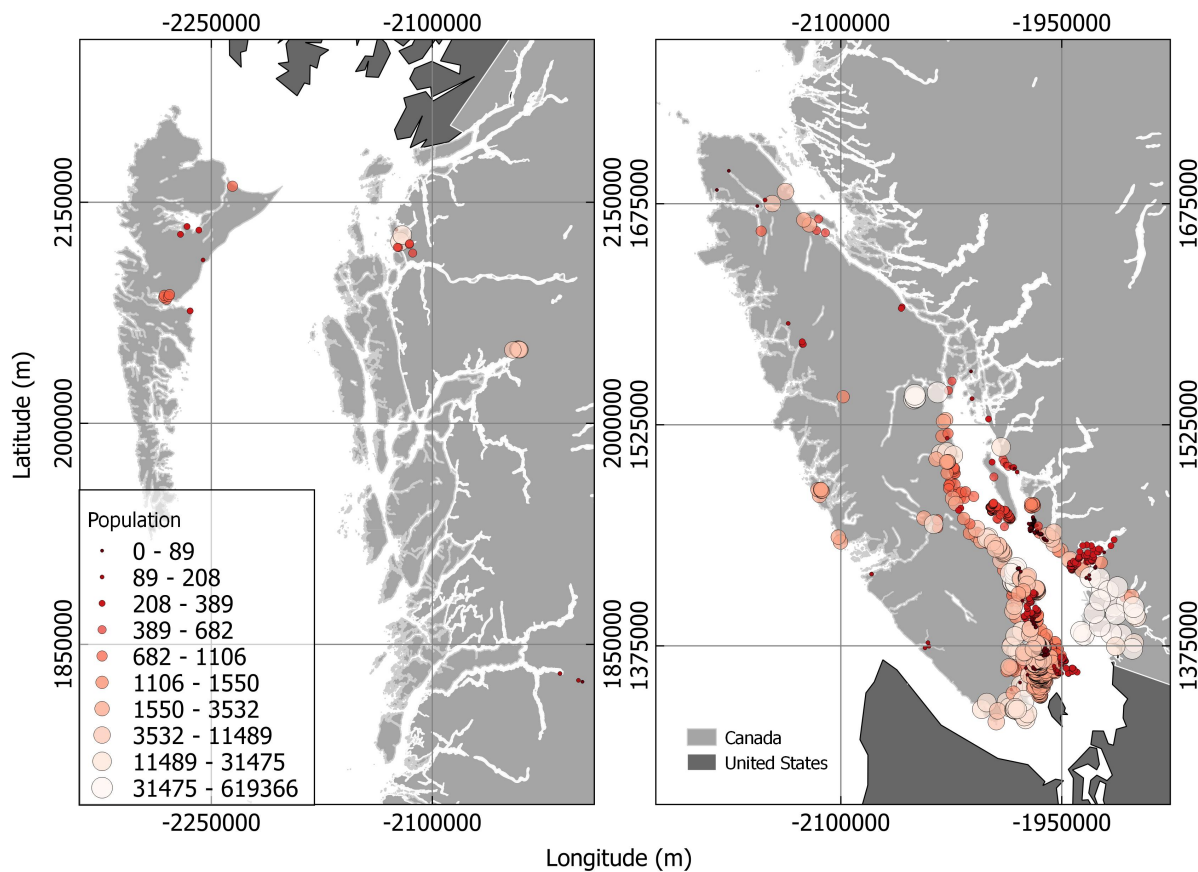


Figure 3.6 Population distribution of non-indigenous communities considered in this study

The largest city in Zone A is Prince Rupert, with a population of 12,802. Most communities in this zone are located on the north coast, near the Alaskan border or in Haida Gwaii (Figure 3.6).

The largest community in Zone B is Kitimat, located at the head of the Kitimat inlet north of the 2,000,000th latitude (Figure 3.6), with 8538 residents. Most other communities in Zone B are located in the north of Vancouver Island.

The highest populated community in Zone C is Port Alberni, with a population of 20,503.

### *First Nations*

The Aboriginal people are an important subgroup of the population, accounting for 4.3% of Canada, and 5.3% of British Columbia. The Aboriginal people in British Columbia are a diverse group, with 198 different First Nations. The majority of the Aboriginal population in BC, 78%,

does not live on a reserve. Reserves are a track of land legally defined by the Crown in the Indian Act for the use of Aboriginal people. Reserves are defined here, following the 2011 census definition, as Indian Reserves (IRI), Indian government district (IDG) and Nisga’a Land (NVL). The body of First Nation people living collectively on a reserve is named a band, governed by a band council. First Nations defines the group of people or bands living on a reserve.

Generally, provincial and federal laws apply to residents living on reserves, but with some exceptions such as marriage, rent regulation, tobacco and gaming. Band councils are therefor also responsible for emergency preparedness within their governing boundaries. Some First Nations, through treaties, are self-governed. Self-government arrangements take diverse form and may command government structure, land management, health care, child welfare, education and economic development.

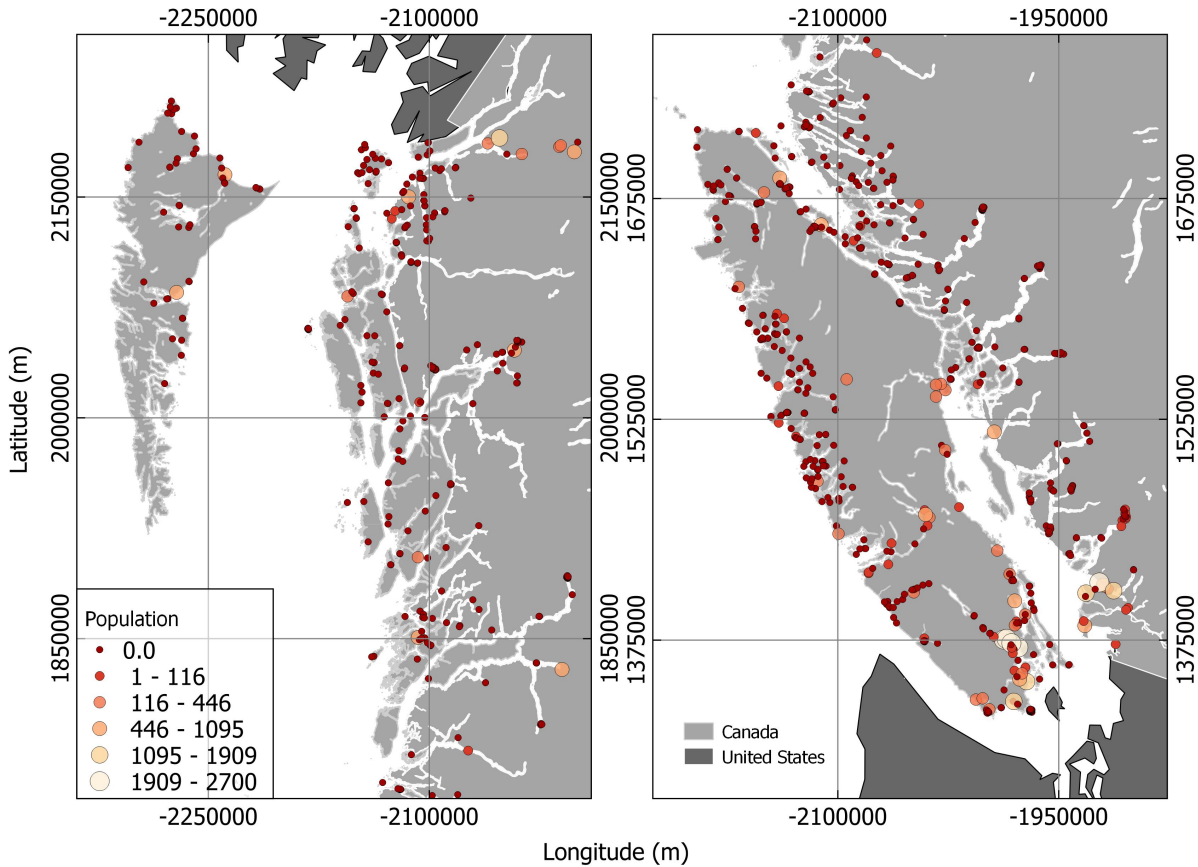


Figure 3.7 Population distribution of First Nation communities considered in this study

First Nations may have multiple reserves, many of which are not inhabited. Moreover, 73.9% of the reserves considered in this study have population reported of 0, denoted as dark red points in Figure 3.7. Some reserves are located within urban centres, notably Ahahswinis-No 1 and Tsahaheh No. 1 adjacent to Port Alberni, Cole Bay No. 3 adjacent to North Saanich and

Capilano No. 5 inside Vancouver. Although most reserves, are located in remote areas distributed throughout the main coast, Haida Gwaii and Vancouver Island (Figure 3.7).

### *Transient Population*

In addition to residents and First Nations, the transient population, temporary workers and tourist, represents an important subgroup. One of which that may have a higher vulnerability due to the fact that they may not be as well educated in the local tsunami hazard and emergency protocols. Seasonal workers are needed in industries such as logging, commercial fishing, aquaculture, recreation, and tourism. The seasonal and temporary labour force is made up of foreign and displaced native workers. The tourism industry in BC is ever growing. The revenue generated from this industry was \$13.4 billion in 2011, following a growing trend from the previous 10 years. In 2015, a total of 1,272,014 tourists visited the province, 313,221 of which visited Vancouver Island and 319,140 visited the coast and mountains. Although an important group, the transient population was not included in the analysis of this study due to a lack of precise information.

In conclusion, the tsunami vulnerability in the province of British Columbia is partly mitigated by their warning capabilities and emergency preparedness. The tsunami warning system, with its three main stages is a collaboration of international, federal and provincial agencies, local governments and the public. The current warning time estimated from the NTWC varies between 3 and 5 minutes. Although the time is small, it still needs to be considered when analysing the amount of time the population has to evacuate tsunami hazard zones. Local emergency plans are the responsibility of local government, as such, some communities are better prepared than others having tsunami warning sirens and tsunami signage. Many disaster educational opportunities exist in hopes of improving resident and emergency official responses, but are mostly geared towards earthquakes and not necessarily tsunami events. The relative tsunami hazard of different areas of the coast was used to divide the province in 5 TNZ, which are used for warning messages dissemination. Run-up planning levels are also provided by TNZ. Although the provided run uses an uncommon methodology based on the potential maximum wave height without consideration for the local bathymetry or areas prone to wave amplifications. The potential population at risk, including permanent residents and First Nations, is mostly located in the Georgia Basin, more precisely in Zone E. The remainder of the coast is populated with small villages and settlement with few population agglomerations with more than 1,000 residents.

## Chapter 4. Methodology

---

This chapter presents the methodology followed for the vulnerability assessment, divided in two main sections: Data Collection and Vulnerability Assessment Methodology. The first presents the data used, including its origin and precision; the second presents the processes used for the vulnerability assessment (VA) in detail. The VA was completed using geographic information systems (GIS), specifically Esri's ArcGIS 10 software and its open source counterpart, QGIS 2. The VA was performed using stand-alone scripts written in Python, employing Esri's ArcGIS ArcPy functions.

### 4.1 Data Collection

Two types of data were collected for this analysis: population and geographical. Population data, from the Canadian census, is used to estimate the population at-risk within the hazard zone. The geographical data is used to construct the area of study, including the topography, the bathymetry, and municipal boundaries.

#### 4.1.1 Population Data

The population data used in this study originates from the 2011 census conducted by Statistics Canada. The census of population is mandatory for everyone, including First Nation peoples living on and off reserves, permanent residents, refugee claimants, and holders of work and study permits and members of their families living with them. The census of population gathers information on: “the Population and dwelling counts; Age and Sex; Families, households and marital status; Structural type of dwelling and collectives; and Language” (Statistics Canada 2015). Although mandatory, 14 reserves within the country did not give permission to enter their territory to conduct the census and no information is available. Only one of these reserves is located in BC: Esquimalt, which is within Victoria. The population count in this area is thus underestimated.

The overall response rate of the census questionnaire in BC was 96.5%, below the national average of 97.1%. The population within dissemination blocks, typically a city block bounded by intersecting streets, which have a population of less than 15, is rounded to the nearest 5. This adjustment carries over to the larger geographic areas used in the census, including census subdivisions, as the adjusted value of the dissemination blocks are summed. However, the total population will always be within 5 of the true value for census subdivisions and federal electoral districts. To meet confidentiality agreements, some data is made unavailable as it is suppressed for areas where the total population is less than 40 (Statistics Canada 2011).

Communities at-risk within the TNZ are identified on their respective maps. However, some of the locations are no longer populated and were not found within the census or any of community boundary files used and were therefore not included in this study. In addition to the identified communities at-risk, many other coastal communities were considered in the study. A list enumerating the suppressed communities from the census and the communities at-risk from the TNZ maps and whether they were included in the study are presented in the Appendices.

#### **4.1.2 Geographical Data**

Two main types of geographical data were used: vector and raster. Vector data, which are sorted into feature classes, can be of three subtypes – points, lines, or polygons – each of which is a collection of vertices and points with coordinates with two or three dimensions. Raster data is a surface separated in a discrete grid where each cell is the average value found within. When cells in a raster represent the average elevation, representing the topography, it is referred to as a digital elevation model (DEM). However, raster data can represent any type of value. Bathymetric data is distributed in the Bathymetric Attributed Grid (BAG) format, which allows for a uniform combination of multiple data sources describing the sea floor and for easy distribution (ONSWG 2013). BAG data is then opened as a raster in the GIS software. A description of the geographical data, including their format, resolution and source is presented in Table 4.1.

Because four distinct datasets were used for the community's boundaries – municipalities, Designated places, population centres and Aboriginal land – some duplicates of communities existed and were manually removed. In addition, the community boundaries were adjusted to the constant higher high water large tides (HHW) coastline used.

The Albert Equal-Area Conic projection is used as the default geographic projection in this study. All geographic datasets were projected to this default. The projection employs the North American 1983 geographic coordinate system, the GRS 1980 spheroid and the NAD83 vertical datum. This Albert Equal-Area Conic projection was chosen as it does not distort area, is similar to the corporate standard mapping of British Columbia and is ideal in applications of small regions or countries. This projection, however, distorts shape and distance. Though, in general, the distortion in distance is minimum in comparison to the conformal Universal Transverse Mercator (UTM) projection, which preserves shape. It was found that difference in distance in the latitude has an average of 0.15% and 0.17% in the longitude (Klinkenberg 1995). The UTM projection was not used as the coast of BC spanned between two UTM zones. Using the Albert Equal-Area Conic projection, the shape is the least distorted between standard parallels. The standard parallel used in the projection are 50° and 70°, encompassing the vertical span of the province, located between parallel 48° and 60°.

Table 4.1 Format, description, resolution and provider of the geographical data used

<b>Name</b>	<b>Data format</b>	<b>Description</b>	<b>Provider</b>
Bathymetry	Bathymetric Attributed Grid (BAG)	Sea floor bathymetry of Canadian waters divided and distributed by NTS grids with a lower low water, large tide (LLW) vertical datum. Resolution: 500-m grid	Canadian Hydrographic Service (CHS), Fisheries and Oceans Canada (CHS 2016)
HHW coastline	Line Feature Class	Higher High Water Large Tides (HHW) coastline of British Columbia.	Canadian Hydrographic Service (CHS), Fisheries and Oceans Canada (CHS 2016b)
BC DEM	Digital Elevation Model (DEM)	DEM of British Columbia in array of 1:50,000 grid tiles in the Canadian Digital Elevation Data (CDED) format in metres of the ground or reflective surface. Resolution: 0.75 arc seconds (north/south)	BC Ministry of Forests, Lands and Natural Resource Operations (GeoBC 2012)
Municipalities	Polygon Feature Class	First Nations (Indian Reserves (IRI), Settlements (SE) and Indian Government Districts (IDG)) and non First Nations (incorporated municipalities and Cities (C), District Municipalities (DM) and Town (T)) communities defined by the 2011 census subdivisions.	Statistics Canada (Statistics Canada Catalogue no.92-160-X 2011)
Designated Places	Polygon Feature Class	Small communities that do not meet the criteria for a defined municipality or population centre according to the 2011 census.	Statistics Canada (Statistics Canada Catalogue no. 92-163-x 2011)
Population Centres	Polygon Feature Class	Urban areas such as with a population of at least 1,000 and a minimum concentration of 400 persons/km <sup>2</sup> classified by the 2011 census.	Statistics Canada (Statistics Canada Catalogue no. 92-166-X 2011)
Aboriginal Lands	Polygon Feature Class	Aboriginal lands of British Columbia, including reserves, Sechelt land and Land Claim Settlements lands.	Surveyor General Branch, Natural Resources Canada (NRCan 2016a)

Additional resources were required for the Tofino case study in order to construct a more complex depiction of the built environment (Table 4.2). The zoning map was digitized in GIS software by overlay and manual tracing. The road network data files for Tofino were incomplete; therefore, the dataset was downloaded directly from OpenStreetMap, an open source web-based mapping service. The built-up area within the Tofino land cover layer only encompassed part of the village located to the north of the peninsula and omitted all other buildings. Buildings were manually found and traced using areal photographs from Digital Globe (2016) and the Tofino civic address map.

Table 4.2 Format, description, resolution and provider of the additional geographical data used in the Tofino case study

Name	Data format	Description	Provider
Tofino Zoning Map	PDF	Zoning map of the District of Tofino established by the zoning by-laws.	District of Tofino (District of Tofino 2015)
Tofino Civic Address Map	PDF	Civic address map as established by the District of Tofino.	District of Tofino (District of Tofino 2010)
Tofino Road Network	Line Feature Class	Road network within the District of Tofino including highways, roads and pedestrian pathways.	OpenStreetMap (OpenStreetMap 2016)
Tofino Land Cover	Polygon Feature Class	Type of land cover of the Tofino area: water bodies, light brush, heavy woods, sand, mud, rocky ledge and built-up areas.	Natural Resources Canada (NRCan 2016b)

## 4.2 Vulnerability Assessment Processes

The VA is measured by available time ( $t_{\text{available}}$ ), that is, the difference between the tsunami's first wave arrival time ( $t_{\text{arrival}}$ ) and the time needed to reach safety ( $t_{\text{safety}}$ ) at a given location. The time to reach safety is a function of the travelling velocity and distance from safety ( $d_{\text{safety}}$ ). The available time symbolizes, when positive, the remaining time before the tsunami wave arrives once safety is reached for a given location, and, when negative, the additional time needed to reach safety after the tsunami wave arrives for that same given location. The available time is used for comparison instead of the time to safety as it accounts for the difference in hazard of a location by being a function of the tsunami arrival time.

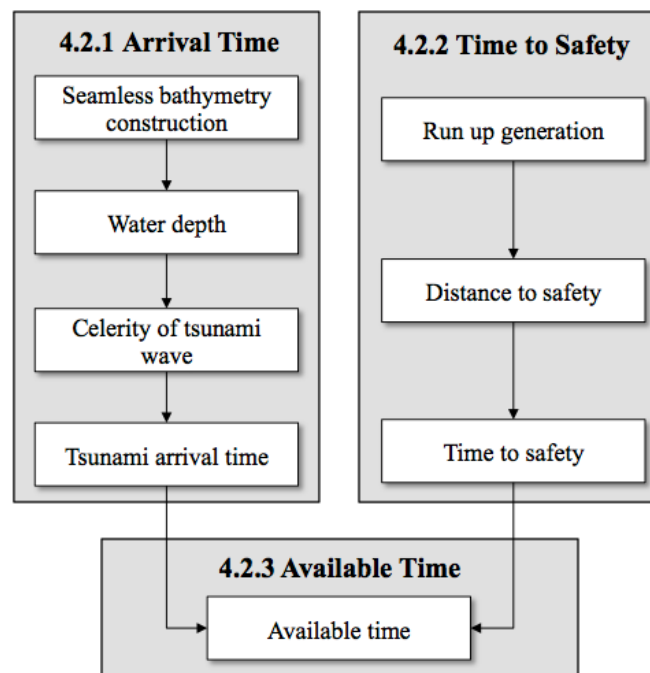


Figure 4.1 Vulnerability Risk Assessment Workflow

The VA workflow, presented in Figure 4.1, has three primary components: arrival time, time to safety, and available time.

### 4.2.1 Arrival Time

The arrival time of the first tsunami wave is the first primary component needed to compute the available time. In calculating arrival time, we assume that linear wave theory is valid, as viscosity, surface tension, and turbulence do not have a large influence on ocean waves (Synolakis 1986, 1987, Hebenstreit and Murty 1989, Tadepalli and Synolakis 1994, Kanoglu 1997, Titov and Synolakis 1997, 1998, Satake, Wang and Atwater 2003). The celerity of a tsunami wave is described by the celerity of a wave in shallow water, a function of the gravitational constant ( $g$ ) and the water depth ( $h$ ) shown in Equation 4.1:

$$c = (gh)^{0.5} \tag{4.1}$$

The shallow water assumption is valid when the ratio of the water depth to wavelength is equal or less than 0.04. Typically, tsunamis generated by earthquakes have a wavelength of 10-500 km (Bryant 2014). Tsunamis, therefore, satisfy this condition in a water depth of 400-20,000 m, which is within range of the average ocean depth of 3700 m (NOAA 2015). Tsunami waves' celerity decreases in true shallow water, where the shallow water assumption is no longer valid. However, using this assumption throughout its propagation yields a shorter propagation time and, thus, a conservative estimate.

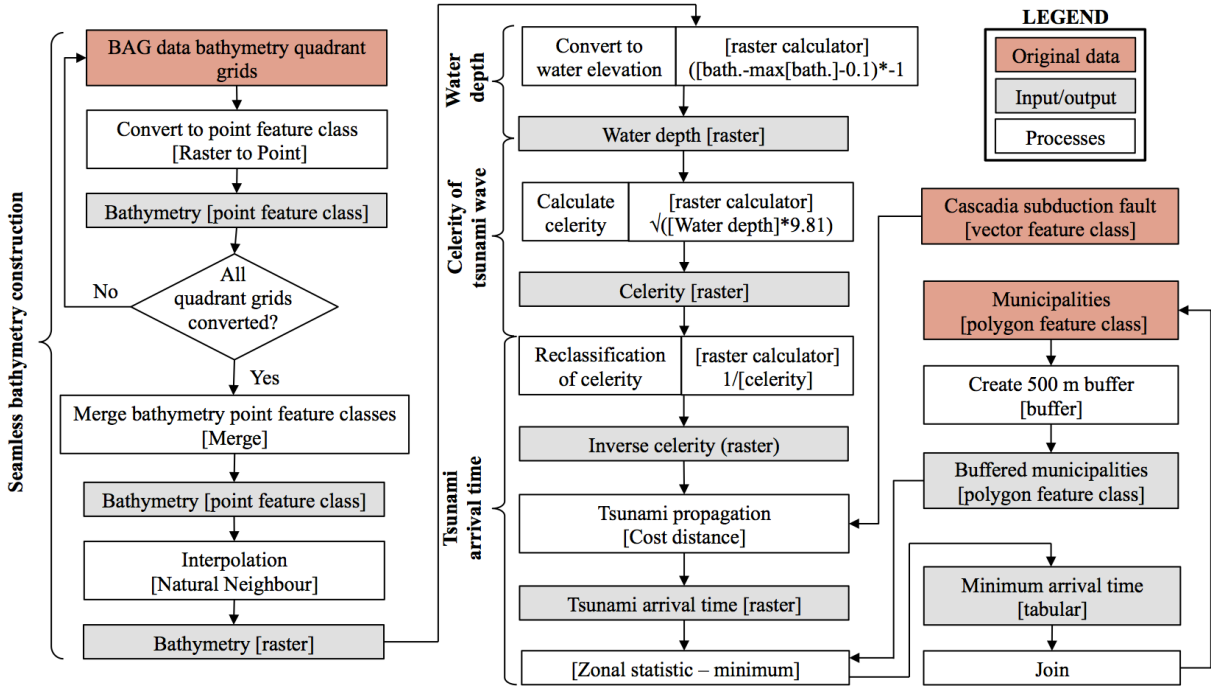


Figure 4.2 Workflow for the first primary component: Tsunami Arrival Time. This section is separated into two components: the seamless bathymetry construction and the first tsunami wave arrival time

The shallow water Equation (4.1) is a function of only the water depth. Consequently, calculating the arrival time (Figure 4.2) starts with finding the water depth using a seamless bathymetry extending from the coast to the tsunami origin. Using the water depth, the wave celerity can be calculated, followed by the propagation time of the wave using a direct step method.

### *Seamless Bathymetry Construction*

The bathymetric data used in this study is from the Canadian Hydrographic Service (CHS), which was obtained through a multi-beam survey. This technique uses multiple sonars attached to the bottom of a ship to evaluate the depth of the seabed. The ship typically surveys an area by travelling in orthogonal grids. Consequently, some areas of the ocean may only have data points within lines sparsely distributed, as demonstrated in grid 92E in Figure 4.3a. As a result, the raw bathymetry grids, in raster format, are converted to points and merged together resulting in a uniform point feature class layer. Interpolating the point file then fills the gaps in data, using Natural Neighbour interpolation, which itself uses an inverse distance weighting method, meaning that the interpolated value of a point is the weighted average of the cluster of points in the surrounded region. The weight of a point is the inverse of its distance to the source point being interpolated. Each cell without a value in the raster is interpolated, while known cells retain their initial value. The result of this interpolation can be seen in the bathymetry of the grid 92E as presented in Figure 4.3b.

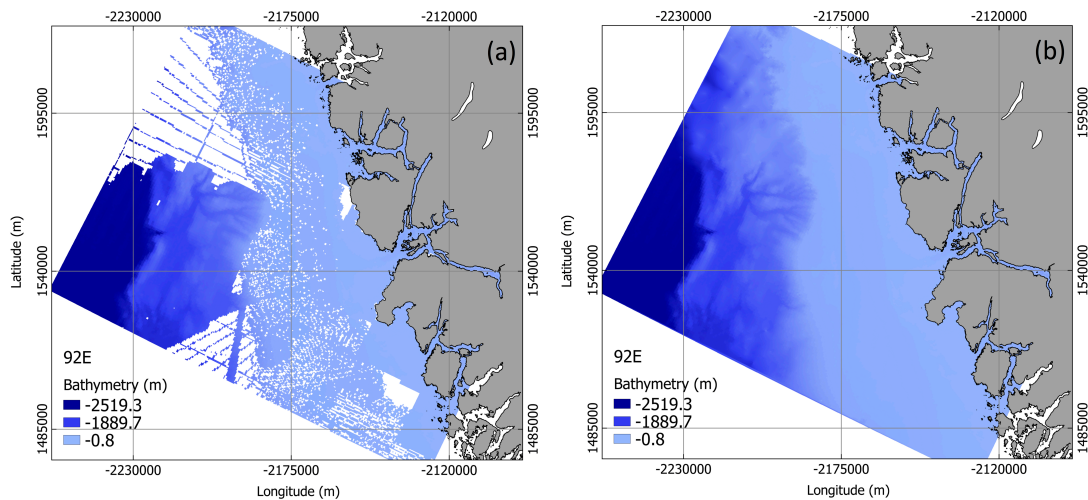


Figure 4.3 Bathymetry of grid 92E: (a) raw BAG data, (b) Natural Neighbour interpolation

The obtained bathymetry data only covers the Canadian portion of the Juan de Fuca strait (Figure 4.4, green). Some bathymetric data from US sources are available; however, the American datasets do not cover all missing parts of the strait (Figure 4.4, blue) and elevations where the datasets overlap were significantly different. Only the Canadian dataset was used since the

fastest tsunami propagation path through the Juan de Fuca strait is likely to pass to the north of the San Juan Islands archipelago, along route 1 in Figure 4.4.

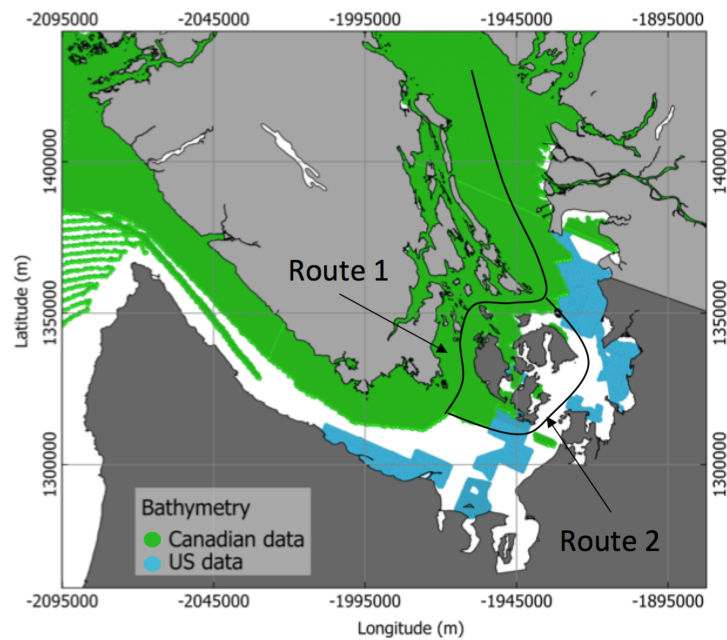


Figure 4.4 Bathymetry limits of the Canadian (green) and American (blue) datasets within the Juan de Fuca Strait, South Vancouver Island

The numerical simulation by Cherniawsky et al. (2007) of a CSZ event tsunami in south Vancouver Island demonstrates that the tsunami propagates first along route 1. The tsunami waves first circulate between Vancouver Island and San Juan Island after 1 hour and 44 minutes following the inducing earthquake (Figure 4.5a). The tsunami waves have already reached Sidney and the Pender islands by the time the tsunami has propagated south of the San Juan Islands (Figure 4.5b).

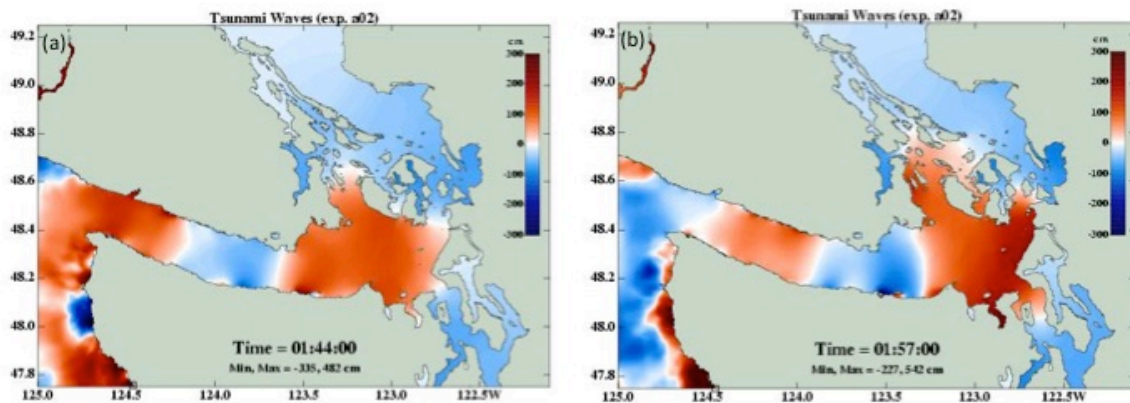


Figure 4.5 Tsunami propagation after: (a) 1:44:00; and (b) 1:57:00 inducing earthquake, within the Juan de Fuca Strait using the MOST3 model (adapted from Cherniawsky et al. 2007)

*Water Depth and Celerity*

Bathymetric data is represented as negative values, since it is the elevation below sea level. The bathymetry datum is the LLW and intertidal areas, or drying areas, have a value above 0. The maximum value in the bathymetry dataset used was of 5.0 m. The desired water datum is the HHW, representing the worst-case scenario for the tsunami arrival time. In order to achieve this, the maximum value of the bathymetry was subtracted throughout to bring the dataset maximum value to 0. To ensure that no water depth was 0 for the analysis, an additional 0.1 m was also subtracted. The final result of the water depth is presented in Figure 4.6.

The bathymetry was converted to water depth using the Esri’s ArcGIS Raster Calculator, which executes an algebraic equation for each cell in a raster. The water depth ( $h$ ) was generated using the Equation 4.2. The bathymetry value for each cell is  $b$  and  $max(b)$  is the maximum value of the bathymetric dataset.

$$h = -(b - \max(b) - 0.1) \tag{4.2}$$

Using the newly found water depth, the celerity is calculated using the Raster Calculator with Equation 4.1.

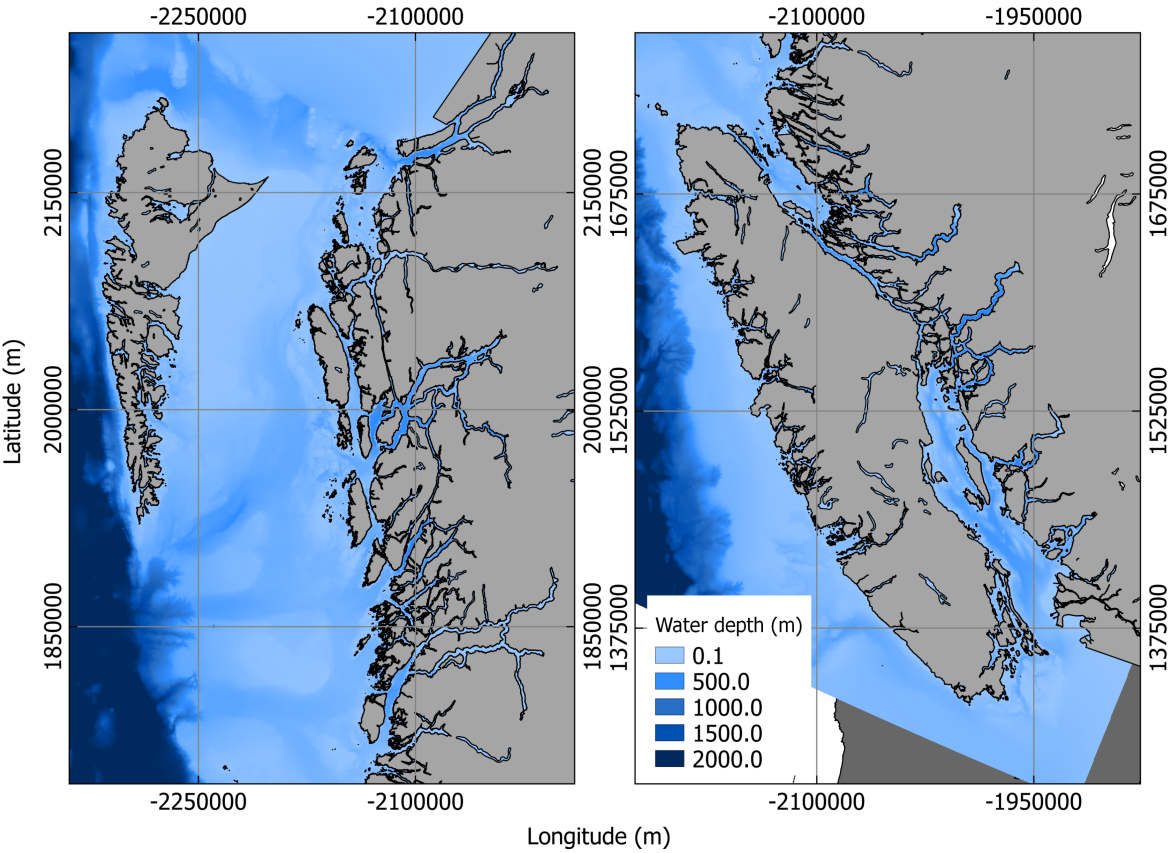


Figure 4.6 Water depth of the British Columbia coastal waters, calculated from the seamless bathymetry constructed

### Arrival Time

The propagation of the tsunami throughout the study area was performed using Esri's ArcGIS Cost Distance tool, which employs a direct step method to calculate the shortest weighted distance from a source to a destination. The tool calculates the accumulated cost for each cell from the source by multiplying the cell cost value by the distance. The distance is determined by the raster cell size. The inputs for this tool are the cost raster and the source raster.

The cost raster used is the inverse celerity, found from the celerity raster using the Raster Calculator. The inverse of the velocity multiplied by the distance results in a time; thus, the accumulated least costly path results in the shortest tsunami arrival time. The shortest tsunami path is ensured as the inverse of the celerity results in the largest velocity having the lowest values, hence the lowest cost. The total time is then determined by summing the time needed to cross each cell within the shortest path, therefore using a direct step method. Possible diffusion of the wave was not computed in this method given that only the celerity of the wave based on depth was considered.

The tsunami source was taken as the limit of the full rupture zone of the Cascadia fault (Figure 4.7) similarly to Cherniawasky et al. (2007). This rupture scenario represents the Long-Narrow scenarios resulting in a  $M_w$  9.0 earthquake described by Satake et al. (2003).

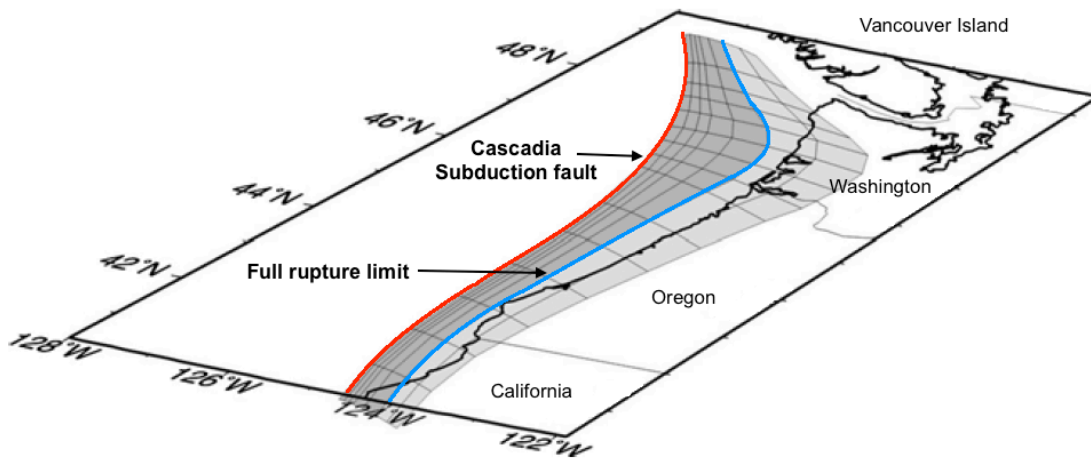


Figure 4.7 Cascadia subduction fault and full rupture zone along North American Pacific Coast, adapted from Cherniawasky, et al. (2007)

Finally, the arrival time for each community, in tabular form, was computed using the minimum function of the Zonal Statistic tool, which calculates the statistics of a raster within specified zones. The zones used were a 500 m buffered municipality feature class, as demonstrated in Figure 4.8. Using the minimum function, the tool yields the minimum value within this zone. A 500 m buffer was necessary, as most municipality boundaries do not extend past the coastline and, therefore, using the original municipality boundaries would have returned no value using

the Zonal Statistic tool. The minimum arrival time was then joined to the original municipality feature class Attribute Table.

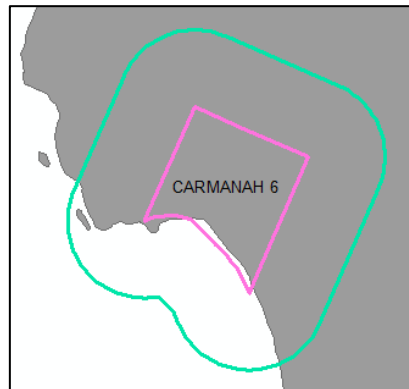


Figure 4.8 Buffer of 500 m radius (green) created around communities boundary (pink) used for the Zonal Statistic tool

#### 4.2.2 Time to Safety

Calculating the time to safety requires three primary steps: run-up generation, distance to safety, and time to safety (Figure 4.9). The time necessary to reach safety is a function of the distance to safety (safe zone), which depends on the run-up, and the travelling velocity. Given that the time to safety is dependent on run-up coupled with the numerous run-up values considered, time to safety is calculated with a “for-loop”, processing one run-up value at a time.

##### *Run-Up Generation*

The run-up, given as an elevation value, describes the vertical limit of the inland intrusion of the tsunami. Above the run-up value, the area is considered the safe zone (SZ), and below or equal to the run-up, it is considered the hazard zone (HZ). As the likely run-ups for the BC coast are not known for most locations, run-ups are generated for elevation values between 3 and 25 m, with a 2 m interval for the entire coast. For each run-up, a SZ and HZ are required, one being the inverse of the other. A minimum of 3 m is used as it is the minimum height to cause serious damage (Leonard, et al. 2013). The maximum run-up considered was taken as maximum run-up observed in BC, located in Port Alberni from the 1700 tsunami, plus 50% for safety in addition to 0.5 m for 50-years sea level rise adaptation, totalling in a value of 24.5 m.

A bare-earth DEM is used in this study, meaning that built surfaces are not included. The initial safe zone is computed using the Raster Calculator. The function *setnull* is used on the DEM to set all elevation below or equal to the run-up value to a new value of “no data”. However, using this method leaves “dry pockets” within the HZ, as can be observed in Figure 4.10. These dry pockets are considered a SZ, as their elevation is above the run-up value. The smaller pockets, varying from a single cell (24.3 m x 24.3 m) to a few cells, cannot be considered potential evacuation sites for the population due to their small sizes, the uncertainty surrounding the built

environment in these areas, and the potential for wave overtopping. If the initial SZ raster is left intact with the dry pockets, the distance to safety could be underestimated. An additional artefact of this method is small gaps within the SZ having a value equal to or below the run-up and, therefore, automatically considered hazardous. To remedy this, a generalization process is used.

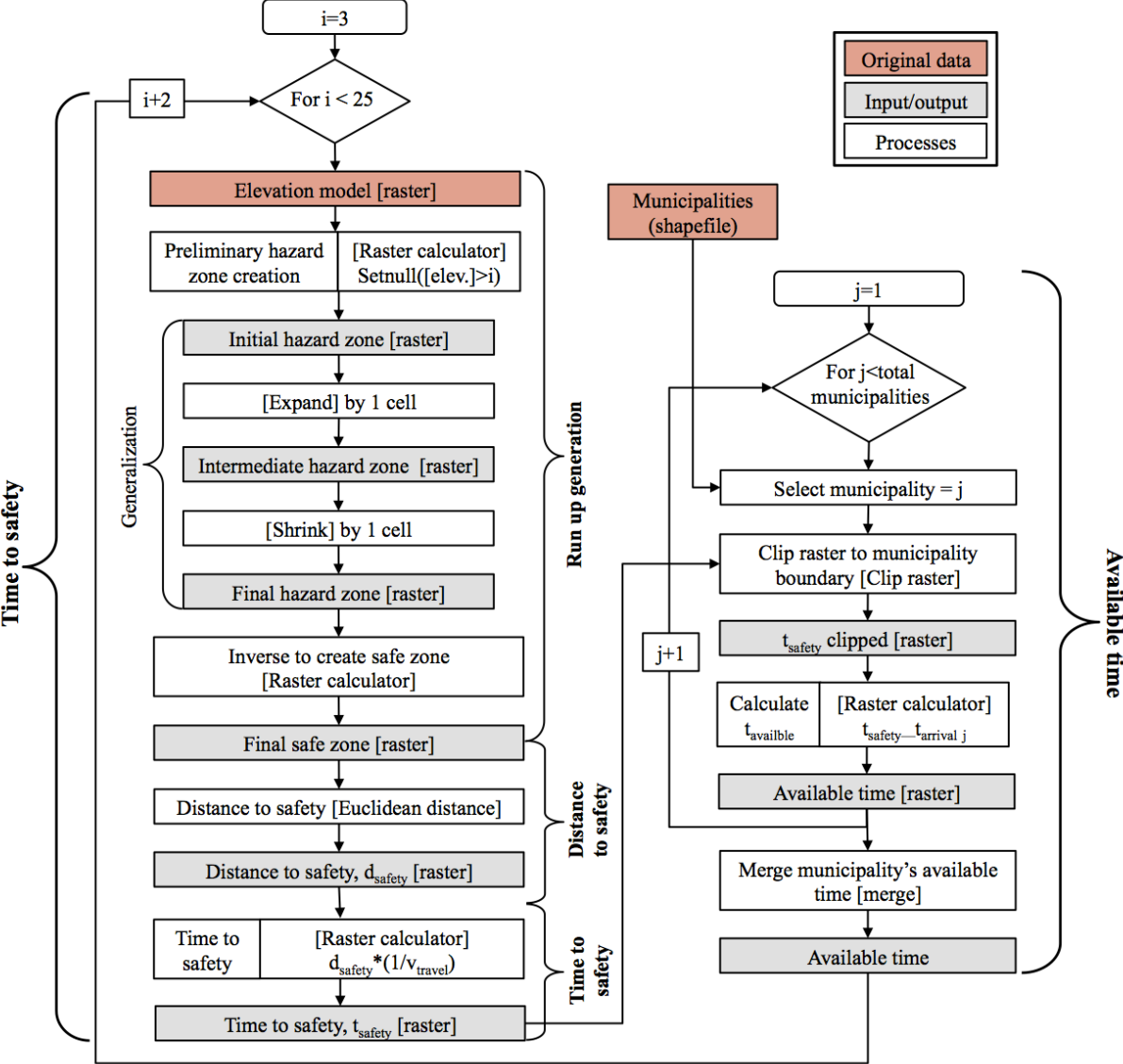


Figure 4.9 Workflow for the time to safety and available time primary method component. The time to safety calculation is separated into three steps: the run-up generation, distance to safety, and time to safety.

Generalization is a process whereby excess details within a raster are removed or smoothed or small gaps are filled. The approach varies based on the desired results. Many tools are available in Esri’s ArcGIS generalization toolset such as: *Nibble*, *Shrink*, *Expand*, *Region Group*, and *Thin* (ESRI 2016). The *Expand* and *Shrink* tools were used to satisfy the two goals of this study’s generalization process: eliminate small gaps within the SZ and eliminate unnecessary dry

pockets with the HZ. The specific generalization process used and its effects on the number and size of dry pockets, the distance to safety, and the surface area of the HZ are further discussed in section 4.2.3.

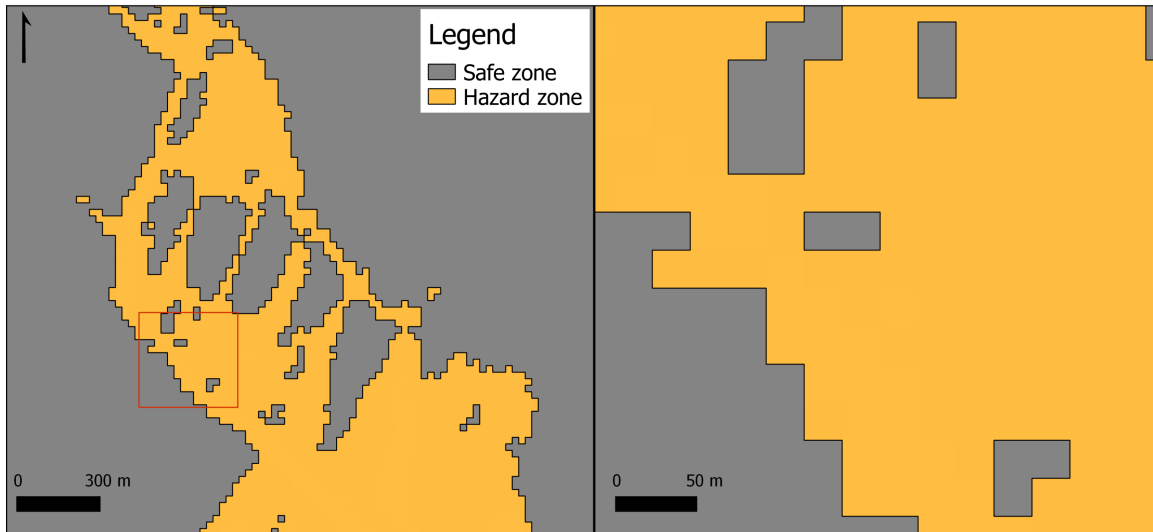


Figure 4.10 Dry pockets created by the run-up generation method within the time to safety

The generalization process was applied to the initial HZ raster ( $HZ_{initial}$ ), resulting in the final form of the HZ ( $HZ_{final}$ ). This raster has a constant cell value of 1, where the HZ is located and a null value is assigned for the SZ. A conditional statement function is used to create the SZ as the inverse of  $HZ_{final}$ . The expression used is presented in Equation 4.3:

$$SZ = Con(IsNull(HZ_{final}), 2, SetNull(HZ_{final}), 1) \quad [4.3]$$

The statement reads as:

1. If a cell in  $HZ_{final}$  is null, evaluated with the *IsNull* function, then assign a value of 2 in SZ raster. A value of 2 is used, which eliminates confusion with the original  $HZ_{final}$  value of 1.
2. Otherwise, assign a null value in the SZ raster if cells in  $HZ_{final}$  have a value of 1, using the *SetNull* function.

#### *Distance and Time to Safety*

The distance to safety ( $d_{safety}$ ) is calculated as the shortest distance for each cell in the HZ raster to the nearest cell in the SZ raster, using the Euclidean Distance tool. Following this, the time necessary to reach safety ( $t_{safety}$ ) at each cell location can be found using the Raster Calculator by dividing the value of the distance to safety raster by the travelling speed.

Only pedestrian evacuation is considered within the scope of this study. In addition, the possible effects of car traffic on pedestrian evacuation were not considered. Pedestrian evacuation is

recommended by emergency managers in the province of British Columbia instead of evacuating with a vehicle, unless impossible, for many reasons. First, congestion is likely to occur with a large quantity of vehicles simultaneously driving in a similar direction. Congestion could drastically reduce the evacuation speed and render emergency personnel travel difficult. Additionally, road conditions following a large earthquake may not be adequate for driving. As noted in Table 4.3, three pedestrian travelling velocities are considered: mobility impaired, average adult ambulatory, and slow run.

Table 4.3 Pedestrian travelling velocities considered for evacuation in model

Category	Velocity (m/s)	Source
Mobility impaired (MI)	0.89	(FEMA P-646)
Average adult ambulatory (AW)	1.22	(Wood and Schmidlein 2013)
Slow run (SR)	1.79	(Wood and Schmidlein 2013)

### 4.2.3 Available Time

The available time is calculated as a nested for-loop passing through each municipality, within the first run-up for-loop. Within the nested loop, the time to safety raster is clipped to the boundary of a selected municipality. The available time is then calculated for each cell of this clipped raster by subtracting the selected municipality's time to safety ( $t_{\text{safety}}$ ) from the tsunami arrival time ( $t_{\text{arrival}}$ ). Once this has been completed for each municipality, the available time rasters are merged back together, resulting in a concise available time ( $t_{\text{available}}$ ) raster for the run-up level being processed. Once finished, the process returns to the start of the first loop, within the time to safety process, to generate the next run-up.

### 4.2.4 Run-Up Generalization Sensitivity Study

The dry pockets are a natural product of the local topography, such as hills and mounds that are higher than the surrounding elevation. Dry pockets are also established in tsunami HZ (or design zones) determined with numerical simulations that meet ASCE standards, as in the case of Hilo in Hawaii (Figure 4.11). The dry pockets could be beneficial to emergency managers as potential evacuation sites or locations for engineered mounds to be used for vertical evacuation. However, site-specific evaluations would be needed for these locations.

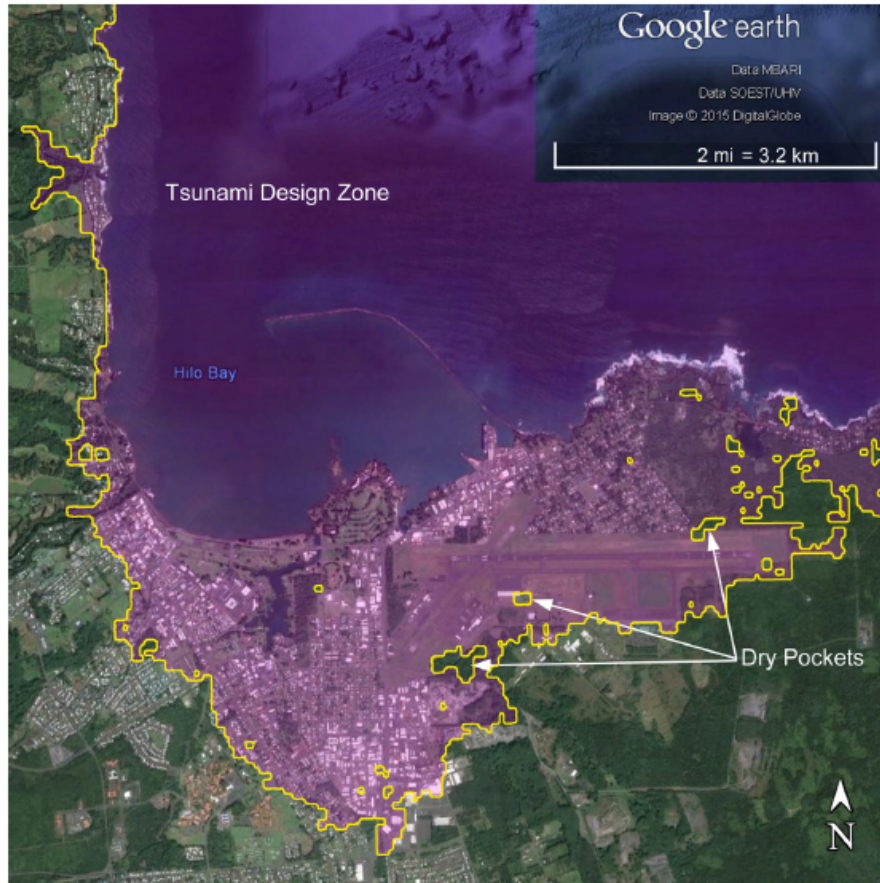


Figure 4.11 Tsunami design zone for Hilo, Hawaii where dry pockets are also observed (Naito, et al. 2016)

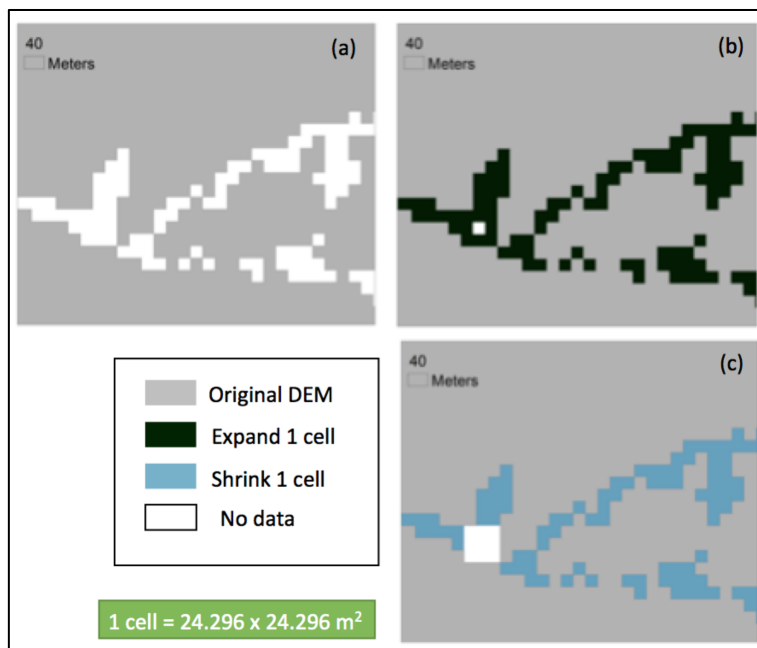


Figure 4.12 Generalization process: (a) initial raster, (b) results of Expand process, and (c) results of Shrink following the Expand procedure.

Care must be taken when using generalization processes, as it impacts the overall shape of a raster: an over-generalized raster will not reflect the real geometry of the area. The primary goal of this process is to limit the amount and size of the dry pockets; the secondary goal is to reduce gaps in the SZ. The two tools used to accomplish these goals are Expand and Shrink. Expand works by expanding a zone of a raster by a specified number of cells. Because the input raster used has one constant value, this adds the specified number of cells to the boundaries adjacent to a null cell, as can be seen from the transition in Figure 4.12a to Figure 4.12b. Shrink does the opposite, reducing valued cells adjacent to null cells (Figure 4.12c).

In order to find the optimal generalization process, various cases were computed to study the effects on the amount and size of dry pockets, the distance to safety, and the surface area of the HZ. The cases considered are presented in Table 4.4. The naming convention used is as follows: the first tool (E for expand and S for shrink), followed by the second tool and the number of cells used in the first and second tool. The number of cells used within Expand and Shrink were left identical to keep the shape of the HZ and SZ as close as possible to the original.

Table 4.4 Cases considered for the run-up HZ generalization sensitivity analysis

Case	Input Raster	Step 1		Step 2	
		Tool	# of cell	Tool	# of cell
E-S 1	HZ <sub>initial</sub>	Expand	1	Shrink	1
E-S 2	HZ <sub>initial</sub>	Expand	2	Shrink	2
E-S 3	HZ <sub>initial</sub>	Expand	3	Shrink	3
E-S 4	HZ <sub>initial</sub>	Expand	4	Shrink	4
S-E 1	HZ <sub>initial</sub>	Shrink	1	Expand	1
S-E 2	HZ <sub>initial</sub>	Shrink	2	Expand	2
S-E 3	HZ <sub>initial</sub>	Shrink	3	Expand	3
S-E 4	HZ <sub>initial</sub>	Shrink	4	Expand	4

### *Effects on “Dry Pockets”*

The effects on the “dry pockets” caused by the generalization are measured by the change in the amount and size (in number of cells) of the pockets from the baseline (i.e., the SZ raster without generalization). As a test case, a 7 m run-up is evaluated and its results are presented in Table 4.5. The baseline has 1,467 dry pockets with a size of 1 cell, 651 pockets of 2 cells, and 390 pockets of 3 cells.

Using the S-E methodology decreases the amount of dry pockets; with a larger decrease the more cells were used in the method. For groups up to 20 cells in size, average decreases of 34.4% for S-E 1, 57.7% for S-E 2, 69.7% for S-E 3, and 75.5% for S-E 4 are observed. The reduction in the number of pockets is a result of the first step (shrink), as seen in the dashed red square in Figure

4.13a. The small and narrow area of the initial HZ is almost eliminated with S-E 1 and completely eliminated using S-E 2-4. The original narrow bands are replaced with concise rectangular masses due to the following expand process. The initial shrink also makes holes in the HZ larger, as seen by comparing the area within the red square of Figure 4.13a to the original HZ in Figure 4.13b. This artefact is problematic, as reducing the HZ means increasing the area of the SZ in locations that are below the run-up elevation and should continue to be considered hazardous and, thus, producing a conservative estimate of the SZ.

Table 4.5 Number of dry pockets as a function of their size in cells for the baseline and test cases E-S 1 to 4 and S-E 1 to 4 for a 7 m run-up

Size of dry pockets (cell)	Surface area ( $\times 10^3 \text{ m}^2$ )	Number of dry pockets								
		Baseline	E-S 1	E-S 2	E-S 3	E-S 4	S-E 1	S-E 2	S-E 3	S-E 4
1	0.59	1467	0	0	0	0	790	524	383	296
2	1.18	651	0	0	0	0	337	216	157	118
3	1.77	390	0	0	0	0	220	131	97	75
4	2.36	256	0	0	0	0	134	93	59	44
5	2.95	191	0	0	0	0	96	64	42	32
6	3.54	143	0	0	0	0	91	47	37	28
7	4.13	104	0	0	0	0	75	62	46	35
8	4.72	85	0	0	0	0	59	42	31	28
9	5.31	93	206	0	0	0	63	36	29	20
10	5.90	70	0	0	0	0	43	30	26	19
11	6.49	55	0	0	0	0	45	30	17	16
12	7.08	48	94	0	0	0	37	20	14	6
13	7.67	51	0	0	0	0	35	24	17	11
14	8.26	50	12	0	0	0	32	23	20	17
15	8.85	47	55	0	0	0	23	15	10	9
16	9.44	33	23	0	0	0	21	15	11	15
17	10.0	36	13	0	0	0	24	16	12	10
18	10.6	23	30	0	0	0	24	14	10	9
19	11.2	38	21	0	0	0	19	10	8	7
20	11.8	25	20	0	0	0	22	13	6	4

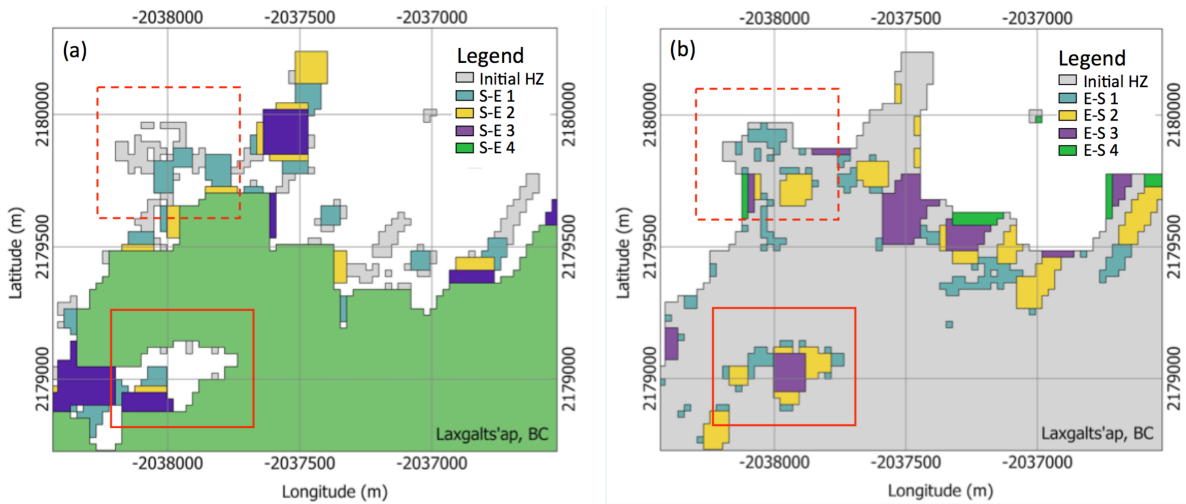


Figure 4.13 HZ computed with the generalization process E-S 1-4 and S-E 1-4 for a 7 m run-up in Laxgalts'ap, BC

Unlike the S-E process, expanding first in the E-S methodology results in filling gaps and narrow openings within the HZ, demonstrated in the solid red square in Figure 4.13b. Larger holes are partly closed. Additionally, adjacent groupings within the threshold distance of the number of cells being used in the method are joined together, as evident in Figure 4.13b in the red dashed square. Even with the shrinking following this expand, the HZ boundary increases with the number of cells being used in the method, thus producing a conservative HZ. Dry pockets in the SZ are completely eliminated up to a size of 9 cells for E-S 1, 25 cells for E-S 2, 49 cells for E-S 3, and 81 cells for E-S 4. A 9-cell grouping has a total surface area of  $5.31 \times 10^3 \text{ m}^2$ , equivalent to 0.9 American football fields. Tsunami shelter guidelines recommend planning for  $0.92 \text{ m}^2$  of space per persons for duration of 24 hours (FEMA P-646). A 9-cell grouping could, therefore, house approximately 5,775 more than the majority of BC communities' populations. It is clear that for the cases E-S 2-4, having a minimum dry pocket size of 25 is overly conservative. The preferred case based on dry pocket elimination is E-S 1.

#### *Effects on the Surface Area and Distance to Safety*

The change in surface area and distance to safety is presented in the following section for the two least conservative cases for E-S processes 1 and 2. As expected, the elimination of dry pockets increases the HZ surface as the SZ is decreased. Additionally, the more cells are used in the process, the more the HZ increases (Figure 4.14a). The increase in the HZ area for both E-S 1 and 2 has a negative correlation with the run-up (Figure 4.14b and c). This increase is rather small, less than 0.16% (approximately  $500 \text{ km}^2$ ) for the entire coast, with E-S 1 resulting in a maximum increase below 0.15%. For run-ups higher than 7 m, the increase is below 0.05%. E-S 2 has a maximum area increase just above 0.15%. Comparatively, run-ups above 11 m (4 m above E-S 1) create a surface area increase below 0.05%. For run-ups greater than 7 m, the area

increase plateaus, with E-S 2 being approximately 180 km<sup>2</sup> greater than E-S 1. The pockets are more significant in lower run-ups, as the percent of the area decreases with run-up, but the total area remains almost the same after 7 m of run-up.

As the SZ surface area decreases, the distance to reach safety increases in some locations. The change in the distance to safety (Figure 4.15a) is much more significant than the increase in the HZ surface area created by E-S 1 and 2. E-S 1 causes an increase just above 50% for 3 m and 5 m of run-up and below 25% for the remaining run-ups. Contrastingly, E-S 2 increases the distance to safety over 120% for a 3 m run-up, approximately 100% for a 5 m run-up, and above 50% for a 7 m run-up. Similarly to the surface area, the percentage increase in the distance to safety decreases with higher run-ups (Figure 4.15b). Also, the difference in distance to safety compared to the baseline case (Figure 4.15c) remains nearly constant with E-S 1, having an average of approximately 30 km, and E-S 2, with approximately 60 km. This sustains the conclusion that the dry pockets have a larger influence at lower run-ups.

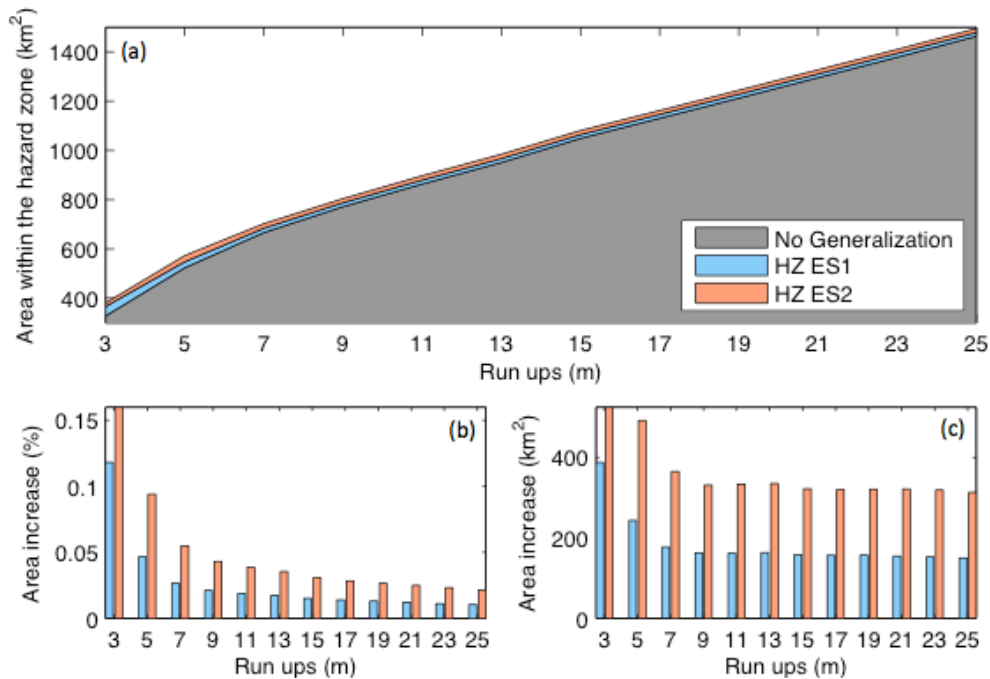


Figure 4.14 (a) Cumulative total area within the hazard of the baseline and generalization cases E-S 1 and 2 for each run-up between 3-25 m, (b) Percent increase in the area compared to the baseline for E-S 1 and 2, (c) Area increase within the HZ compared to the baseline for E-S 1 and 2

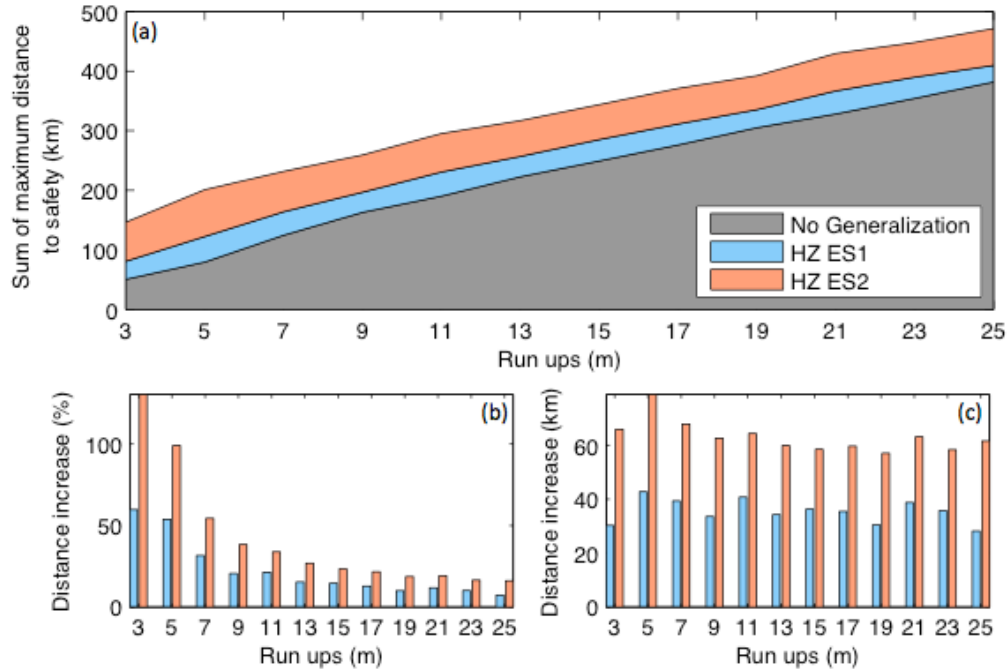


Figure 4.15 (a) Cumulative sum of the maximum distance to safety of each community for the baseline and generalization cases E-S 1 and 2 at each run-up, (b) Percent increase in the sum of the maximum distance to safety between the baseline and cases E-S 1 and 2, (c) Difference in the maximum distance to safety increase from the baseline for E-S 1 and 2

In conclusion, the process outlined by case E-S 1 is the best methodology for the generalization, because it satisfies the first objective of reducing the dry pockets. Although the S-E method also decreased the number of dry pockets, up to half still remain. Additionally, the S-E process reduced the HZ in unwanted locations. The E-S process using 1 cell instead of 2 or more is preferred, as those cases were overly conservative, removing all dry pockets smaller than 25 cells in size. This is substantiated by the fact that E-S 2 increases the distance to safety for the entire coast by over 100% for the lower run-ups of 3 and 5 m.

## Chapter 5. Tsunami Vulnerability of the West Coast

---

This following chapter presents the results obtained from the vulnerability assessment. First, a range of run-ups determined from the literature and suggested for each zone as a probable run-up range, the arrival time results are presented and compared to known values, followed by the hazard zone assessment, the available time results and finally communities with a greater vulnerability are discussed.

### 5.1 Run-Up Range

The maximum wave height and run-ups for known locations from the literature is presented in Table 5.1. The empirical method of doubling the tsunami wave height (zero-to-peak amplitude) is used to calculate the potential run-ups. This method is used as other empirical methods required knowledge of the offshore slope, onshore slope or roughness coefficient (Section 2.1.1).

The run-ups in Zone C vary greatly, mostly between locations directly on the coast and locations within bays and inlets. The maximum wave height was found in southern Vancouver Island with a value of 8.0 m, resulting in 16.0 m run-up. Followed by 7.0 m wave height in Port Alberni, which translates to a 14 m run-up. However, modeling coupled with geological evidence suggests that a run-up of 16.0 m occurred during the 1700 tsunami. This maximum exceeds the planning level for this zone of 10 m, which includes a factor of safety, by 60%. The maximum wave height is from Barkley Sound, 13.9 m, but is not taken as a maximum for this zone as it was an isolated maximum in the model and does not accurately represent the tsunami behaviour within the bay (Cherniawasky, et al., 2007). Adding a 50% for safety to the maximum run-up of 16.0 m results in 24.0 m.

Cherniawasky, et al. (2007) found a maximum wave height of 2.0 m in Zone D, near Victoria, resulting in 4.0 m run-up (6.0 m including FS). The planning level of 4.0 m (including FS) in this zone was found using maximum wave height of 1.3 m, which is underestimated compared to the results obtained by Cherniawasky, et al. (2007). The same authors found a maximum wave height of 1.5 m in the Strait of Georgia near Richmond in Zone E, resulting in a 3.0 m run-up, 4.5 m with FS. The wave height found is a 200% increase from the planning level wave height of 0.5 m.

Scarce evidence for Zone A and B make it difficult to assess probable run-ups. The maximum run-up observed in Zone A, in Haida Gwaii, is 13.9 m. This run-up occurred on the west coast of the island away from populated regions, which are located on the north and east coast. This value is likely an overestimation for this area, as this location directly faces the tsunami source, unlike

the populated northern and eastern side of the archipelago. However, the township of Masset, in Zone A, currently uses a planning level of 10 m. The planning level for these zones, 6.0 including the FS, is based on a 4.0 m run-up. However, as the recommended panning levels are underestimated for Zone C, D and E, a value of 4.0 m is also likely underestimated.

Table 5.1 Summary of maximum wave amplitude and run-up within the Canadian West Coast from the literature review of historical and modelled tsunamis. Maximum run-up calculated as twice the maximum wave height at the shore.

Zone	Location	Maximum wave height (m)	Maximum probable run-up (m)	Run-up including factor of safety	Source
A	Haida Gwaii (west coast)	2.0	4.0 13.9 <sup>1</sup>	6.0	(Ng, et al. 1990)b (Leonard and Bednarski 2014)
C	Cape Scott	0.8	1.6	2.4	(Whitmore 1993)
C	San Josef Bay	1.4	2.8	4.2	(Whitmore 1993)
C	Tofino	5.8	11.6	17.4	(Cherniawasky, et al. 2007)
C	Ucluelet	6.0	12.0	18.0	(Cherniawasky, et al. 2007)
C	Barkley Sound	7.0	14.0	21.0	(Cherniawasky, et al. 2007)
C	Port Alberni	7.0	16.0 <sup>2</sup>	24.0	(Ng, et al. 1990)b
C	South Vancouver Island	8.0	16.0	24.0	Ng, et al. 1990)b
D	Victoria	2.0	4.0	6.0	(Cherniawasky, et al. 2007)
E	Vancouver	1.5	3.0	4.5	(Cherniawasky, et al. 2007)

<sup>1</sup> Historical maximum run-up from the Haida Gwaii tsunami 2012

<sup>2</sup> Maximum run-up computed from numerical model

The minimum value for the probable range of run-ups is taken as the lowest run-up that has significant damage potential which is 3 m as described by Leonard et al (2013). The maximum value is taken as the sum of the maximum run-up for the zone (Table 5.1), including an additional 50% for safety in addition to 0.5 m for the 50-year sea level rise adaptation, as recommended by BC officials. The maximum for Zone A and B was taken as the maximum run-up used for emergency mapping in Masset, 10 m, plus the sea level rise adaptation. The effects of high tides are not added as the run-ups were computed from the HHW coastline. The range of run-ups considered, rounded to the nearest run-up computed, for each zone is as follows:

- Zone A: 3.0 – 11.0 m
- Zone B: 3.0 – 11.0 m
- Zone C: 3.0 – 25.0 m
- Zone D: 3.0 – 7.0 m

- Zone E: 3.0 – 5.0 m

## 5.2 Arrival Time

The vulnerability is primarily assessed using the available time ( $t_{available}$ ). As defined by Equation 4.1, it is a function of the tsunami first wave arrival time ( $t_{arrival}$ ) and the time to safety ( $t_{safety}$ ). Thus, it is imperative that the arrival time is as accurate as possible. However, as no tsunami propagation model has been performed for the entire BC coast providing consistent tsunami arrival times for all communities considered, data to validate the arrival time process is scarce.

The general trend of the arrival time results (Figure 5.1) follows what is theoretically expected. The arrival time is greater as the distance from the source (directly west of Vancouver Island, Figure 4.7) increases, as more distance is covered. Additionally, as the celerity, and therefore the arrival time, is a positive radical function (Equation 4.2) of the water depth (Figure 4.6), the arrival time is expected to be smaller in shallower areas compared its deeper counter parts. This phenomenon can be best observed in the area between the main coast and east of Haida Gwaii where the water depth is less than on the west coast of Haida Gwaii, resulting in a greater arrival time.

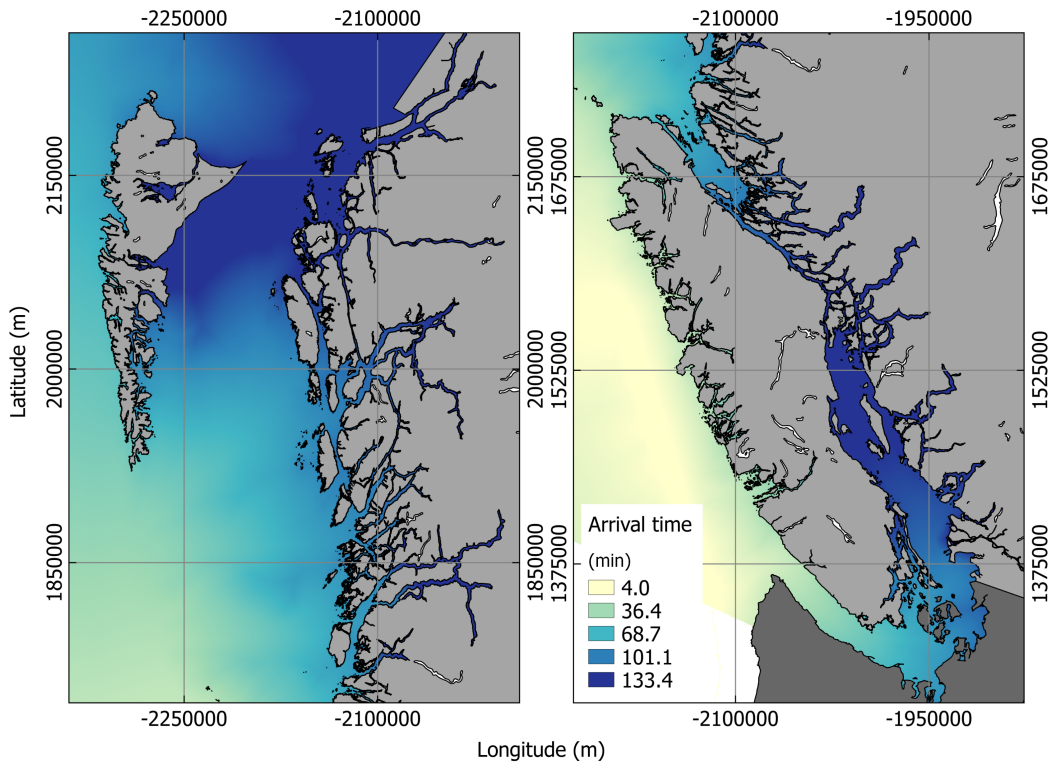


Figure 5.1 First tsunami wave arrival time ( $t_{arrival}$ ) in minutes for British Columbia, found using the arrival time process

As expected, the West coast of Vancouver Island has the shortest arrival time, approximately 30 min, as it is the closest area to the CSZ fault. The arrival time significantly increases in the Juan de Fuca Strait, south of Vancouver Island, in the most populous area near Victoria and Vancouver. North of Vancouver Island, on the main coast, the arrival time is approximately 70 min, with greater values in the adjacent inlets.

The BC Earthquake Alliance Society (2016) presents estimates of a tsunami first wave arrival time for some sites in the province based a numerical model of a CSZ earthquake of M 9.0. The numerical model, or the specific scenario considered is not specified. An M 9.0 CSZ earthquake can be produced by the Long-Narrow (used in this model), Long-Splayed and Short-North scenario defined by Satake, Wang and Atwater (2003). All three scenarios have a similar fault break near Vancouver Island and should not result in large discrepancies in the distance of the initial tsunami source. Arrival times are only available for 14 sites, five of which are within Zone C (Tofino, Ucluelet, Port Alberni and Winter Harbour), 4 are within Zone D (Sooke Harbour, Esquimalt, Victoria and Sidney) and 3 within Zone E (Delta, Richmond and Nanaimo). Only one site is presented for both Zone A and B: Prince Rupert and Bella Bella, respectively.

Underestimation of the arrival time is preferred rather than overestimation as an arrival time that is greater than the reality would overestimate the available time and not represent the risk appropriately. All sites in Zone C, except for Port Renfrew, are overestimated, as the difference between the estimated and calculated value is negative (Figure 5.2a). The largest differences are in Winter Harbour and Tofino, a difference of -12.3 min and -8.1 min, resulting in approximately 40% error. The difference for the remaining sites in Zone C range between -3.3min and 2.3min with an error between -8.4% and 6.6%. The difference in arrival time for sites in Zone D have a range between 4 min and 25.3 min, and the error is between 5.7% and 21.1%. For Zone E, the difference ranges from 14.9 min and 30 min and the errors between 11.0% and 22.2%. For Zone C, D and E, the difference in arrival time increases linearly with the site's distance from the tsunami source (Figure 5.2a). The error follows a similar trend (Figure 5.2b) but within a smaller slope. Tofino and Winter Harbour do not fit within the linear trend line of the error but do fit for the difference in arrival time.

The trend seems to indicate that some sites within Zone C may be overestimated because they are closer to the source. This may be due to the shallow-water assumption. As they are closer to the source near shallow water, a major portion of the water depth used to calculate the arrival time is shallower than the values within the shallow-water assumption (Figure 4.6). However, except for Tofino and Winter Harbour, the error is the smallest for Zone C. The sites in Zone D and E are within the area of limited bathymetry (Section 4.2.1, Figure 4.5). Considering that the error for these two zones is below 23%, the limited bathymetry and likely tsunami route does not seem to have a major effect on the arrival time results. Additionally, as all calculated arrival

times in these zones were less than the estimated values, this further proves that route 1 was a conservative assumption.

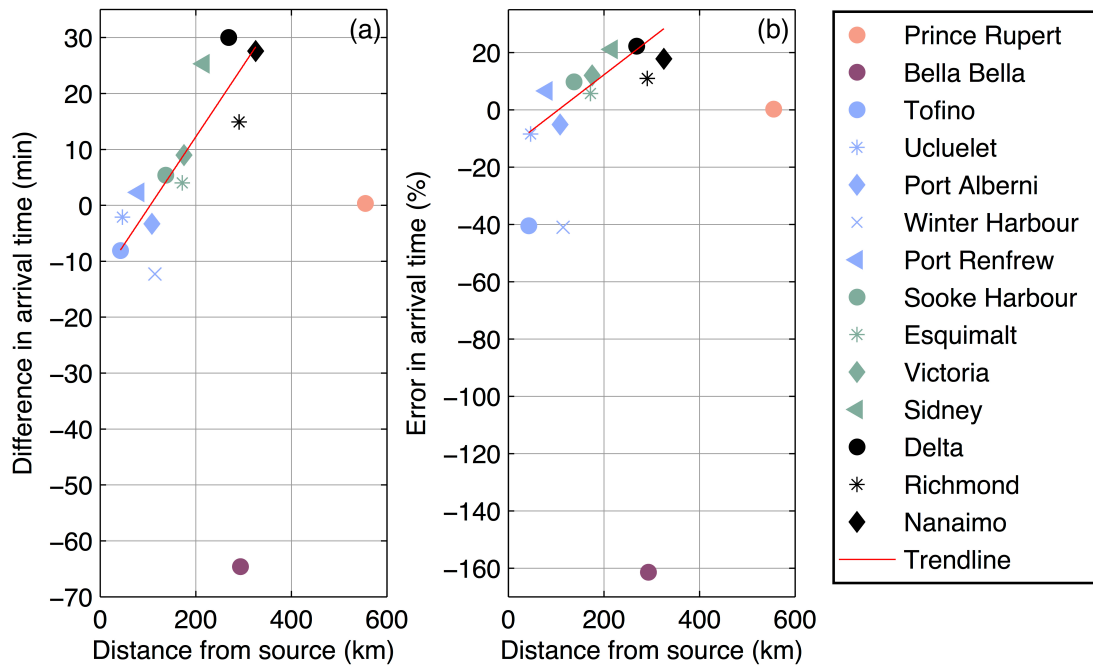


Figure 5.2 Validation of tsunami arrival time with estimate values from BC Earthquake Alliance Society (2016): (a) Difference in arrival time between estimated and calculated values; (b) Error of the calculated arrival times values as a function of the site distance from the tsunami source

The only arrival time value for Zone A, Prince Rupert, is the furthest site from the source and has the lowest difference with the estimated arrival time of 0.3 min resulting in an error of 0.2%. Contrastingly, the only site in Zone B, Bella Bella, has the largest difference in arrival time of -64.6 min, resulting in an error of -161.5%. Neither of these sites follows the linear trend of Zone C, D and E and no information can be concluded for sites North of Vancouver Island due to the limited dataset.

Bella Bella is located on the main coast approximately halfway between the southern tip of Haida Gwaii and the northern tip of Vancouver Island. Its arrival time estimated value of 40 min is likely underestimated, as it does not align with results from numerical models. The MOST simulation of the historical CSZ event of M 9.0 from 1700 shows that the tsunami wave first arrives near Bella Bella after 65 min (Witter, et al. 2011). In fact, at 40 min, the wave is at the edge of the northern tip of Vancouver Island. This is further supported from results Xie, et al. (2012) where a 2 hour isoline crosses the location of Bella Bella.

The few sites compared with the BC Earthquake Alliance Society (BC EA) for the first tsunami wave arrival time located in the Georgia Basin and on Vancouver Island south of Tofino are within 23% of the estimated value. The error increases as the distance from the source increases.

Tofino and Winter Harbour, located in central and North Vancouver Island follow the linear trend of the difference between calculated and estimated value similarly to their counter parts in Zone C, D and E unlike for the error. Nothing can be determined for Zone A and B, as only two locations are included and are both outliers. However, due to the few sites included in the BC EA dataset and the uncertainty attached to its source, few conclusions can be made. Nevertheless, the calculated arrival time using the Arrival Time process in GIS software follow general trends expected tsunami propagation behaviour. Additionally, as 10 of 14 points are within 23% error with the estimated values, the results are deemed acceptable.

### **5.3 Hazard Zone**

The severity of the hazard posed by the tsunami run-up is dependant on the local topography. Areas with steep mountainous terrain will have less area within the HZ as the elevation increases rapidly. In contrast, low run-ups may negatively affect valleys and floodplains, as flat and low-laying areas are flooded. The province of BC has both steep mountains and flood plains created by low-laying areas.

BC is covered by dense forests on vast plateaus located between two major mountain chains stretching north-south on either side of the province. More specifically, the Pacific Cordillera to the west creates the Insular Mountain range and Coast Mountain Range. The Coast Mountains extend from south-western Yukon to the Fraser River covering the entire BC coast. The uppermost part of the Insular Mountains creates Haida Gwaii and Vancouver Island and is the reason for the many islands and deep fjord-like inlets seen on the coast. At the southern base of the Coast Mountains, east of the Strait of Georgia is a low-laying basin, often referred to as the Lower Mainland. This area lies at the mouth of the Fraser River and encompasses the Greater Vancouver area. This creates a floodplain in the Delta and Surrey regions. On Vancouver Island, other coastal floodplains exist in Cowichan 1 reserve, Campbell River, Comox, Parksville, Nanaimo, Tahsis, Zeballos and Port Hardy. On the main coast, floodplains are also found in Kitimat, Stewart, Bella Coola and Squamish.

The surface area within the HZs created for the range of run-ups considered in this study, 3 to 25m, is presented in Figure 5.3. The surface area is cumulative as higher run-ups will also include the previous run-ups area. Only the areas within communities were compiled.

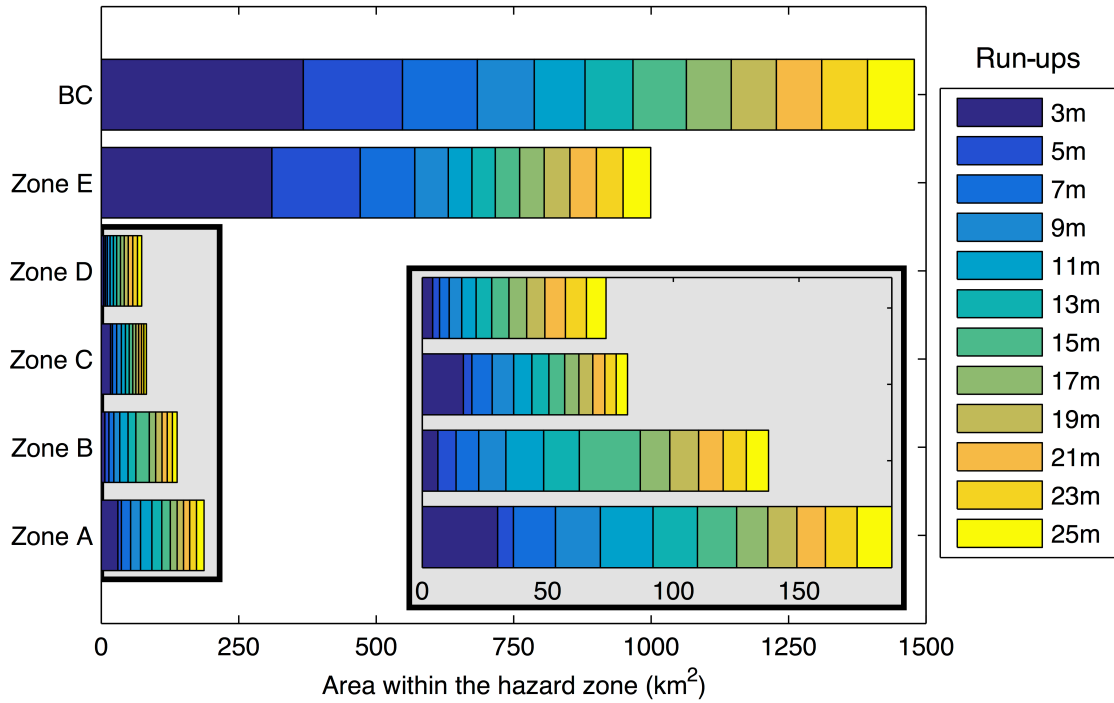


Figure 5.3 Cumulative surface area within the hazard zone (HZ) for run-ups between 3-25 m for each Tsunami Notification Zone (TNZ)

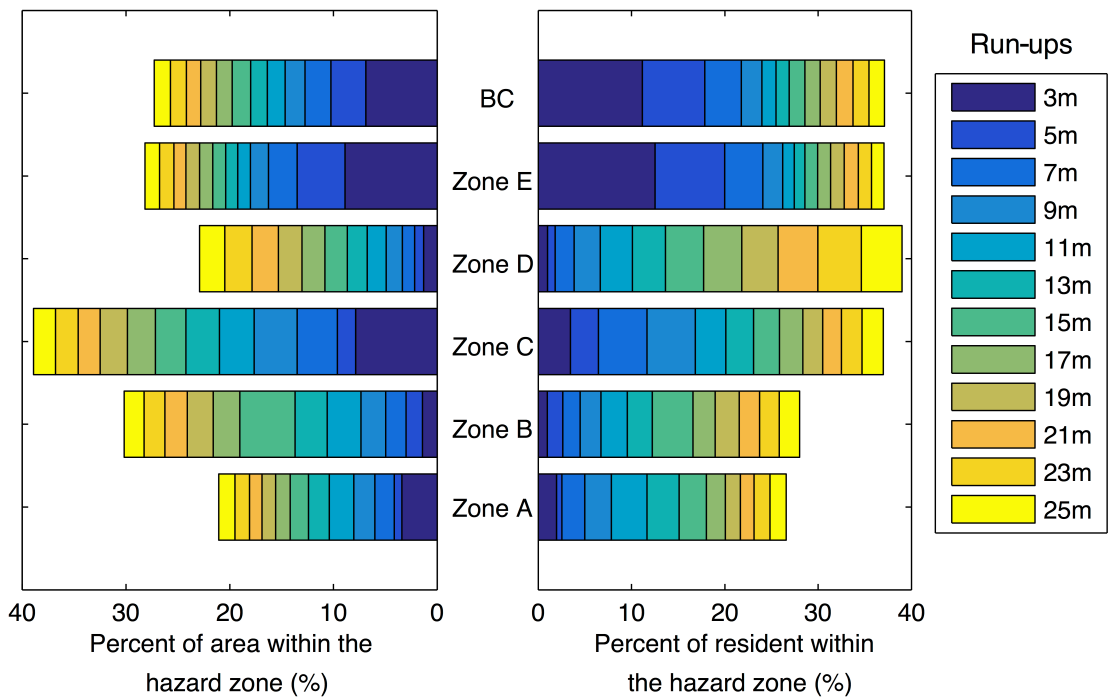


Figure 5.4 Cumulative percentage of the inundated area and resident population within the hazard zone (HZ) for run-ups between 3-25 m for each Tsunami Notification Zone (TNZ)

Zone E, having 37.5% of all communities, is the major contributor of the surface area within the HZ of the entire province, representing 67.6% of the total at the maximum run-up of 25 m. Because of the lower-mainland, lower run-ups affect Zone E the most. A 3 m run-up produces 31.0% (310.1km<sup>2</sup>) of the total flooded area created by run-ups up to 25 m. At the maximum probable run-up of this zone, 5.0 m, a total of 470.9 km<sup>2</sup> are inundated, representing 14.1% of the the zone (Figure 5.4).

Unlike Zone E, which is primarily characterized by low-laying areas, Zone A to D have primarily mountainous terrain. Zone D has the least amount of surface area of all zones, which correlates with the fact that it has the least amount of communities. The total area within the HZ at 25 m run-up is only 73.2 km<sup>2</sup>. At the maximum probable run-up of 7.0 m, the total inundated area is 10.7 km<sup>2</sup>, representing 3.7% of its total area. The HZ surface area increase in Zone D is almost consistent, which suggests consistent terrain sloping. Zone B follows a similar trend, however has a slightly larger increase occurring at 15 m. The total area within the HZ at the maximum probable run-up of 11 m for Zone B is 91.9 km<sup>2</sup>, 11.2% of its total.

Zone C and A experience their largest increase in HZ at the initial 3.0 m run-up. For Zone C this results in 20.1% of the total HZ (81.7 km<sup>2</sup>) and 16.1% for Zone A. Following this, the HZ increases steadily, by 7.3% and 8.1% for Zone C and A. This suggest that Zone A and C have generally a larger low-laying area below 3 m elevation followed by average sloping grounds. At the maximum probable run-up of 25 m and 11 m, 81.7 km<sup>2</sup> and 91.9 km<sup>2</sup> are inundated in Zone C and A respectively. This represents, 38.6% and 10.8% of the total surface area of each respective zone.

The resident population within the HZ (Figure 5.5) is calculated as the surface area within the HZ times the population density obtained from the 2011 census. At the maximum run-up of 25 m, a maximum of 1.12 million residents were found to live within a hazard zone, 36.9% of all the total population living within a coastal community (Figure 5.4). Zone E, is again the main contributor to the HZ population due to the large urban centre found in the Strait of Georgia, contributing 88.0% of the total for the province. At the maximum probable run-up of 5 m, approximately 534,000 individuals are within the HZ, representing 17.8% (Figure 5.4) of the total population of Zone E. The population within 5 m run-up of Zone E is significantly more than the entire population within all other zones. The second most populous zone is Zone D. At the maximum probable run-up of 7 m, approximately 11,000 residents are within the HZ, representing 3.84% of its population.

Zone C has the largest percentage of its area within the HZ at the maximum run-up level, 39.6%, resulting in the highest percent of its population at-risk, 37.0%. But as Zone C is comprised of small towns and village, the total population at-risk is still low, 11,469 at 25 m run-up. The

population at-risk increases more rapidly from 3 m to 11 m run-up, with an average increase of 1238 people, followed by an increase of 753 people from 13 m to 25 m.

Zone A and B have a very similar population at-risk distribution. The total residents within the hazard zone for the maximum probable run-up of these two zones of 11 m is 2540 and 1995 respectively. This represents 11.7% and 9.6% of their total population.

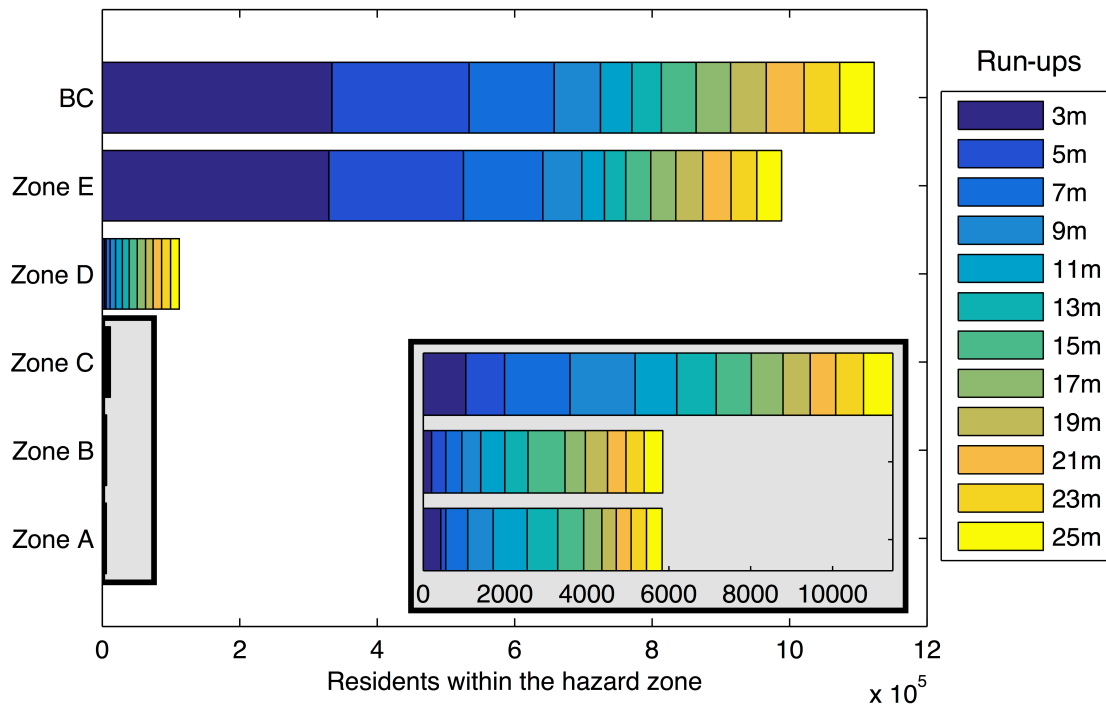


Figure 5.5 Cumulative resident population within the hazard zone (HZ) for run-ups between 3-25 m for each Tsunami Notification Zone (TNZ)

The average increases in population with 2 m run-up for Zone A, B and C are 486, 487 and 955 respectively. If the increase in population at-risk is distributed evenly throughout the communities, each community only experiences an increase of a few individuals in the HZ as the average community size is 183, 131 and 205 for Zone A, B and C respectively. However, the population at-risk is more likely to be disproportionately distributed. Even with low population at-risk compared to Zone E, the fact that these communities in these three zones are distributed throughout a large area, could translate into a high demand on the emergency personnel and infrastructure. In Zone C, this situation is aggravated by the fact that a large percentage of communities could potentially be inundated, further limiting resources and space to house a large portion of their population.

### 5.4 Available Time

The following section presents the statistical distribution of the communities’ minimum available time by TNZ, followed an examination of communities with the greatest vulnerability. A vulnerability scale (Figure 5.6) is established to better evaluate the community’s relative risk. A high vulnerability is established for available times of 15 min or less. The life safety threshold is an available time of 0, as a negative value implies insufficient time for pedestrians to evacuate to safety. A value of 15 min is used as the upper threshold of the high vulnerability category, instead of the life safety threshold, for consideration of the duration of the earthquake, tsunami warning message dissemination and personal effect gathering, such as the emergency kits. It was also chosen that distance to safety is the most direct route to safety and did not consider the built environment. In reality, the distance to safety may be longer due to obstacles. The moderate vulnerability upper threshold is taken as twice the value of the high vulnerability, 30 min. Finally, low vulnerability is any available time above moderate. High vulnerability is interpreted as areas where there is not enough time to evacuate or has little time to spare before evacuating to higher ground. Moderate vulnerability, on the other hand, is an area where there is sufficient time to evacuate with considerable time to spare.

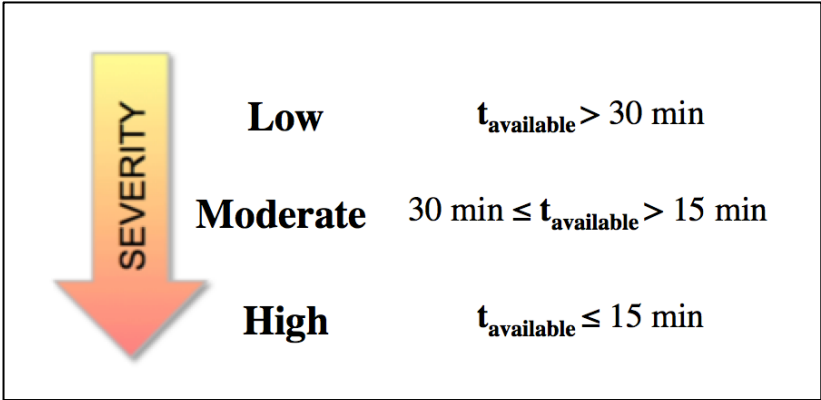


Figure 5.6 Available time vulnerability scale

#### 5.4.1 Available Time by Zone

The statistical distribution of the minimum available time for each community for three evacuation velocity – mobility-impaired (MI), average adult ambulatory (AW) and slow run (SR) – is presented in Figure 5.7-5.12.

##### *Zone A and B*

All communities in Zone A (Figure 5.7) have a low vulnerability, as they all have an available time above 80 min at the maximum probable run-up of 11 m. At the most extreme run-up of 25 m, all communities remain within the low vulnerability category as the minimum available time

is 50.2 min. The available time distribution is symmetrical with an average median available time of 152.2 min for all three velocities for the considered run-up range. There is little variation in available time between the three pedestrian velocities until 21 m.

The community minimum available time is slightly skewed to the right for Zone B (Figure 5.8), having many communities as outliers with large available time. Few outliers are present below the 95<sup>th</sup> percentile at run-ups above 3 m. The median is 107.2 min and the minimal value is above 50 min for all run-ups. Similar to Zone A, all communities have a low vulnerability for the entire range of run-ups and at the extreme run-up of 25m.

The uncertainty of run-up value in Zone A and B from a Cascadia tsunami is great due to the limited evidence. But even without reliable run-up, it's determined that these two zones have a low vulnerability to a CSZ tsunami. This is primarily due to their large arrival times, having a minimum value of 83.1 min and 66.3 min for Zone A and B. The second closest tsunami source, the Aleutians, would likely produce a low vulnerability for the communities in these two zones as the arrival time would be even greater than a CSZ event, with values of 2 hours or greater. The largest threat to these areas is likely from a local tsunami, such as ones produced by landslides or submarine landslides, as they would have much shorter arrival times.

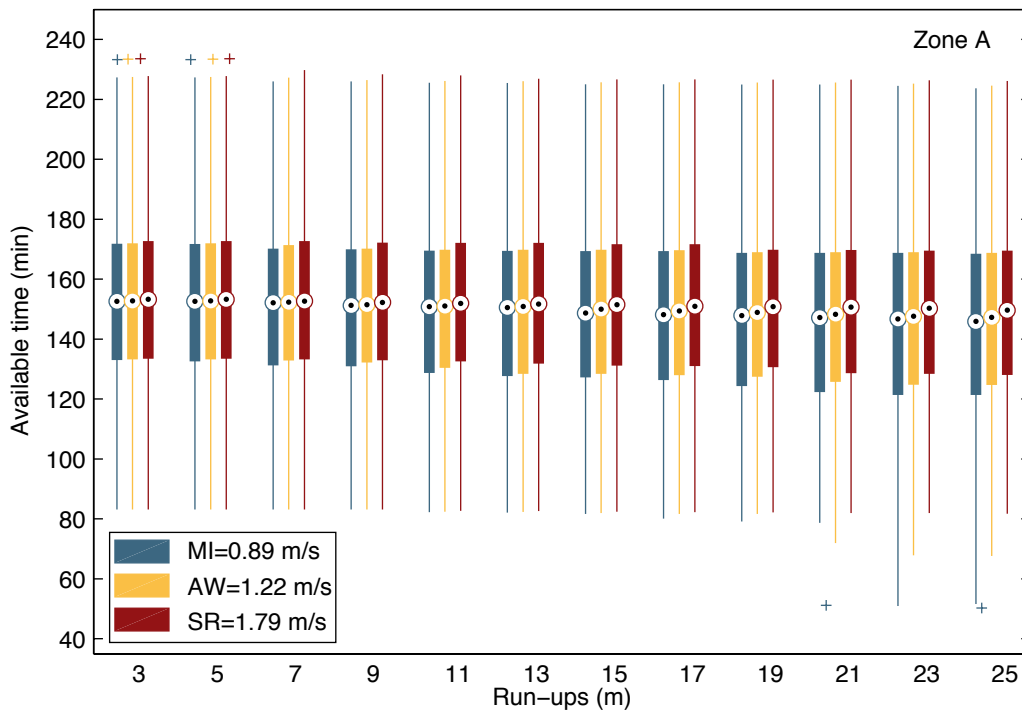


Figure 5.7 Boxplot of the minimum available time of communities within Zone A for run-ups between 3 and 25 m

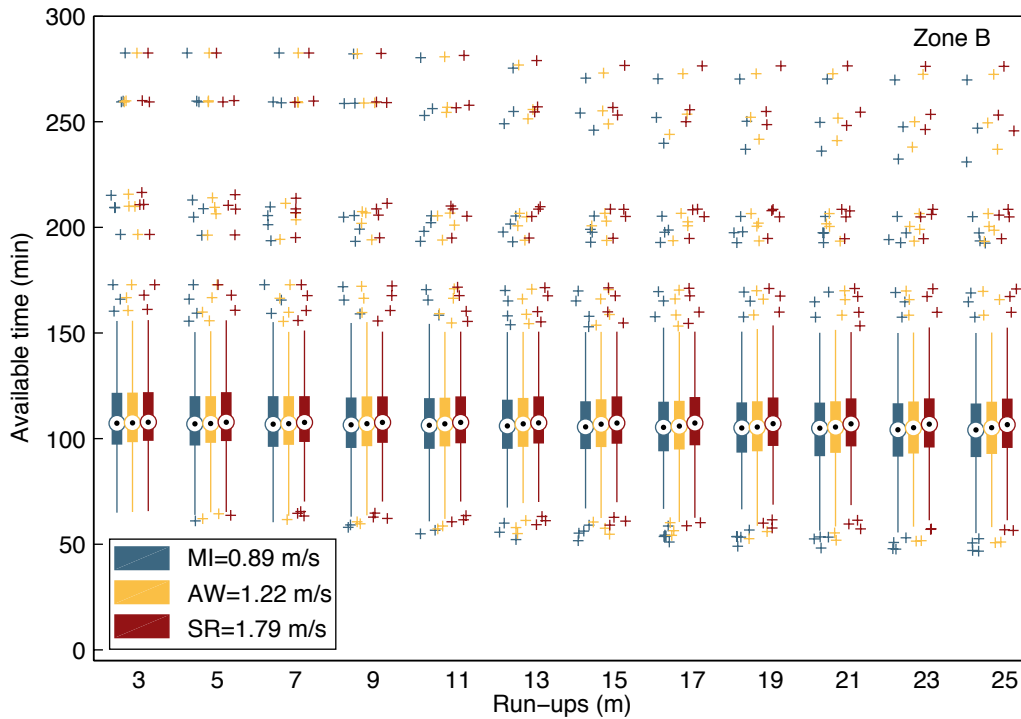


Figure 5.8 Boxplot of the minimum available time of communities within Zone B for run-ups between 3 and 25 m

### Zone C

The range of probable run-ups for Zone C is the largest in the province, being between 5 and 25 m. The median available time in this zone is 35.1 min for all run-ups and velocities, meaning that more than 50% of the communities have a low vulnerability (Figure 5.9). Additionally, 75% of the communities have a low vulnerability 11 m run-up. Subsequently, 25% of the communities have a moderate vulnerability at 9 m run-up and above for MI velocity, 11 m run-up for AW and 13 m run-up for SR, as the 75<sup>th</sup> percentile is less than the 30 min threshold. The first community to reach the high vulnerability threshold occurs at 7 m run-up for MI, 9 m run-up for AW and 17 m run-up for a SR. Starting at 11 m run-up, one community is below the life safety threshold, Grassy Island No. 17. Additional communities breach this threshold at 21 m run-up.

The Zone C dataset is slightly skewed to the right, towards larger values. Many more outliers exist above 1.5 standard deviations from the media (large available time) than do below (small available times). The average standard deviation is 16.2 min. The difference in the median and minimal value of the available time for the three pedestrian velocity is less than 1 min for run-ups up to 5 m. The difference increases with run-ups, due to the short arrival times and large increase in distance to safety with increasing run-ups.

Individuals that may have a slower walking speed than the average adult – people with disabilities, seniors or adults with young children – are at higher risk in Zone C, as high vulnerability is reached as early as 7 m run-up. However, even healthy adults able to travel at a SR pace are still at risk as SR available time breaches the high vulnerability thresholds at 21 m. In addition, as the run-up increases, so does the distance to safety and an individual would need to maintain the SR pace for longer distances and for over 25 min, which can be a difficult task.

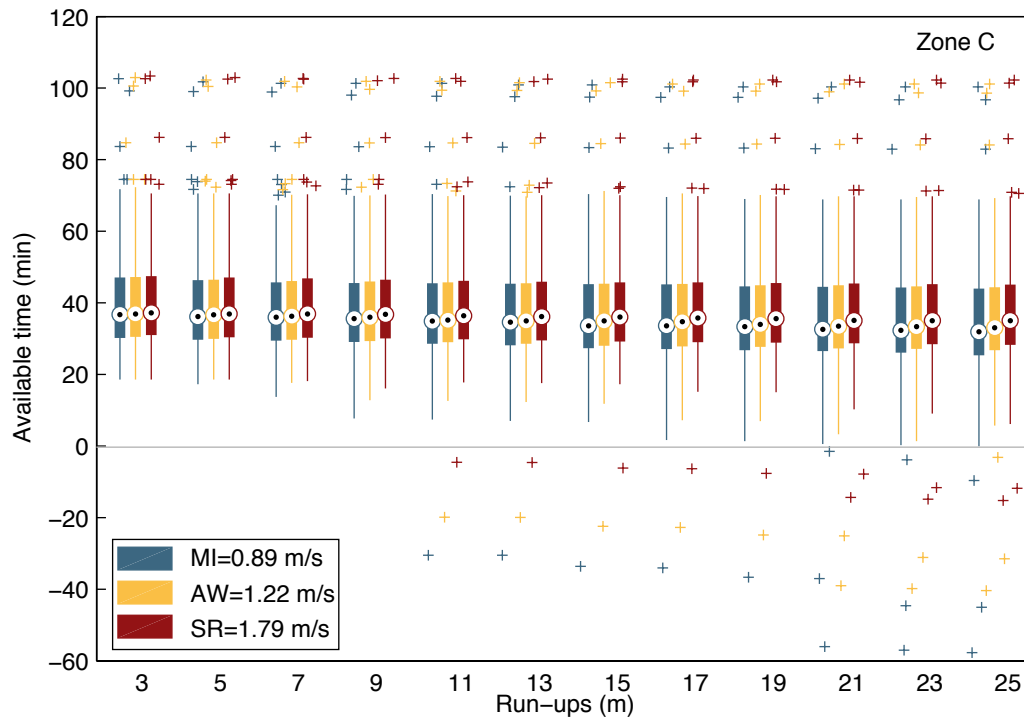


Figure 5.9 Boxplot of the minimum available time of communities within Zone C for run-ups between 3 and 25 m

### Zone D

As the waves are attenuated while passing through the Strait of Juan de Fuca, the probable run-up range for Zone D is rather small, from 3 m to 7 m. For this range, all communities have a low vulnerability at all velocities and have an average median available time of 58.7 min (Figure 5.10). This high median is caused by the high arrival time in this zone, averaging 64.9 min. Moderate vulnerability threshold is first breached by an outlier at 15 m run-up for a MI available time, and at 25 m for AW available, well beyond the probable maximum run-up of 7 m. The maximum difference in the MI and SR available time, at 7 m run-up, is 6.25 min. Zone D has the smallest sample sizes with only 24 communities, and this limited dataset is not normally distributed.

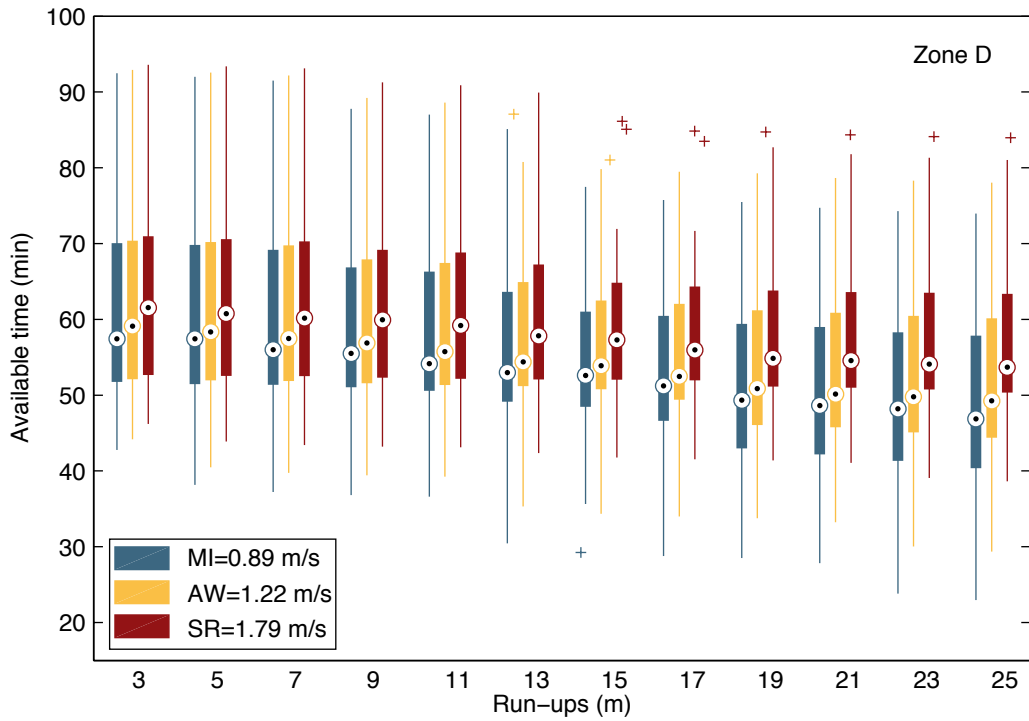


Figure 5.10 Boxplot of the minimum available time of communities within Zone D for run-ups between 3 and 25 m

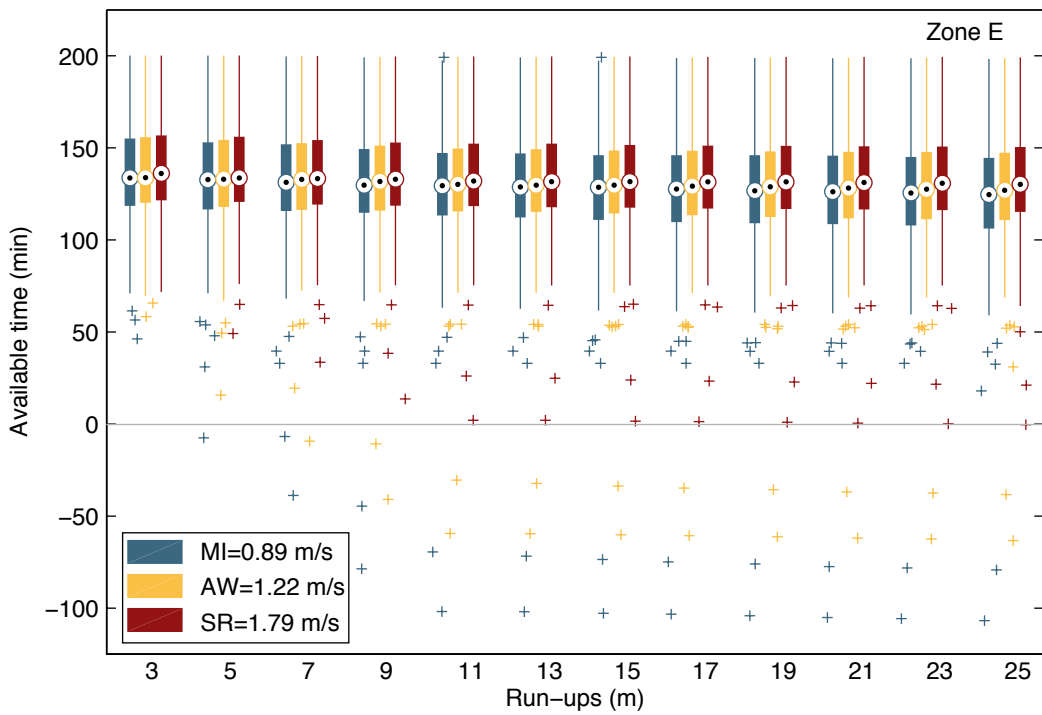


Figure 5.11 Boxplot of the minimum available time of communities within Zone E for run-ups between 3 and 25 m

## *Zone E*

Similar to Zone D, Zone E has a very small probable run-up range, between 3 and 5 m, due to tsunami wave attenuation. The attenuation and wave propagation through the Strait of Juan de Fuca and then Georgia results in the highest arrival times, with an average of 137.8 min. Consequently, the available time average median is also the highest of all zones, 133.9 min (Figure 5.11). The dataset contains many outliers below 1.5 standard deviations from the median. All communities have a low vulnerability at the 5 m run-up, except for one community at the MI and AW velocity, which has a high vulnerability. However, because the arrival time is so large, individuals evacuating at a SR velocity would need to maintain this pace for over an hour, which is unlikely. Two communities are below the life safety threshold at a 7 m run-up, 2 m above the maximum probable run-up. For such high arrival times, evacuation by car may be possible. The communities in this zone have a low vulnerability to a CSZ tsunami. This tsunami hazard is further decreased by the fact that the greater Vancouver region is protected by an elaborate system of dykes and flood control measures, which may reduce the run-up from a tsunami wave. However, the run-up could also be increased if the dikes are breached. Tsunami waves overtopping the protective structures during the Tohoku tsunami in 2011 were accelerated due to the shape of the structures. This could be of concern in the Vancouver area for larger tsunami waves that may occur due to landslides or if tsunami waves are coupled with extremely high tides. The vulnerability to the zone would definitely increase for local tsunamis from landslides as the arrival time would be decreased significantly.

### **5.4.2 Moderate and High Vulnerability Communities**

Communities with a high or moderate vulnerability within their probable run-up range are further discussed below. All the communities are within Zone C, of which are 5 non-indigenous communities and 45 First Nations communities. The First Nations communities are separated within 6 sub-regions along Vancouver Island. Where the data is provided, the available time is also computed with the BC EA estimated arrival times and compared with the computed available time. Two communities from Zone E, Delta and Richmond, are also further examined as they have a significantly lower available times than their counter parts and reach life safety within or near the range of probable run-ups.

#### *Zone C Non-Indigenous Communities*

Tofino was found to have the lowest available time computed with both the model and BC EA arrival time. Tofino is located on the Esowista Peninsula on the west coast of Vancouver Island (Figure 5.12), directly in the trajectory from a CSZ tsunami. This results in a low arrival time, calculated as 28.1 min, 8.1 min above the BC EA estimate value. The peninsula has higher grounds at the north, where the main village is located, and residential and commercial areas in

the low-laying parts to the south. The low-laying area has an elongated shape resulting in large distances to safety. This effect combined with the small arrival time causes the low minimum available times.

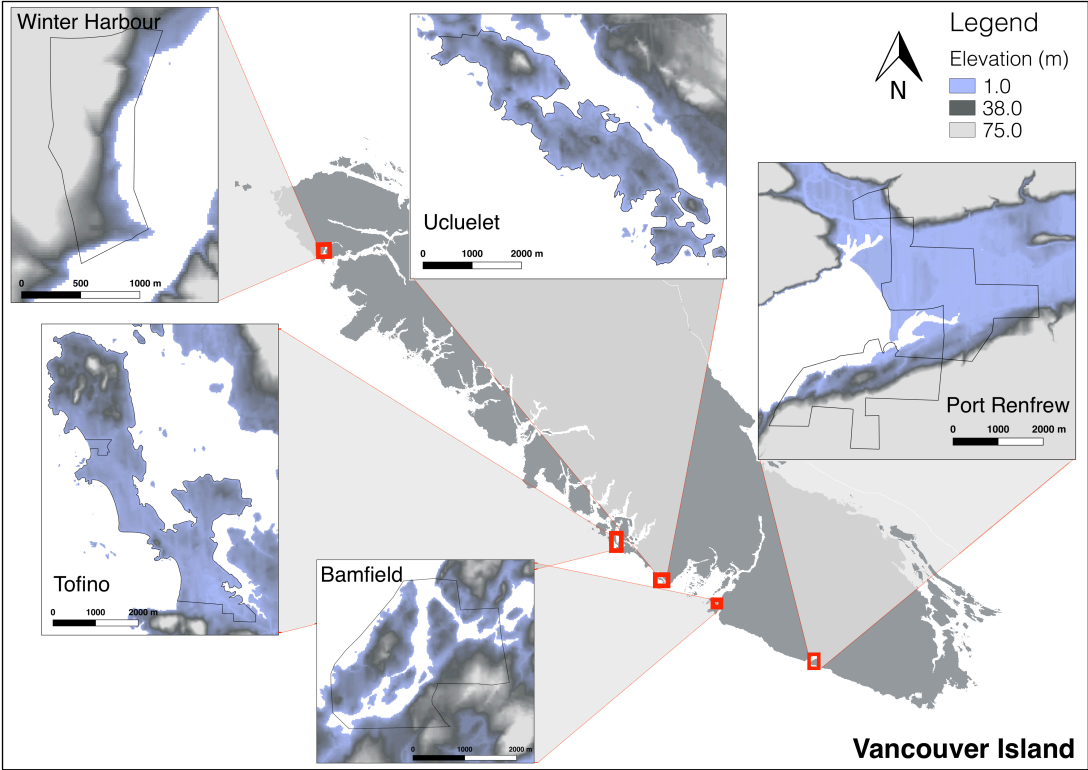


Figure 5.12 Location of non-indigenous communities with high and moderate vulnerability communities within Vancouver Island (Zone C)

At the lowest probable run-up of 5 m (Figure 5.13), the minimum available time is within the moderate vulnerability for all velocity. For the best case scenario, an adult capable of a slow run, high vulnerability is reached at 21 m run-up and 11 m run-up using the model and BC EA arrival time respectively. The life safety threshold is not breached at this velocity. For an AW velocity, the high vulnerability is reached at 15 m and 9 m using the model and BC EA arrival time, similarly using the MI velocity, the high vulnerability is reached 13 m and 7 m. The 8 min difference in the arrival time decreases high vulnerability run-up by 6 m. However, it causes an 8 m decrease in the life safety threshold run-up for the MI velocity, occurring first at 17 m. The life safety threshold is only breached with the AW velocity using the BC EA arrival time, at 21 m run-up.

Tofino has an average available time of 10.9 min, for all data points in the probable run-up range. The available time decreases with run-up from 3 m to 21 m at a rate of -1.4 min/m, -1.1 min/m and -0.70 min/m for MI, AW and SR velocity. For run-ups greater than 21 m the decreasing rate has an average of -0.12 min/m. This is due to small increases in the HZ from

steep hills. Tofino is further examined as a case study in the following chapter including a study of possible life safety mitigation systems from vertical evacuation structures.

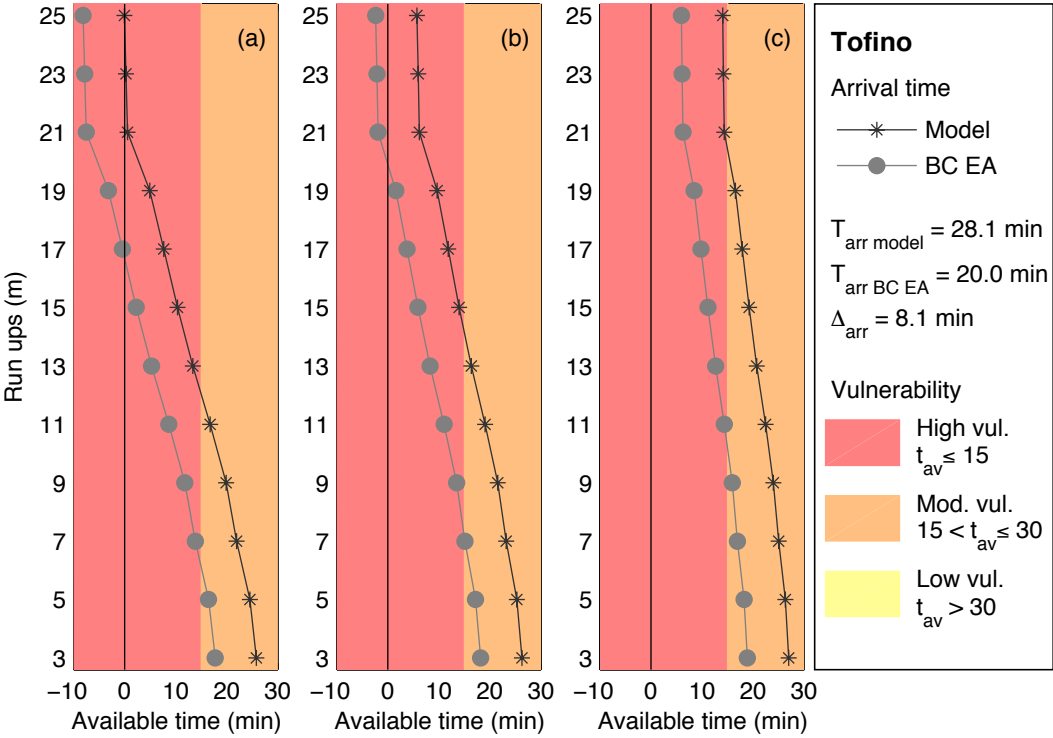


Figure 5.13 Minimum available time of Tofino using the model and BC EA tsunami arrival time for a range of run-ups between 3 and 25 m for three velocities: (a) Mobility impaired pedestrian ambulatory speed (MI); (b) Average adult ambulatory speed (AW); (c) Slow run (SR)

Ucluelet has a similar shape to Tofino, located 40 km south, on the Ucluth peninsula (Figure 5.13). However, its topology differs greatly, as it does not have a major low-laying area, but instead has higher elevations in the centre of the municipality and on the edges of smaller outcropping peninsulas, sloping downwards toward to shore. This change in topography is reflected in higher available times (Figure 5.14). The computed arrival time of 27.1 min is 2.1 min larger than the BC EA value of 25 min.

The available time decreases linearly with run-up until 21 m, at an average rate of -0.46 min/m and -0.36 min/m and -0.23 min/m for the MI, AW and SR velocity. A larger decrease in the available time, between 3.8 min and 7.7 min, occurs at 21 m. The initial small decreasing rate results in the small difference of 2.1 min in the computed arrival times and BC EA data increases the run-up at which the high vulnerability category is reached for the MI velocity by 6 m, from 23 m to 17 m. The change in arrival time does not affect at which run-up the high vulnerability threshold is reached for the AW velocity, occurring uniformly at 23 m. The SR available time only reached high vulnerability with the BC EA arrival time at 25 m run-up. The life safety threshold is not breached at any velocity in Ucluelet.

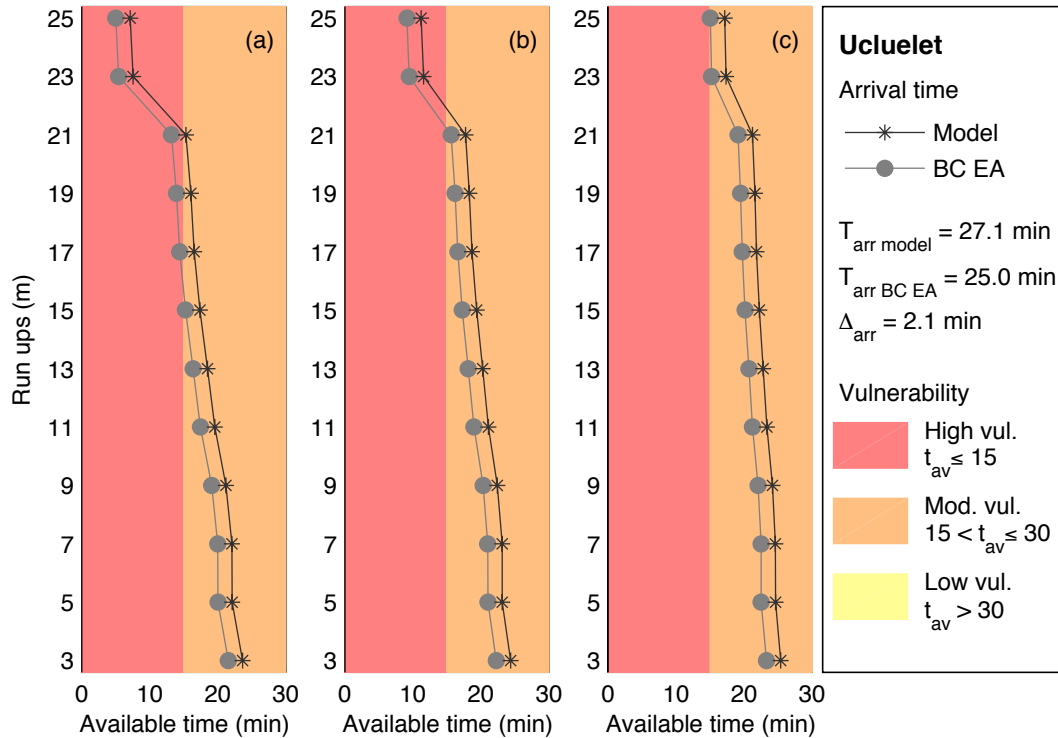


Figure 5.14 Minimum available time of Ucluelet using the model and BC EA tsunami arrival time for a range of run-ups between 3 and 25 m for three velocities: (a) Mobility impaired pedestrian ambulatory speed (MI); (b) Average adult ambulatory speed (AW); (c) Slow run (SR)

The current tsunami evacuation plan in Ucluelet designates elevation above 20 m as safe. The minimum available time at this run-up is approximately 14 min, indicating that life safety should be maintained in this community.

These results are underestimated compared to the agent-based evacuation modeling that was performed in Ucluelet by Johnstone and Lence (2012) as life safety threshold is not surpassed. For run-ups ranging between 10 m and 20 m (the hazard scenario did not cause even run-ups within the community) and an arrival time of 20 min, the authors projected casualties between 237 and 1149 depending on the season and time of day. The authors found that pedestrian evacuation is the most efficient and that 80% of individuals would reach a safe haven within 45 min. The results of this study are likely underestimated compared to the agent-based simulation that was limited to the road network and individuals were only considered safe when they reached limited safe havens instead of any elevation above the run-up. Using the road network increased in the agent-based model also because of congestion on connecting bridge. Direct comparison cannot be done as the pedestrian velocity used by Johnstone and Lence (2012) is not specified.

Port Renfrew is located along the southeast portion of Port San Juan bay, at the entrance of the Juan de Fuca Strait (Figure 5.13). A portion of the town borders the bay and has an elongated

shape at the foot of larger mountains and the remaining portion is located within a low-laying basin at the head of the bay. The computed arrival time is 2.3 min larger than the BC EA value of 35 min. The available time decreases rapidly until a 9 m run-up at an average rate of 4.4 min, 3.5 min and 2.2 min for MI, AW and SR velocity (Figure 5.15), due to the low-laying basin. After 9 m, the ground slope increases rapidly resulting in insignificant increase in the hazard zone. This causes the available time slope to be almost zero, ranging from -0.062 min/m to -0.13 min/m. The high vulnerability threshold is reached at 7 m and 9 m run-up for the MI and AW speed. The threshold is never surpassed for the SR velocity.

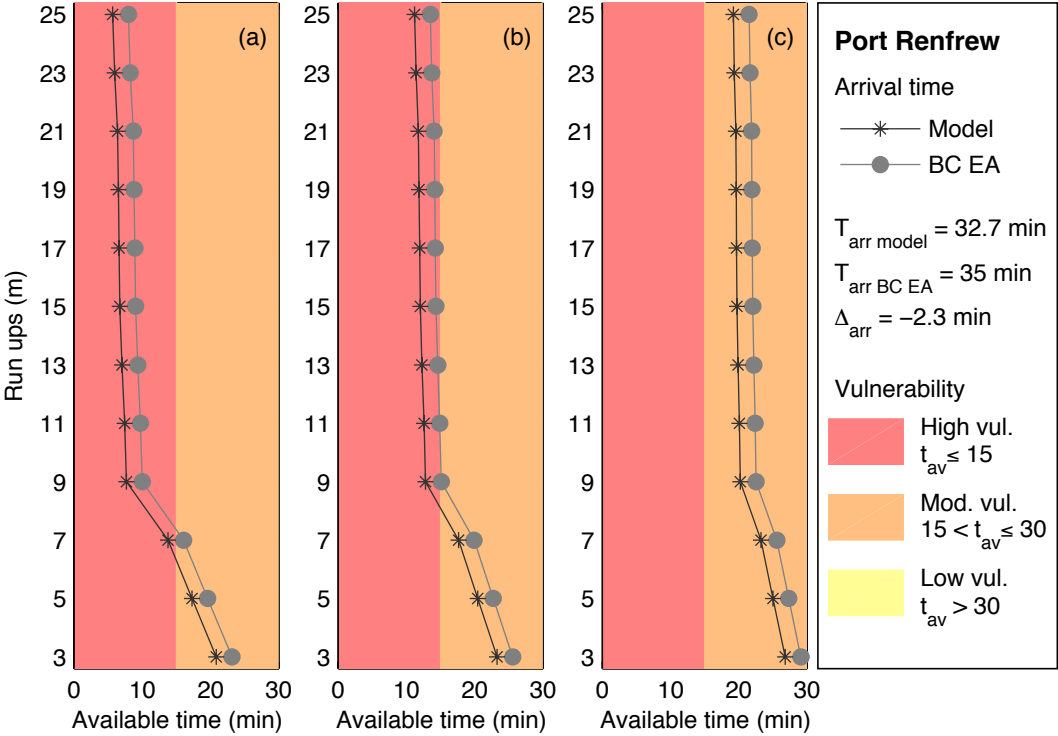


Figure 5.15 Minimum available time of Port Renfrew using the model and BC EA tsunami arrival time for a range of run-ups between 3 and 25 m for three velocities: (a) Mobility impaired pedestrian ambulatory speed (MI); (b) Average adult ambulatory speed (AW); (c) Slow run (SR)

Step slopes are harder to climb and more time consuming than walking on flat ground, as described Nalsmith’s rule and Toblers hiking function (Langmuir 1984, Tobler 1993). The available time for the run-ups within the steepest slopes, between 9 m and 25 m, differ only by 2.0 min for the worst case-scenario, MI velocity, ranging from 5.7 m to 7.7 min. It is likely that more time would be required for an individual to travel uphill, mostly if such an individual has mobility impairment. Careful consideration to this aspect should be taken for the evacuation planning above 9 m run-up at this location, which is likely as the wave heights in south Vancouver Island were found to be as high as 8 m, resulting in a 16 m run-up without including the factor of safety. In addition, wave amplification may occur, as it is located within a bay.

Winter Harbour is a small village located north of Vancouver Island, located within a small harbour (Figure 5.13). Its small size and location on steep slopes causes very small difference in the distance to safety resulting in a difference in available time of 1.4 min between the 3 m and 25 m run-up (Figure 5.16). The average available time computed with the model arrival time is 39.5 min, within the low vulnerability category. Using the BC EA arrival time, which is 12.3 min less than the computed value, results in an average available time to 27.2 min, on the higher end of the moderate vulnerability category.

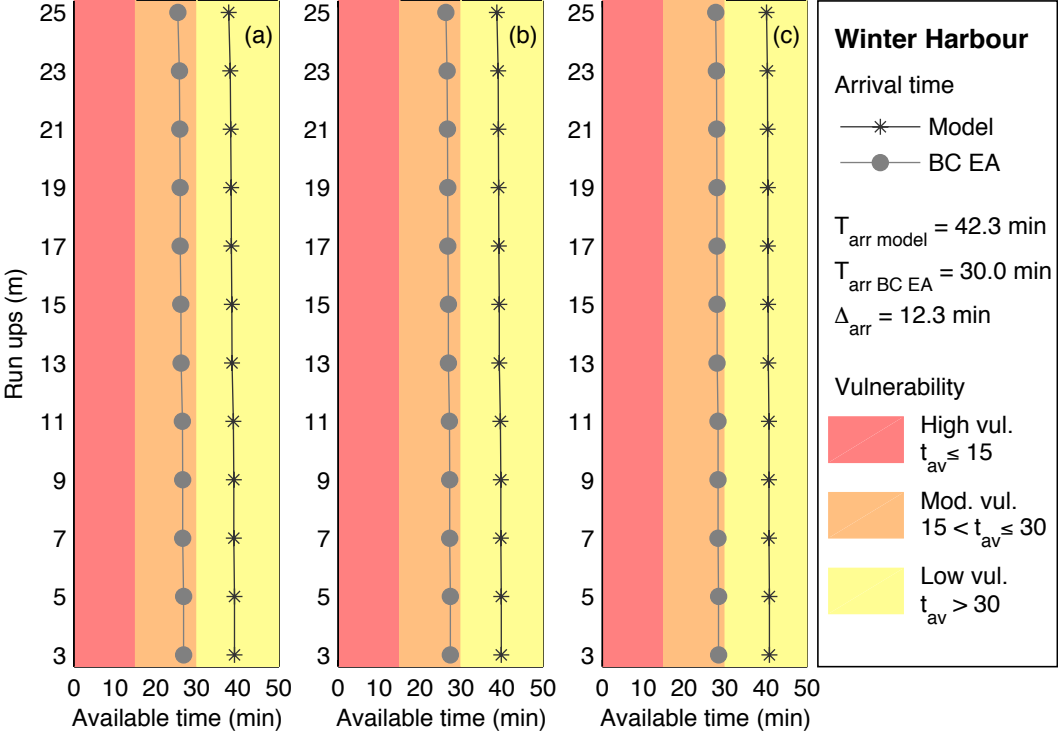


Figure 5.16 Minimum available time of Winter Harbour using the model and BC EA tsunami arrival time for a range of run-ups between 3 and 25 m for three velocities: (a) Mobility impaired pedestrian ambulatory speed (MI); (b) Average adult ambulatory speed (AW); (c) Slow run (SR)

The available time in Bamfield, located on the southeast entrance of Barkley Sound (Figure 5.13), follows a similar behaviour. The available time of this community varies a maximum of 5.8 min between 3m and 25 m run-up (Figure 5.17). The available time decreases at a maximum average rate of -0.26 min/m. The moderate vulnerability threshold is surpassed at 5 m run-up for VI velocity and 13 m for the AW velocity, and not reached at all for the SR velocity. The geometrical characteristics of Barkley Sound amplify the waves in this region, and as a result run-ups in Bamfield may be very high. For the worst-case scenario of a maximum run-up of 25 m the minimum available time is 24.8 min, also on the higher end of the moderate vulnerability range. The risk of casualties in Bamfield and Winter Harbour is therefore low as the minimum available times are 24.7 min and 25.4 min respectively.

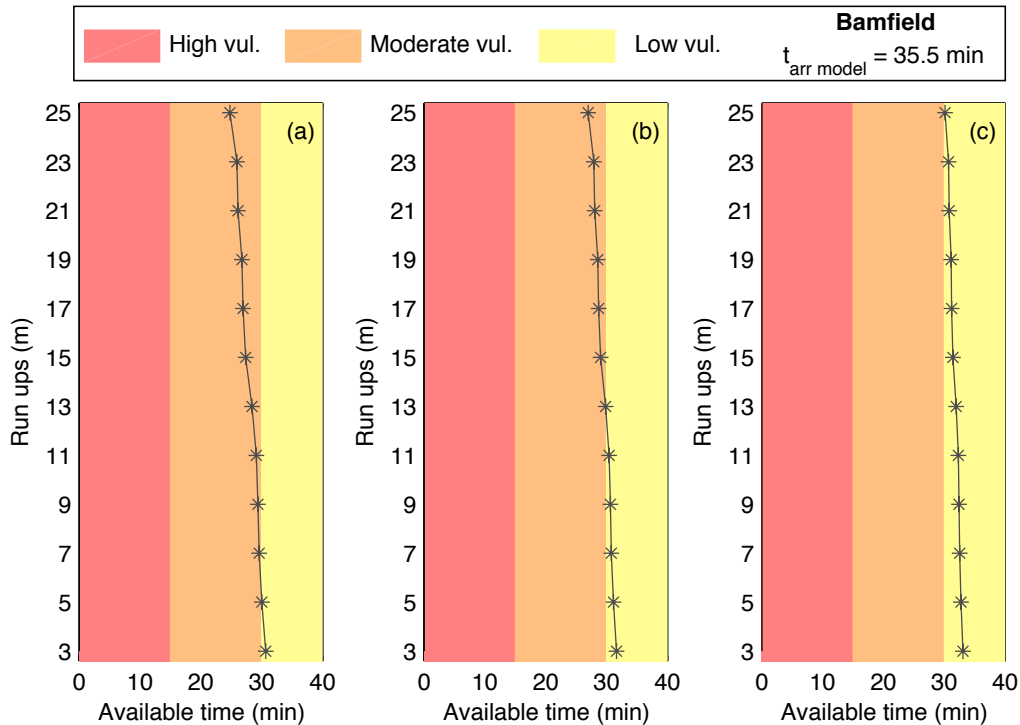


Figure 5.17 Minimum available time of Bamfield for a range of run-ups between 3 and 25 m for three velocities: (a) Mobility impaired pedestrian ambulatory speed (MI); (b) Average adult ambulatory speed (AW); (c) Slow run (SR)

### Zone C First Nation Communities

Due to the large number of First Nation communities that have a moderate or high vulnerability, they are analysed through 8 sub-regions spanning north-south on the west coast of Vancouver Island, C1-C8. Not all First Nation communities (reserves) are permanently inhabited, and therefore have a population of zero in the 2011 census. This is the case for the five communities within the most northern sub-region, C-1 (Figure 5.18). Klaskish 3 and O-Ya-Kum-La 11 have a relatively small available time decrease rate with run-up, with a minimum MI available time of 26.7 min and 29.6 min respectively. The available time decreases much more rapidly with run-up for Semach 2 and Telaise 1, especially at 21 m for the latter, suggesting that a large flood plain at this run-up. The average available time decrease at a rate for all three velocities is  $-0.41$  min/m and  $-0.21$  min/m. The maximum difference between the MI and SR minimum available time is 6.1 min and 3.2 min for Telaise 1 and Semach 2 respectively. Clataux 9 has a low-laying basin to an elevation of 7 m causing a large decrease in the available time, followed by a small decreasing rate, averaging at  $-0.057$  min/m. The difference between minimum MI and SR available time is 7.0 min. This community has the lowest minimum available time, with a value of 22.7 min, just above the halfway mark of the moderate vulnerability range.

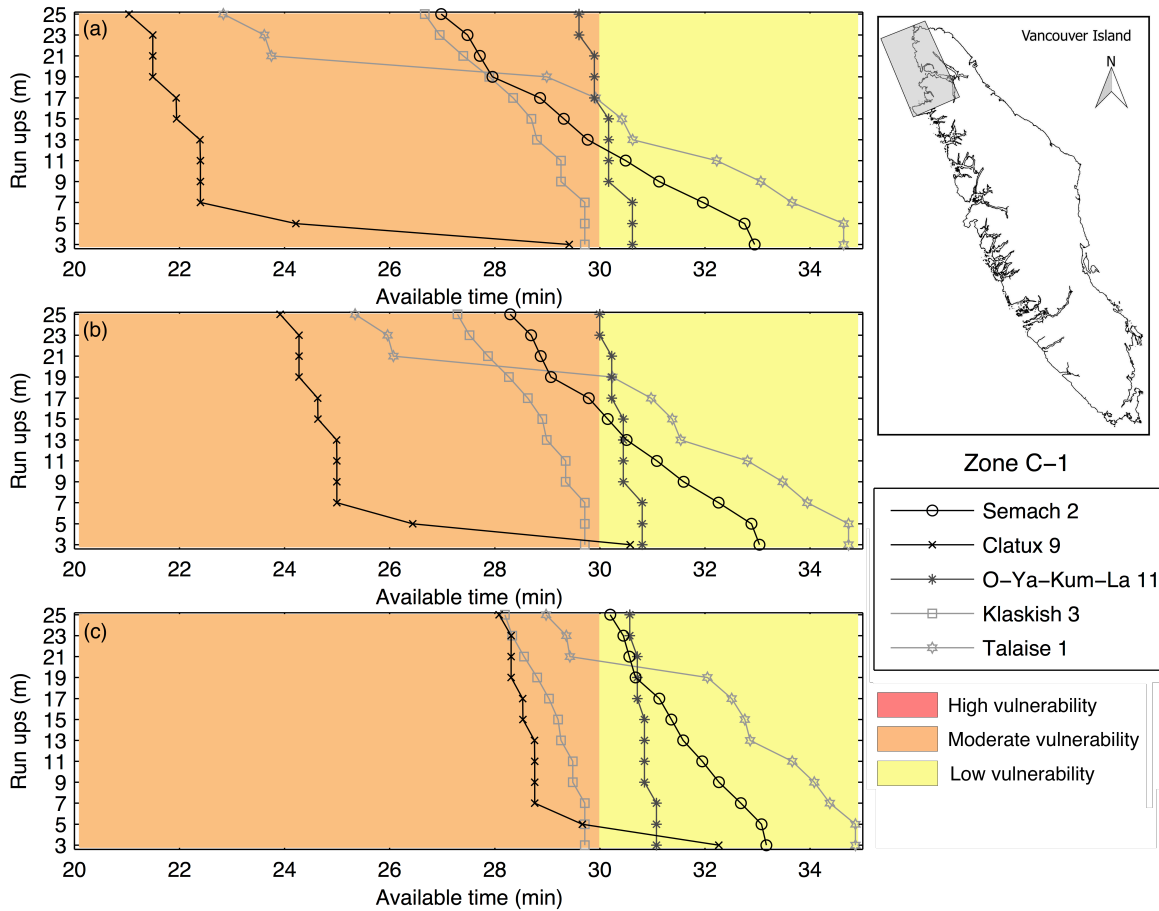


Figure 5.18 Available time (min) of First Nation communities located within sub-region C-1 for the range of run-ups between 3 and 25 m for three velocities: (a) Mobility impaired pedestrian ambulatory speed (MI); (b) Average adult ambulatory speed (AW); (c) Slow run speed (SR)

Sub-region C-2 contains 8 First Nations communities (Chenahkint 12, Houpsitas 6, Village Island 1, Tatchu 13A, Chiseuquis 9, Klitsis 16, Grassy Island 17 and Tachtchu 13; Figure 5.19), of which only one is permanently inhabited, Houpsitas 6. Except for Grassy Island 7, the vulnerability does not significantly change with run-up for communities within this sub-region. The average available time decreasing rate with run-up for these 7 communities is very small, -0.135 min/m. Grassy Island 7 has the second smallest available time of Zone C, with a minimum of -45.0 min, -31.5 min and -11.8 min for MI, AW and SR velocity. The vulnerability remains moderate until 7 m run-up as the available time remains near constant. A large flood plain between 5 m and 9 m creates a large increase in the available time. The vulnerability becomes high and the life safety threshold is surpassed within this flood plain, making run-ups above 7 m very dangerous.

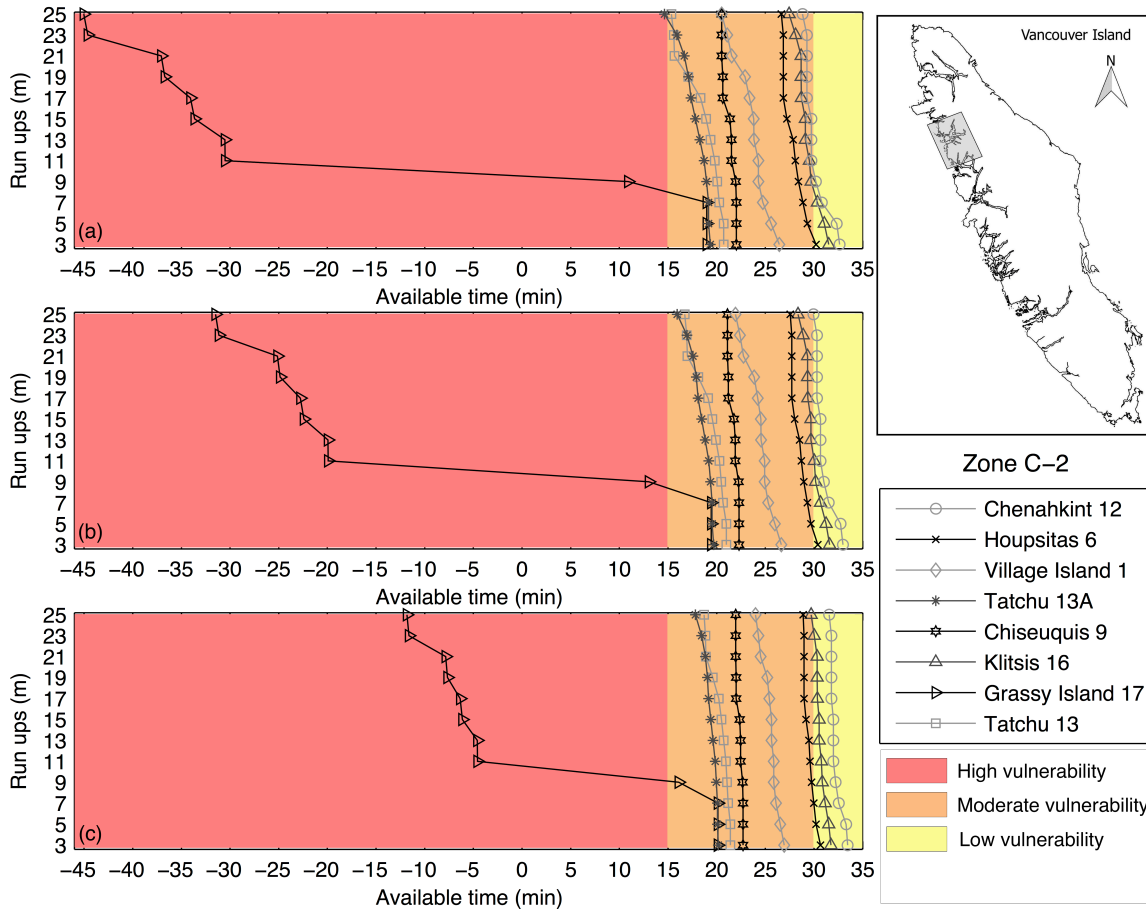


Figure 5.19 Available time (min) of First Nation communities located within sub-region C-2 for the range of run-ups between 3 and 25 m for three velocities: (a) Mobility impaired pedestrian ambulatory speed (MI); (b) Average adult ambulatory speed (AW); (c) Slow run speed (SR)

All 8 First Nation communities within sub-region C-3 (Figure 5.20) are not permanently inhabited. The vulnerability does not vary significantly for five of the communities, Ahpukto 3, Hoke Point 10B, Hesquis 10A, Owossitsa 6 and Oke 10, with run-up and therefore remain within the higher portion of the moderate vulnerability. The minimum available time is 27.0 min and the communities have an average available time decreasing rate of  $-0.063$  min/m. Opemit 4 follows a similar trend until 17 m, where the available time starts to decrease more rapidly to reach an minimum MI available time of 26.7 min, only 1.2 min less than its SR counterpart. Nuchalt 1 experiences a large increase in the available time following 7 m run-up followed by an average decrease of rate of  $0.59$  min/m. Nuchalt 2 is the only community reaching the high vulnerability with the MI and AW velocity, occurring at run-ups above 23 m. Its available time decreases exponentially.

Two First Nations Reserves are permanently inhabited in sub-region 4, Yuquot 1 and Hesquiat 1, with population of 10 or less. Hesquiat 1 reaches high vulnerability at all three velocities, at run-ups of 19 m, 19 m and 21 m (Figure 5.21). Life safety is also reached at 21 and 25 m for MI and

AW, with a minimum available time of -9.6 m. The available time decreases more rapidly following 7 m run-up, as does for Yuquot 1, Homais 2, Tsarksis 2 and Aass 3. However, Hesquiat is the only community to breach the life safety threshold. Yuquot 1, which is populated, reaches high vulnerability at 19 m and 23 m for the MI and AW velocity. Homais 2 reaches high vulnerability at 17 m, 17 m and 21 m for MI, AW and SR and 17 m, 19 m and 23 m for Aass 3. Tsarksis only reaches high vulnerability at 25 m for MI velocity. The vulnerability does not vary significantly for Coopte 9, Teahmit 3, Mooyah 16 and Hoiss 8, with an average decreasing rate of -0.099 min/m and a minimum available time of 26.8 min, in the high range of the moderate vulnerability.

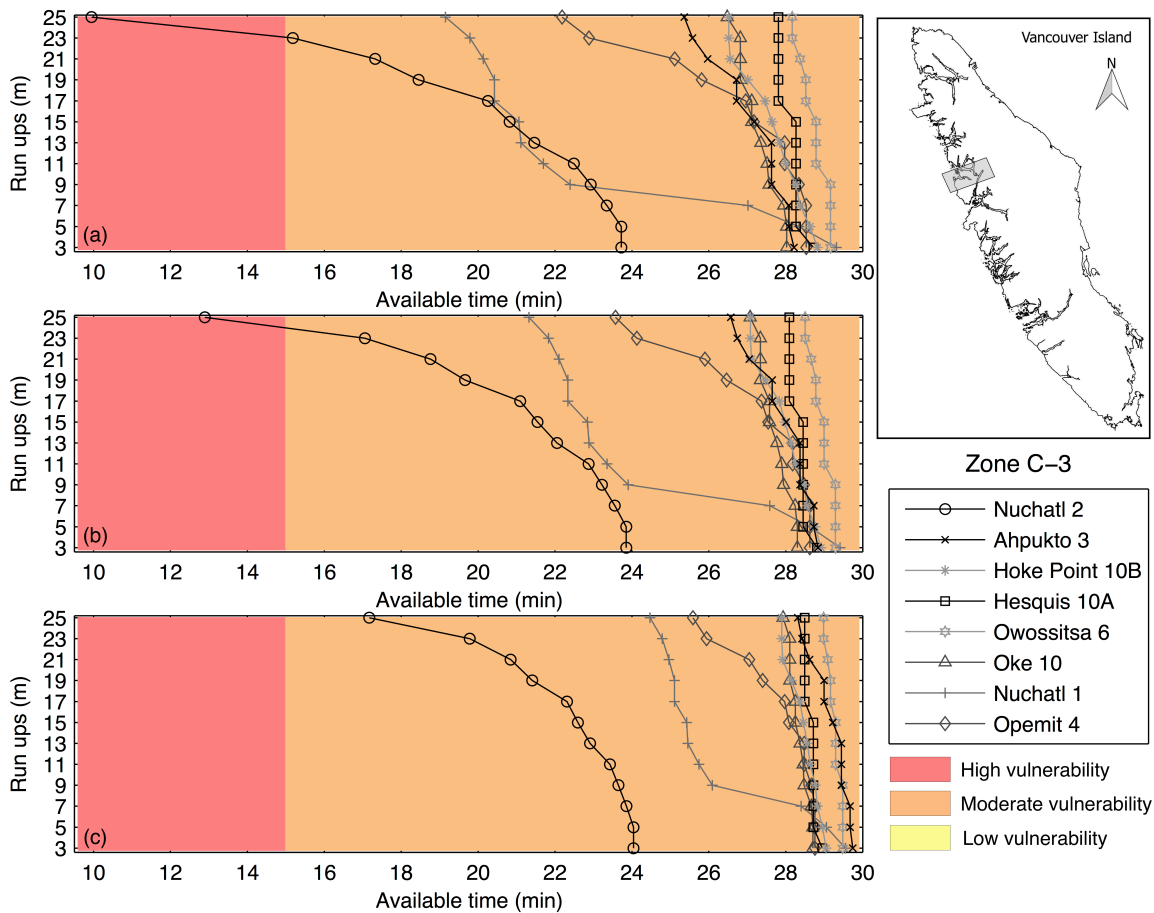


Figure 5.20 Available time (min) of First Nation communities located within sub-region C-3 for the range of run-ups between 3 and 25 m for three velocities: (a) Mobility impaired pedestrian ambulatory speed (MI); (b) Average adult ambulatory speed (AW); (c) Slow run speed (SR)

Two First Nations Reserves are permanently inhabited in sub-region 4, Yuquot 1 and Hesquiat 1, with population of 10 or less. Hesquiat 1 reaches high vulnerability at all three velocities, at run-ups of 19 m, 19 m and 21 m (Figure 5.21). Life safety is also reached at 21 and 25 m for MI and AW, with a minimum available time of -9.6 m. This community The available time decreases more rapidly following 7 m run-up, as does for Yuquot 1, Homais 2, Tsarksis 2 and Aass 3.

However, Hesquiat is the only community to breach the life safety threshold. Yuquot 1, which is populated, reaches high vulnerability at 19 m and 23 m for the MI and AW velocity. Homais 2 reaches high vulnerability at 17 m, 17 m and 21 m for MI, AW and SR and 17 m, 19 m and 23 m for Aass 3. Tsarksis only reaches high vulnerability at 25 m for MI velocity. The vulnerability does not vary significantly for Coopte 9, Teahmit 3, Mooyah 16 and Hoiss 8, with an average decreasing rate of  $-0.099 \text{ min/m}$  and a minimum available time of 26.8 min, in the high range of the moderate vulnerability.

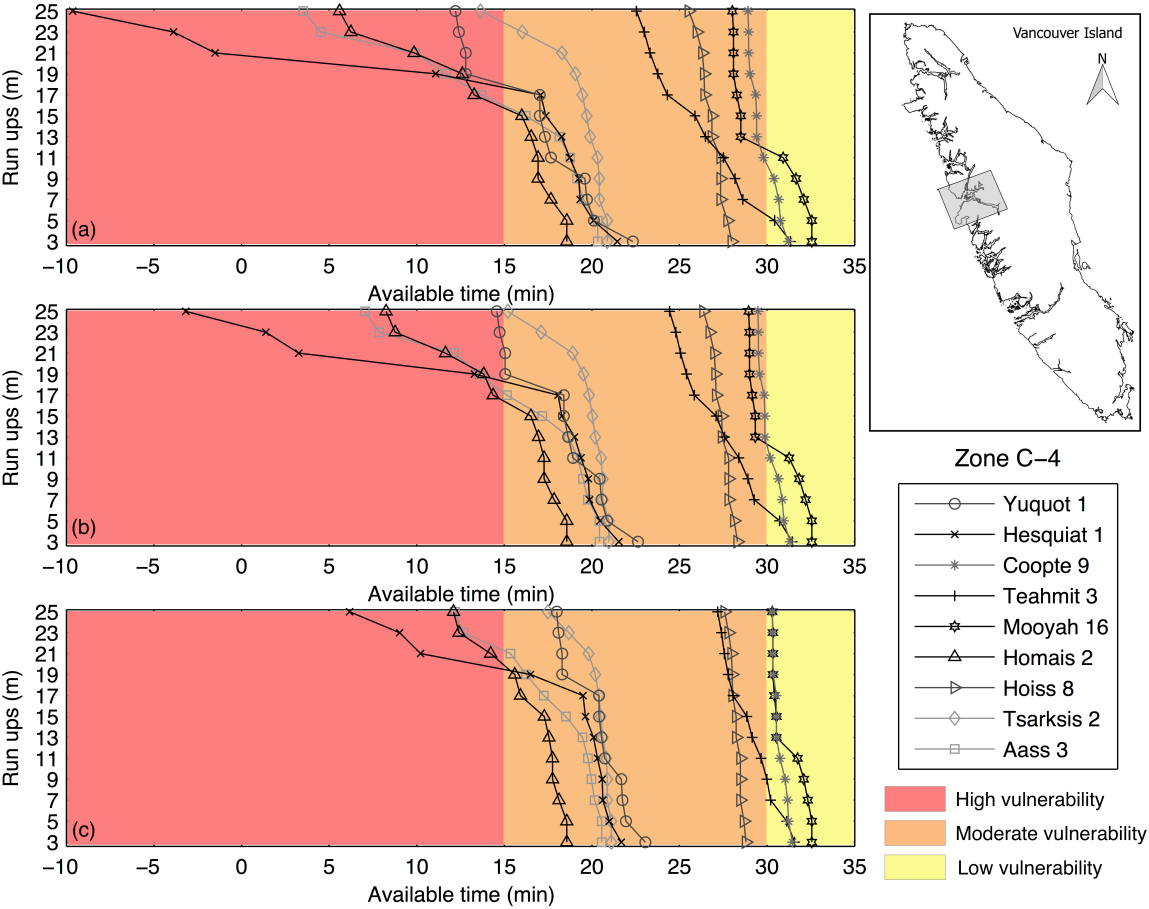


Figure 5.21 Available time (min) of First Nation communities located within sub-region C-4 for the range of run-ups between 3 and 25 m for three velocities: (a) Mobility impaired pedestrian ambulatory speed (MI); (b) Average adult ambulatory speed (AW); (c) Slow run speed (SR)

The lowest available time is found in sub-region C-5 at Barlett Island 32, with a minimum available time of 57.7 min (Figure 5.22). The available time of this community does not vary significantly except for two large jumps between 13 m and 15 m, and 19 m and 21 m run-up. The latter decreases with a maximum of 24.9 min at the MI velocity. The minimum available time differs greatly between the MI and SR velocity, with a maximum difference of 42.5 min. The high vulnerability threshold is breached at 13 m for MI and AW and 19 m for SR and the life safety threshold is surpassed following 17 m uniformly for all velocities. Fortunately, this

community is not permanently populated, as the two large floodplains create a very dangerous area for loss of life. Kutchous Point 33 is the second most vulnerable community within sub-region C-5. A mild slope between 15 m and 17 m run-up causes a large decrease in the available time, where it enters the high vulnerability threshold at the MI and AW velocity. A steep hill follows, causing almost no change in the available time, averaging a value of 1.2 min, 6.8 min and 14.9 min for MI, AW and SR velocity. Although the life safety threshold is not surpassed, the available time value remains very close for run-ups between 19 m and 25 m for the MI velocity. The vulnerability does not vary significantly for Refuge Cove, Hisnit Fishery 34, Openit 27, Tootowiltena 28, Chetarpe 17 and Marktosis 15. Their available time varies between 19.2 min and 35.1 min, with an average available time decreasing rate of -0.14 min/m. Refuge Cove is the only community with a permanent population, with a value of 72.

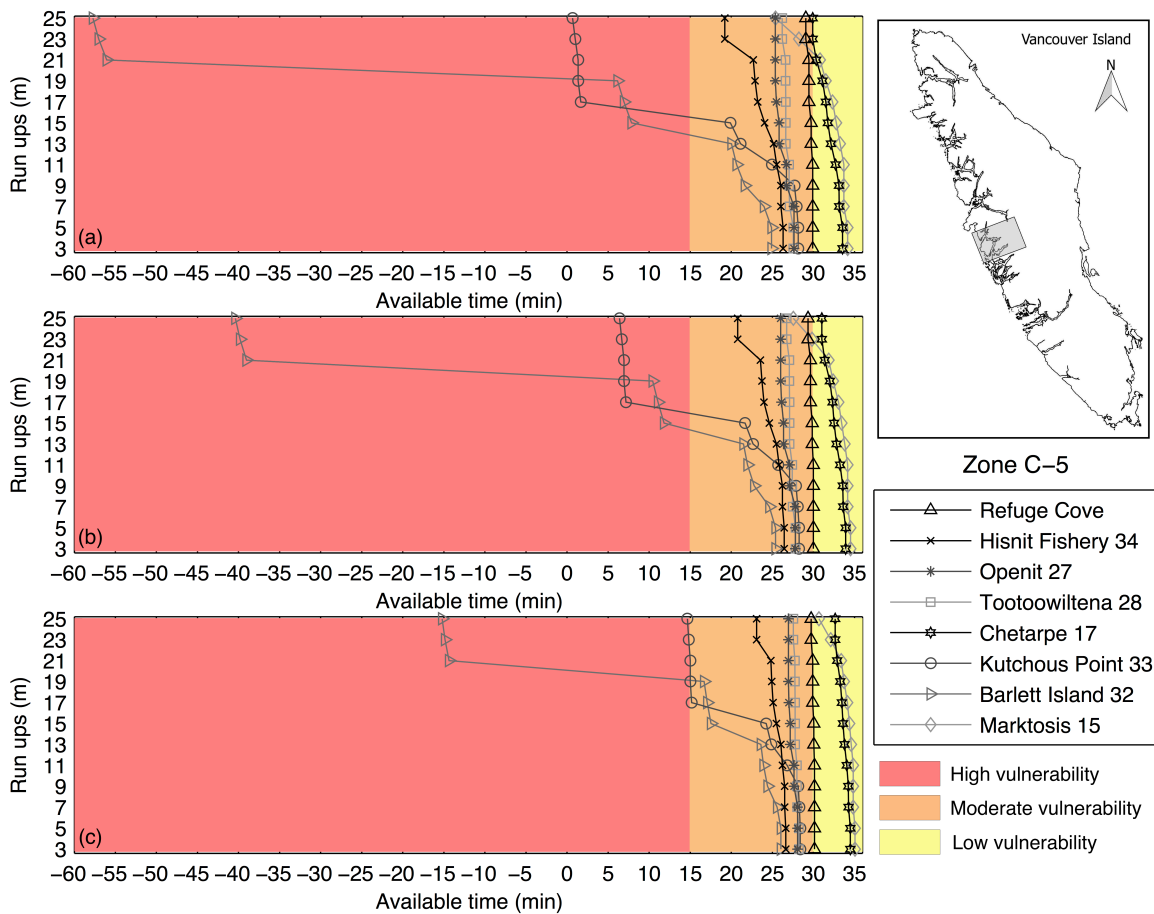


Figure 5.22 Available time (min) of First Nation communities located within sub-region C-5 for the range of run-ups between 3 and 25 m for three velocities: (a) Mobility impaired pedestrian ambulatory speed (MI); (b) Average adult ambulatory speed (AW); (c) Slow run speed (SR)

Opitsat 1 is the only populated community of sub-region C-6 (Figure 5.23), with a total of 173. Fortunately, this is the community with the lowest vulnerability within this sub-region, only reaching the moderate vulnerability with the MI velocity at 23 m run-up. The available time

decreases with run-up at an average rate of  $-0.36 \text{ min/m}$  in this sub-region. The available time ranges from low to moderate vulnerability except for Ahous 16. This community reaches high vulnerability a MI and AW velocities following 19 m. This is due to a large increase in available time between 19 m and 21 m due to a mild terrain sloping. The life safety threshold is not surpassed, with a minimum available time of 10.6 min.

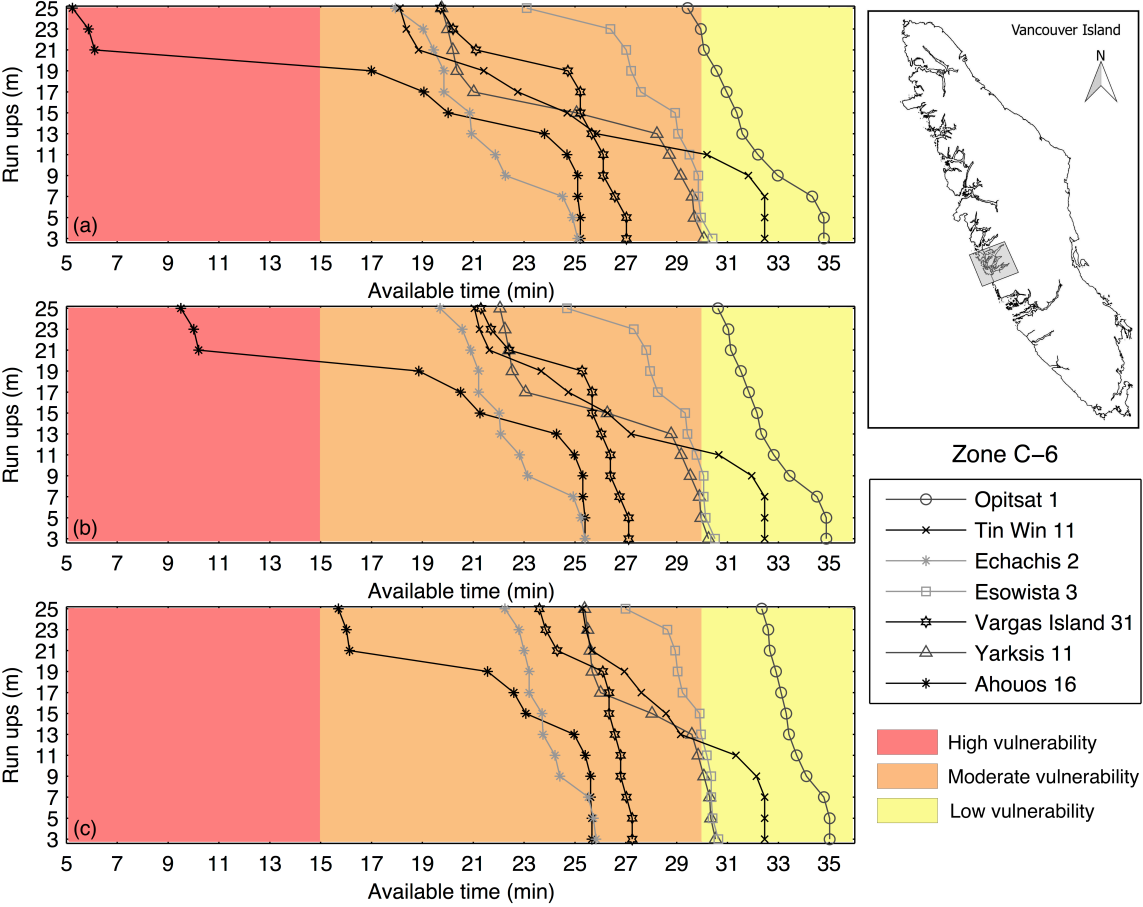


Figure 5.23 Available time (min) of First Nation communities located within sub-region C-6 for the range of run-ups between 3 and 25 m for three velocities: (a) Mobility impaired pedestrian ambulatory speed (MI); (b) Average adult ambulatory speed (AW); (c) Slow run speed (SR)

Sub-region C-7 encompasses Barkley Sound, where wave amplification is prominent and run-ups at the higher end of the Zone C’s range could be expected. At a SR pace, all communities (Anacla 12, Numukamis 1, Nettle Island 5, Omoah 9 and Keith Island 7) except for Ittatsoo 1 are within the low vulnerability (Figure 5.24). Ittatsoo reaches the moderate vulnerability range at 11 m run-up for both MI and AW velocities. The average available time decreasing rate of the sub-region (excluding Omoah 9) is  $-0.35 \text{ min/m}$ . Omoah 9 has a much smaller decreasing rate of  $-0.044 \text{ min/m}$ . Ittatsoo1, Anacla 12 and Numukamis 1 have a permanent population of 240, 73 and 10 people respectively.

Gordon River 2 is the only inhabited community within the most southern sub-region C-8 (Figure 5.25) with a population of 96. It is also the community with the lowest available time in this sub-region. Following a large decrease between 3 m and 9 m run-up, ranging from 6.0 min to 15.0 min, the available time does not vary significantly, averaging a value of 15.3 min, 19.8 min and 26.3 min for MI, AW and SR velocity respectively. Although the high vulnerability is not reached, the average MI available time above 9 m is only 0.3 min less than the threshold. The remaining communities have an available time below 25.7 min.

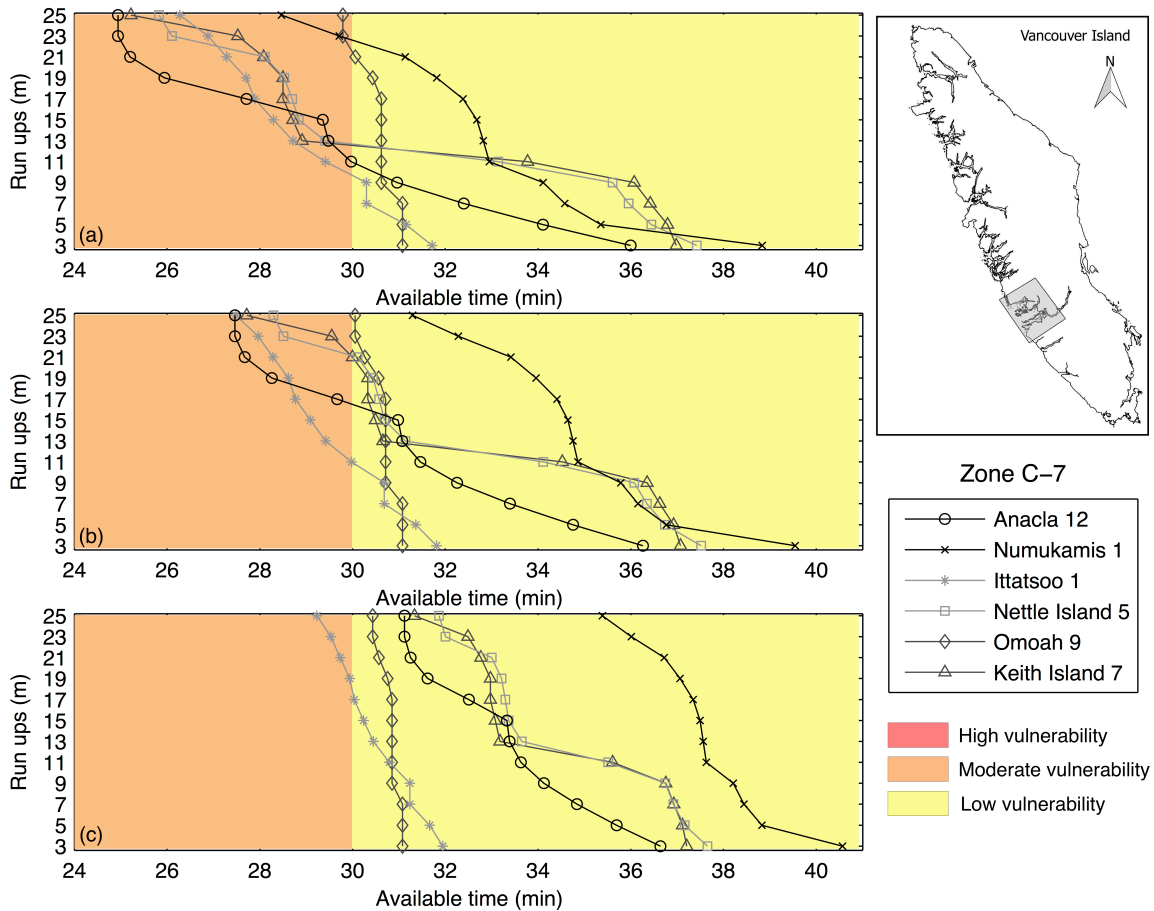


Figure 5.24 Available time (min) of First Nation communities located within sub-region C-7 for the range of run-ups between 3 and 25 m for three velocities: (a) Mobility impaired pedestrian ambulatory speed (MI); (b) Average adult ambulatory speed (AW); (c) Slow run speed (SR)

First Nations communities that are not permanently inhabited will not have comprehensive tsunami evacuation plans. Individuals who are present in the regions, especially locations with a high vulnerability, should educate themselves on the locations of higher grounds and know where to evacuate in an emergency. Additionally, as these communities are not permanently inhabited, a built environment may not be present and travelling through thick forest may require longer times. The communities with the highest vulnerability are Barlett Island 32, Grassy Island 17 and Hesquiat 1. Only the latter is permanently populated. No trend could be determined by

sub-region for the variation in the available time per run-up. As the available time is dependent on the local topography, trends could potentially be found for communities with similar topography based on their location: coast, inlet or island. However, many communities were found in sub-region C-2 to C-5 with a very low available time decreasing rate with run-up.

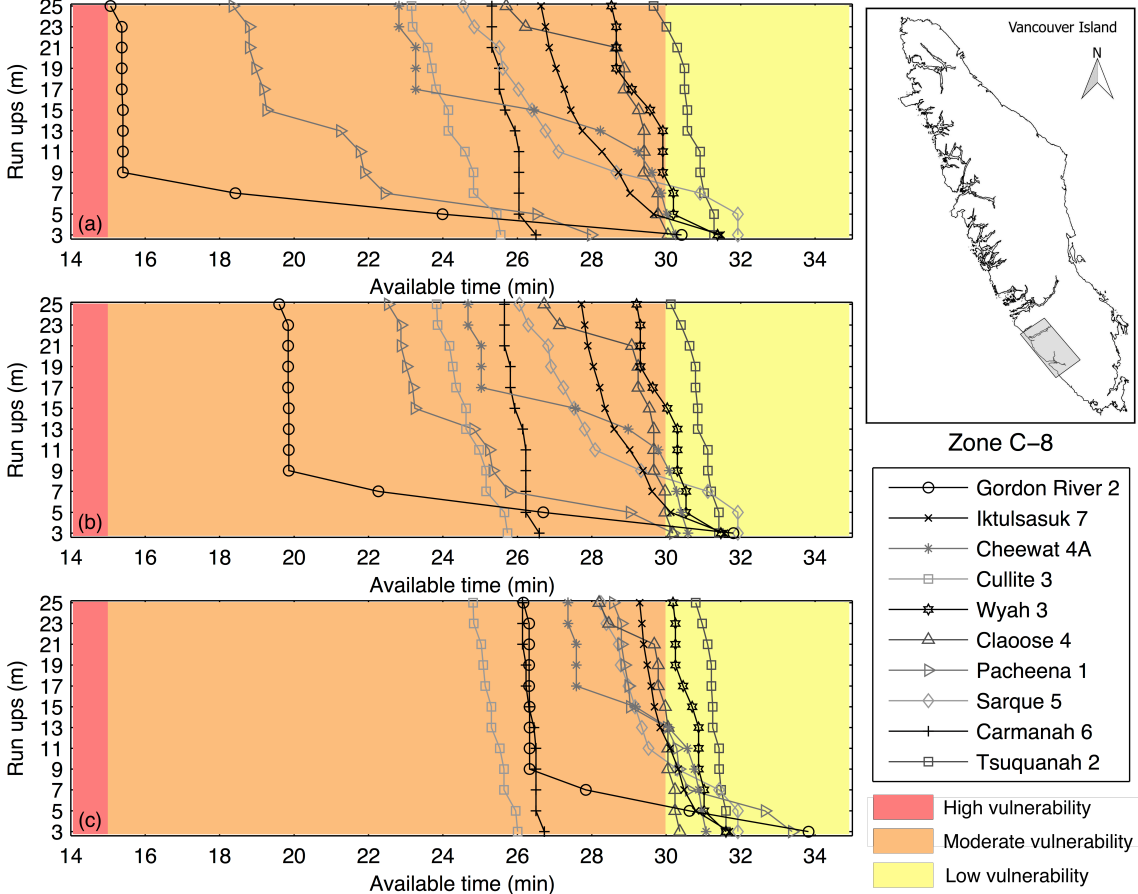


Figure 5.25 Available time (min) of First Nation communities located within sub-region C-8 for the range of run-ups between 3 and 25 m for three velocities: (a) Mobility impaired pedestrian ambulatory speed (MI); (b) Average adult ambulatory speed (AW); (c) Slow run speed (SR)

*Zone E*

Delta and Richmond are two municipalities within the Greater Vancouver region. Richmond is located directly south of Vancouver and Burnaby, connected through three bridges spanning over a Fraser River’s tributary (Figure 5.26). Further south, a second tributary separates Delta from Richmond, with two possible bridge crossings. Two First Nations communities are located within the Delta boundary: Tsawwassen and Musqueam 4. Richmond and Delta have the lowest elevations of the municipalities located within the Lower Mainland, consequently having the lowest available times in Zone E.

The computed arrival time value for each municipality is taken as the minimum within 500 m from the municipality boundary. For Delta, this value, 105.0 min, is found within Boundary Bay, to the south. The arrival time for Richmond is 20.1 min greater, as the value was taken off its western coast, northwest of Boundary bay. This suggests that the arrival time for the northwest portion of Delta is underestimated, as it open coast is located more closely to Richmond than to boundary bay. The arrival time computed is 30.0 min and 14.9 min less than the BC EA estimate value for Delta and Richmond respectively.

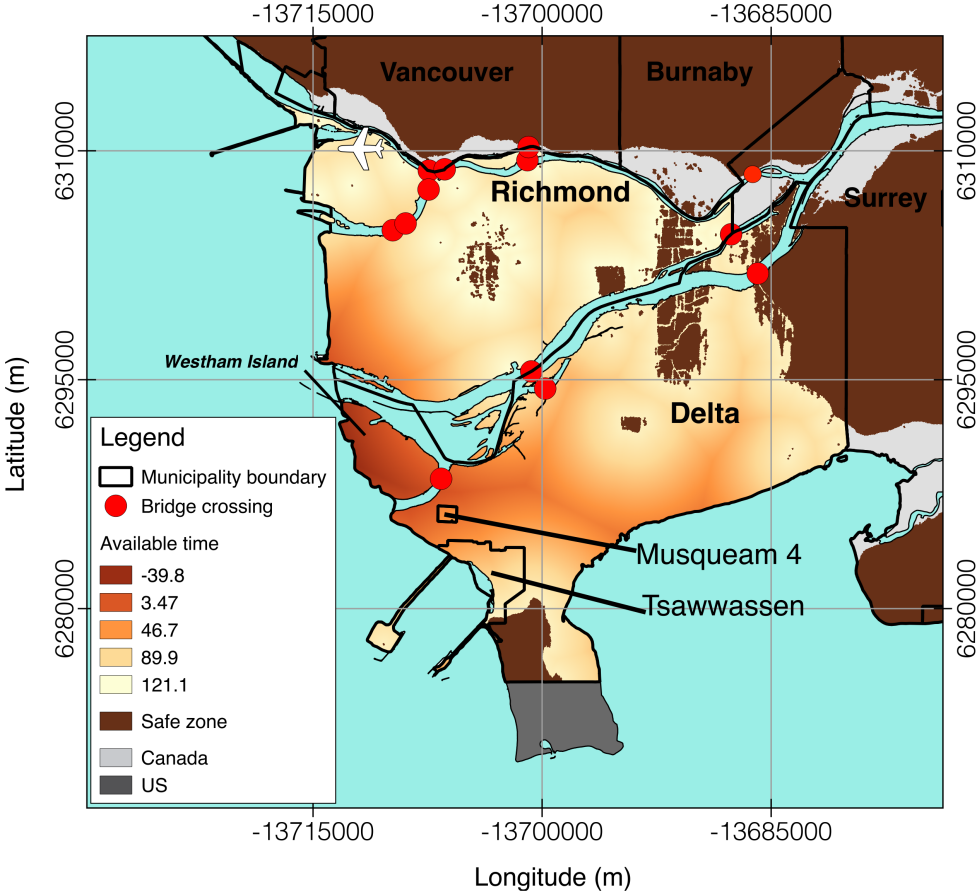


Figure 5.26 Available time computed with model arrival time for Richmond and Delta for a 7 m run-up.

The available time for both Richmond and Delta follow a similar pattern: the available time decreases at a near uniform rate until 11 m run-up, followed by an almost zero slope. Until 11 m run-up, Delta decreases at an average rate of -18.5 min/m, -14.7 min/m and -9.23 min/m for the MI, AW and SR velocities (Figure 5.27). Richmond’s decreasing rate until 11 m run-up is 15% lower, with values of -15.7 min/m, -12.5 min/m and -7.86 min/m for MI, AW and SR velocities (Figure 5.28). Delta has a low vulnerability at 3 m run-up for all velocities. At 5 m run-up, the upper bound of the probable run-up range, the MI available time found with the computed arrival time is within the high vulnerability, and below the life safety threshold with a value -7.47 min.

However, due to the large difference with the BC EA arrival time of 30.0, the available time at this same run-up using this value yields 22.5 min, within the moderate vulnerability. The remaining velocity also yields available times within the moderate or low vulnerability. Two metres above the maximum probable run-up, the available time is below the life safety threshold for the MI velocity using both arrival times (-38.8 min and -8.83 min respectively) and AW velocity using the computed arrival time (-9.30 min).

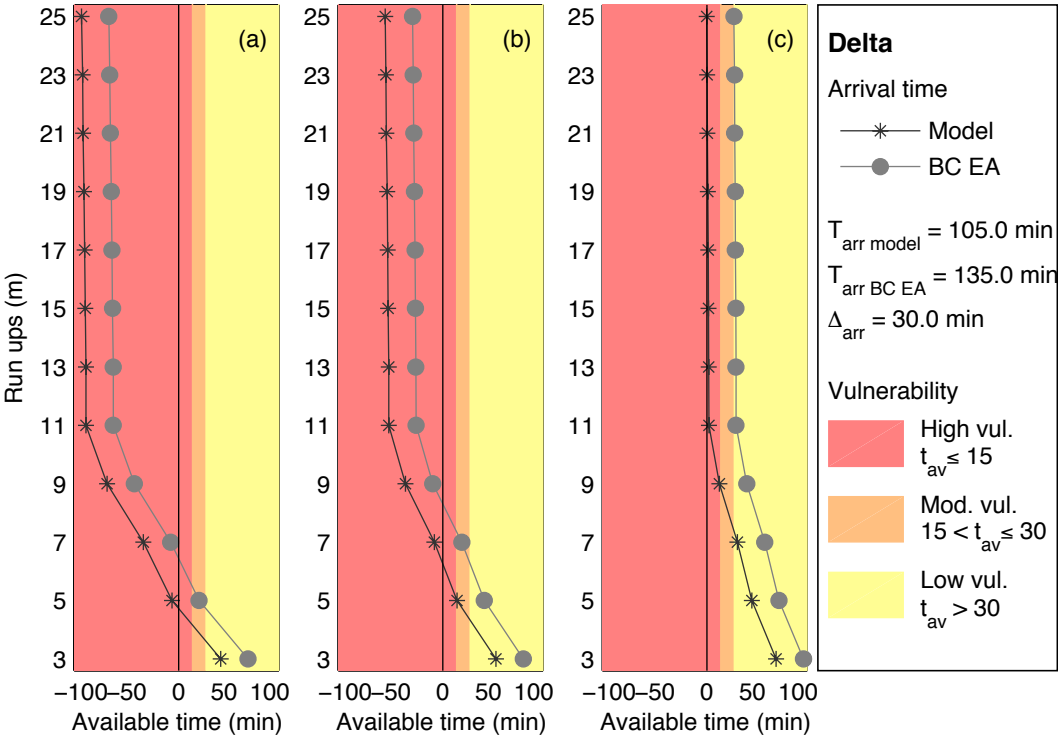


Figure 5.27 Minimum available time of Delta using the model and BC EA tsunami arrival time for a range of run-ups between 3 and 25 m for three velocities: (a) Mobility impaired pedestrian ambulatory speed (MI); (b) Average adult ambulatory speed (AW); (c) Slow run (SR)

Richmond on the other hand has a low vulnerability at all velocities for 3 m and 5 m run-up. At 7-m run-up, 2 m above the maximum probable run-up, the high vulnerability is reached using the BC EA arrival time (8.17 min) and the life safety threshold is surpassed using the computed arrival times (-6.72 min). The remaining velocities yield a moderate or low vulnerability.

The SR available time may provide misleading results as this pacing would need to be maintained for long period of time as the arrival time is large in this region, with a minimum of 105 min. However, running is not necessary as the AW velocity yields value above the life safety threshold below 7 m run-up for both Richmond and Delta. The available time also depends on the designated safe zone. The largest safe zones near Richmond are located in the surrounding municipalities of Vancouver and Burnaby, which are only accessible by bridge. As the distance to safety is computed using direct distances, the time of safety is likely to increase due to the

additional distance required to reach a bridge. Additionally, the distance to safety is underestimated in the north portion of Richmond due to remaining small dry pockets. The area the most at risk the southwest portion, directly on the coast. The largest safe zone for Delta is located east in Surrey. Additional safe zones are also located northeast and southwest of the municipality. Delta is mostly agricultural land with two areas with high population density, one in the northeast, with a portion within the safe zone and the second is in the neighbourhood of Ladner, south of the dual bridge linking to Richmond. The latter is within the area the most at risk for loss of life with Westham Island. The distance to safety within Westham Island is likely underestimated here as well as it is connected to Delta by only one bridge. As the arrival time and distance to safety are quite large, the merits of vehicle evacuation should be studied for this area. Traffic jams could occur in the region of Ladner as the population density is high, but not likely Westham Island as it is a rural area.

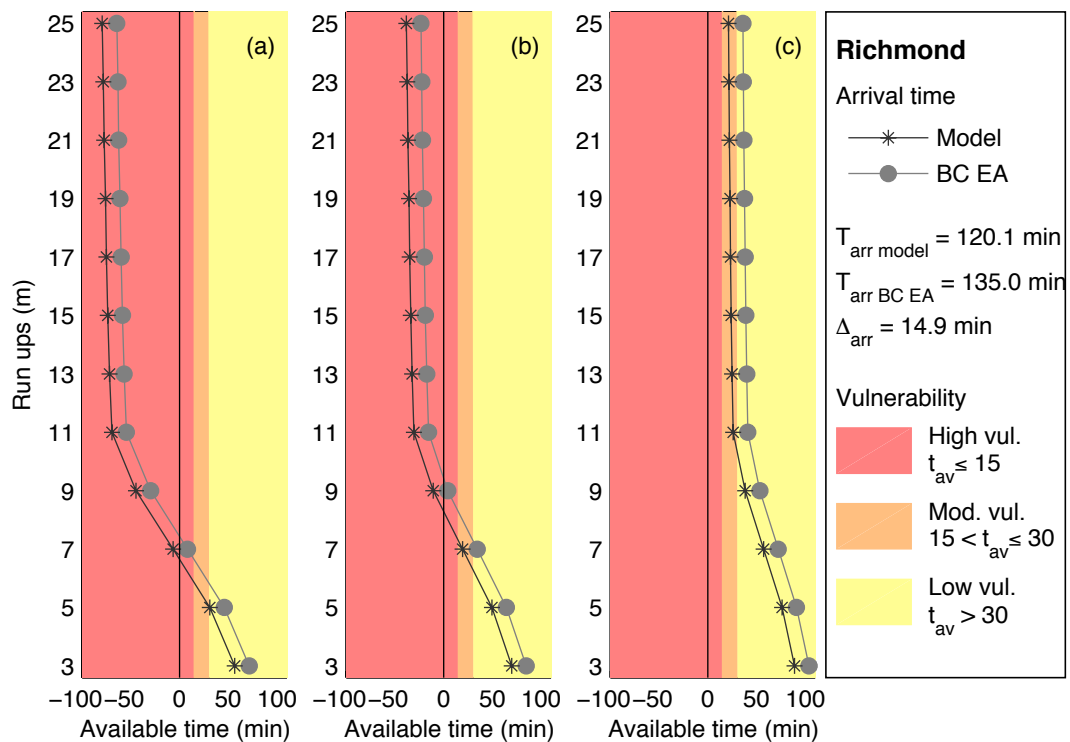


Figure 5.28 Minimum available time of Richmond using the model and BC EA tsunami arrival time for a range of run-ups between 3 and 25 m for three velocities: (a) Mobility impaired pedestrian ambulatory speed (MI); (b) Average adult ambulatory speed (AW); (c) Slow run (SR)

Dikes protecting against flooding from storm surges surround Greater Vancouver, including Richmond and Delta. The dikes are design for a 200-year flood level 1.3 m crest heights. However, a recent report states that most dikes do not meet the provincial standard for seismic stability and crest height (Northwest Hydraulic Consultants 2015). Additionally, some dikes in Delta have been previously overtopped. The maximum wave height modelled by Cherniawasky,

et al. (2007) was 1.5 m in the Strait of Georgia, greater than the 200-year flood level. The dikes may also be overtopped if they fail during the preceding earthquake.

### **5.4.3 Conclusion**

In conclusion, Zone E is the primary contributor to the total province surface area within a HZ due to its large number of communities included within the zone and the low-laying areas of the Lower Mainland. At the maximum probable run-up of 5 m, 14.1% of Zone E surface area is inundated. Zone B and D have an on average a consistent sloping causing steady increases in HZ area at each run-up, with 11.2% and 3.67% % of their total surface area inundated at the maximum probable run-up, respectively. Zone D has the least inundated surface area due to its mountainous terrain and small number of communities. Zone C and A have large low-laying areas below 3 m following by steady sloping terrain. The inundated surface area of each zone at their maximum probable run-up is 39.7% and 11.2% for Zone C and A.

Although the probable run-up range is the lowest in Zone D and E, due to the large population centres, the most at-risk residents are found here. At the maximum probable run-up of 5 m, 17.8% of the population of Zone E is at risk, approximately 534,000 people. This value is significantly more than the total population at the maximum probable run-up of all other zones: 11,000 for Zone C and D and 2,540 and 1,995 for Zone A and B. Zone C has the highest proportion of its population at-risk, with a total of 37.0% at the maximum probable run-up of 25 m.

Zone C has the highest vulnerability of all zones, agreeing with previous evidence that the outer Vancouver Island is the most at risk. Not only does it have the largest probable run-ups, but it has the lowest median available time, with an average of 35.1 min, just above the moderate vulnerability threshold. In addition, 25% of the communities have a moderate vulnerability starting at 9 m run-up. Zone A, B, D and E have a low vulnerability at their maximum probable run-up. Landslides and tsunamis may pose a larger threat in these zones, as the arrival time would be smaller than that of a CSZ tsunami.

The life safety threshold is surpassed by 4 communities in Zone C, Barlett Island 32, Grassy Island 17, Hesquiat 1 and Tofino, at minimum run-ups of 19 m, 11 m, 21 m and 7 m. Hesquiat and Tofino are the only populated communities and Tofino reaches life safety at the lowest run-up. Ucluelet and Port Renfrew, also have a high vulnerability, reached at a minimum run-up of 17 m and 7 m.

Although the CSZ tsunami hazard is low and the arrival time is high, the available time is below the life safety threshold in Richmond and Delta at 5 m and 7 m run-up due to the vast low-laying areas. Dikes in the area may not provide protection as they may fail during the preceding earthquake or be overtopped by the tsunami waves. Landslides tsunamis may pose a greater risk

in this region as the tsunami arrival time would be much smaller than that of a CSZ event and the distances to safety are quite large. The vulnerability to communities due from landslide tsunamis should be evaluated. Additionally, the merits of vehicle evacuation should be studied in this area.

The available time was computed with a bare-earth elevation model, constant evacuation speed and distance-only model for the distance to safety. These assumptions may underestimate the available times in some locations, as the distance to safety may be longer due to obstacles caused by the built environment, as demonstrated by Wood and Schmidlein (2012). Additionally, the time to safety may also be longer due to speed degradation from fatigue or slower pedestrian velocity from climbing steep hills. Though not within the scope of this research, further studies on the differences in the life safety threshold should be considered for vulnerable groups such as people with disabilities, children and the elderly, as the data is based on normal circumstances and abilities of the population. Future models should consider these criteria to better predict the available time by using more precise models such as path-distance models. However, information such as land cover is required for such model. Wood and Schmidlein (2012) also demonstrate that the resolution of the digital elevation model (DEM) used plays an important role in the time to safety calculated. As the DEM used in this study is rather coarse, the available time is also likely underestimated because of this factor. Therefore, locations with available time within the high or moderate category within their respective probable run-up range, should be further examined using more precise path-distance models using DEMs with better resolution. Many tourists and residents visit the numerous parks, beaches and hiking trails to enjoy the natural beauty of the province. Some of these areas may prove to be very vulnerable to tsunamis due to their remoteness, and lack of evacuation plans in place for non-residential areas. Further studies should be conducted on remote attractions that fall within the study area.

## Chapter 6. Case Study: Tofino

---

Tofino is a municipality located on West coast of Vancouver Island on the Esowista peninsula. The village is a renowned surf town due to its ample beaches with large breaking waves and its location just 20 km north of a popular surfing destination, Long Beach. Tofino is also very popular among tourists for its whale and storm watching, fishing and rugged nature. The southern portion of the Esowista peninsula has a low elevation, which causes Tofino to have large, elongated hazard zones at low run-ups. Because of this, and the fact that Tofino is one of the only non-indigenous communities that was found to have an available time lower than the life safety threshold within probable run-ups, it was chosen for further examination. The primary goal of this case study is the life safety, as such the population distribution is estimated and presented, followed by a more specific study of the available time distribution within the community, and finally optimal locations for vertical evacuation structures are presented.

### 6.1 Population

Tofino is a small village with a permanent population of 1,876 people. Its economy was once primarily resource-based, but since 2006 has shifted towards the tourism industry (Centre for Sustainability Whistler 2014, Vaugeois, et al. 2013). During the summer, its population can more than double due to the peak tourism season and the influx of seasonal workers. Because of its extensive tourism opportunities and numerous resorts, Tofino is considered a resort community.

#### 6.1.1 Population Estimation Methodology

The tourism industry creates a large seasonal employment opportunity. Seasonal workers are believed to increase the population of Tofino during the summer to somewhere between 4,000 and 5,000 people (Centre for Sustainability Whistler 2014). The summer resident population for the summer is taken as median value, 4,500 and the winter resident population is taken as the 2011 census value of 1,876. No value exists for the tourist population, and was therefore estimated. The tourist population represents an important population subgroup as they might not be as well educated on the emergency procedures, and thus may be more vulnerable than the residents.

First, all structures within the boundaries of Tofino are identified, presented in Figure 6.1, and assigned to one of 9 categories:

1. Commercial
2. Industrial
3. Park
4. Industrial

5. I Institutional
6. Residential
7. Tourism and accommodation
8. Short term rental

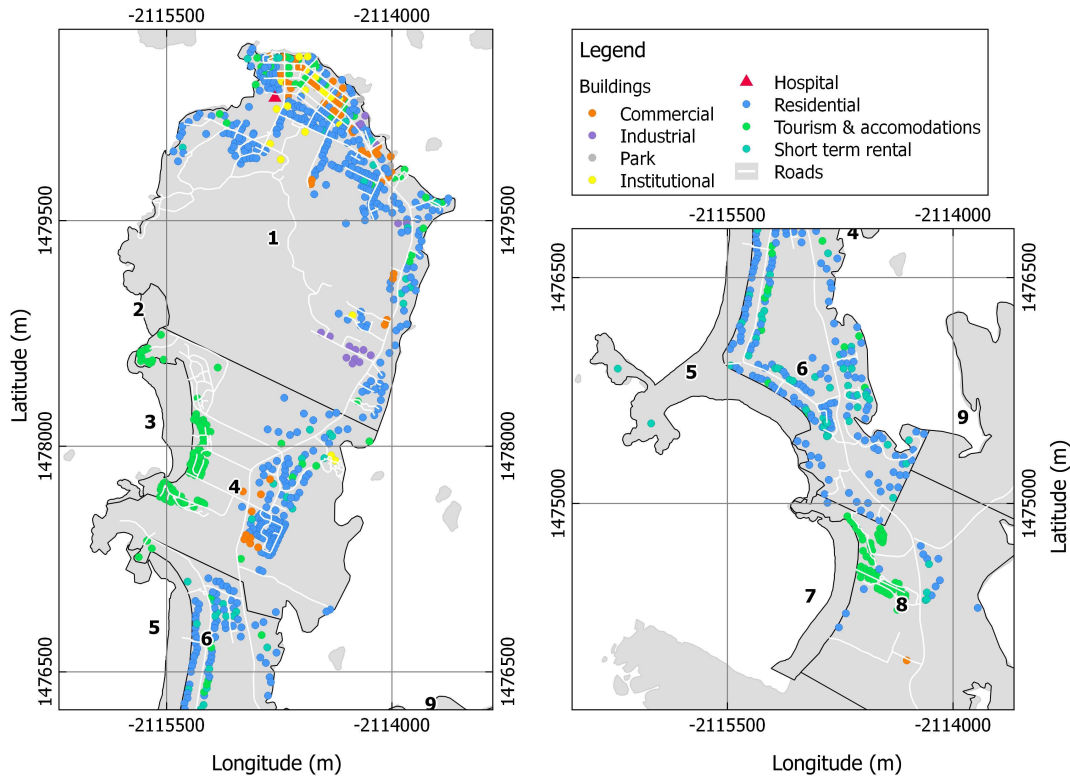


Figure 6.1 Structures distribution within the Tofino, mapped by type: commercial, industrial, park, institutional, residential, tourism and accommodation and short term rental

The structures were identified using aerial imagery and open-sourced maps. The categories were assigned using the zoning bylaw (Zoning Bylaw No. 770, 2012) and panoramic street-level images. Residential structures were further identified as single or multiple units. The residential structure counts were cross-referenced with the census data.

The population was estimated for two scenarios: winter night and summer night. The assumption of the night scenario is that the majority of the population will be found at their domicile (Johnstone and Lence 2012). The resident population distribution was found by multiplying the number of residential units with the summer or winter average population density per household. The number of private dwellings found was 26 less than the census value of 1,033. From this, 88 are used for short-term rentals, and were considered as tourist accommodations instead of residential housing.

The tourism population was first estimated by surveying all accommodations' and campgrounds' number of units and unit capacity within Tofino. The number of rooms sold is the primary

tourism tracking mechanism. Accommodations are reported to be near or at capacity during the busiest month of the summer season, August (Centre for Sustainability Whistler 2014). The summer tourist population was therefore taken as the maximum capacity of all accommodations and campgrounds. The winter tourist population was taken as the maximum occupancy of the winter season, occurring in March, with 56.9% occupancy rate. The population estimates are presented in Table 6.1.

Table 6.1 Tofino resident and tourist population estimates for the winter and summer night scenario

Population	Summer	Winter
Resident	4500	1876
Tourist	4621	2630
Total	9121	4506

Only a night scenario was considered as estimation of the whereabouts of residents and tourists, since a daytime scenario involved too many uncertainties due to the inability to calculate people at work, participating in leisure activities or travelling.

### 6.1.1 Population Distribution

For ease of analysis, Tofino was separated into 9 zones (Figure 6.2). Zone 2, 3, 5 and 7 are beaches and are not populated, except for Chesterman Beach (5) that includes Frank Island to its west, which has 2 short-term rental houses. West (9) is not developed.

The highest density of structures is within the Village (1), demonstrated in Figure 6.3. The buildings within the village are limited to the northern part of the peninsula and the remaining portion is undeveloped. The village has a combination of all structure categories. The village also has the highest resident population (Figure 6.3a) and most multi-unit residential structures are located there. The second highest resident population is found in Chesterman (6). This zone is mainly comprised of single-family homes. MacKenzie (4) is also comprised of a residential neighbourhood of single-family homes to its west.

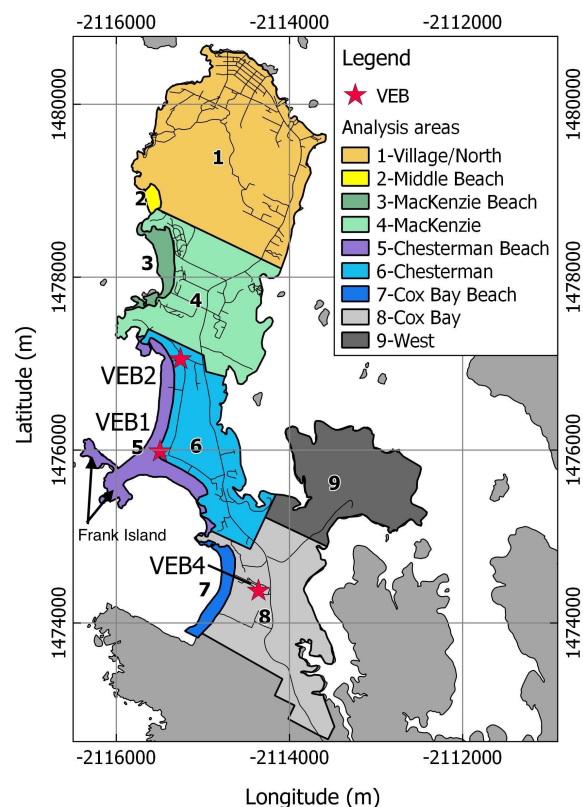


Figure 6.2 Tofino analysis zones

The tourist population is dispersed throughout the community (Figure 6.3b). The tourist accommodations with the highest capacities are the resorts. The resorts are located along the coast, near the beaches, seen as the high population clusters. Short-term rentals and bed and are dispersed in the residential neighbourhoods in MacKenzie, Chesterman and Cox Bay, but some are also found in the Village. Located within MacKenzie is the Tin Wis First Nations Reserve. This Reserve is not inhabited but instead the land is allocated to the Best Western Tin Wis Resort.

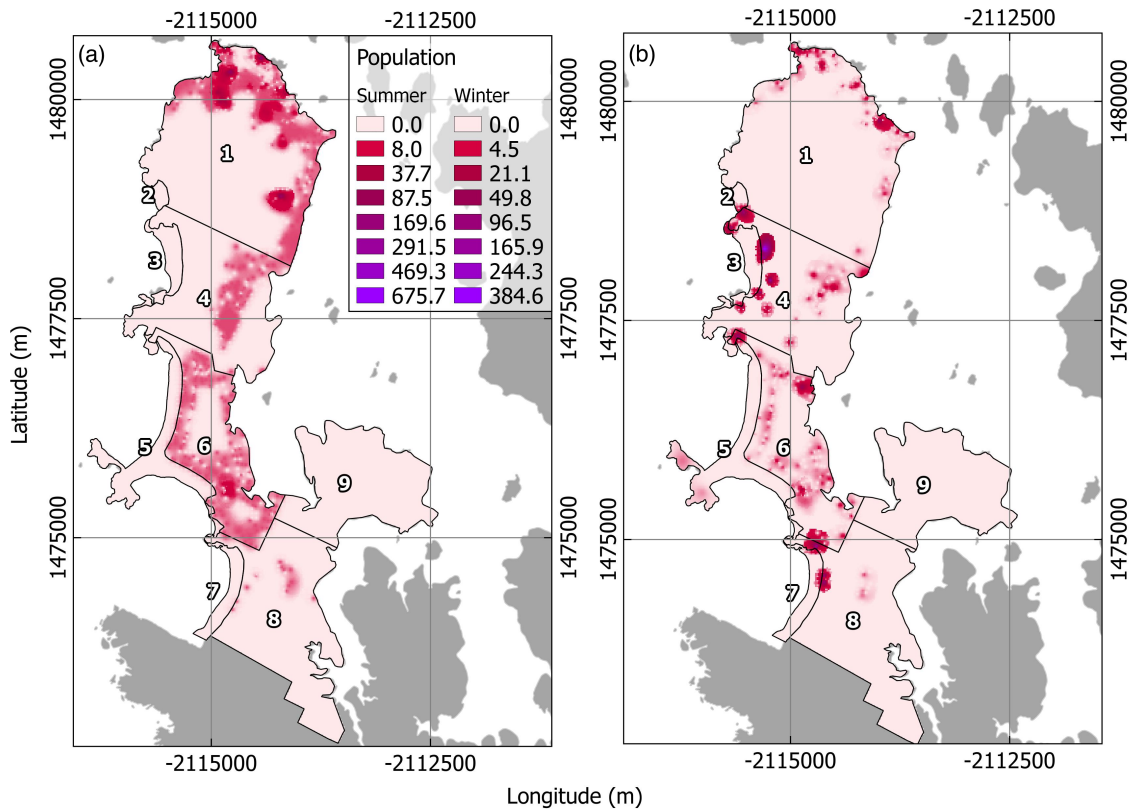


Figure 6.3 Population distribution for summer and winter night scenario: (a) resident population; (b) tourist population

## 6.2 Pedestrian Evacuation Tool

The time to safety in the case study was computed using the USGS Pedestrian Evacuation Analyst extension for Esri's ArcGIS (Wood and Schmidlein 2012, 2013). The Pedestrian Evacuation Analyst uses an anisotropic path-distance (APD) model that calculates the least-costly path to safety in terms of time and energy expenditure using Esri's ArcGIS path-distance geoprocessing tool, the same tool used for the tsunami wave propagation model. This model is more comprehensive than calculating the shortest path using the Euclidean distance (path-only model) as it considers the slope, land cover and travel directionality.

The travel velocity is adjusted based on land cover type, using a speed conservation value (SCV). The SCV represents the percentage of the maximum speed that will occur on the specified ground type. The SCV values proposed by Wood and Schmidlein (2012) are used (Figure 6.4). The SCV assumes that your maximum speed will be achieved on surfaces made for travel, such as roads. Where pedestrian travel is impossible, such as water and building footprints, a value of 0 is assigned. The road network, including pedestrian pathways, and building footprints were also added to the Tofino land cover.

The travel velocity is further adjusted based on the anisotropic (directionally dependent) ground slope derived from Tobler’s hiking function (Wood and Schmidlein 2012), thus individuals will have a higher velocity travelling downhill than uphill. Multiplying the SCV value, slope adjustment value and travelling velocity results in the cost-surface raster.

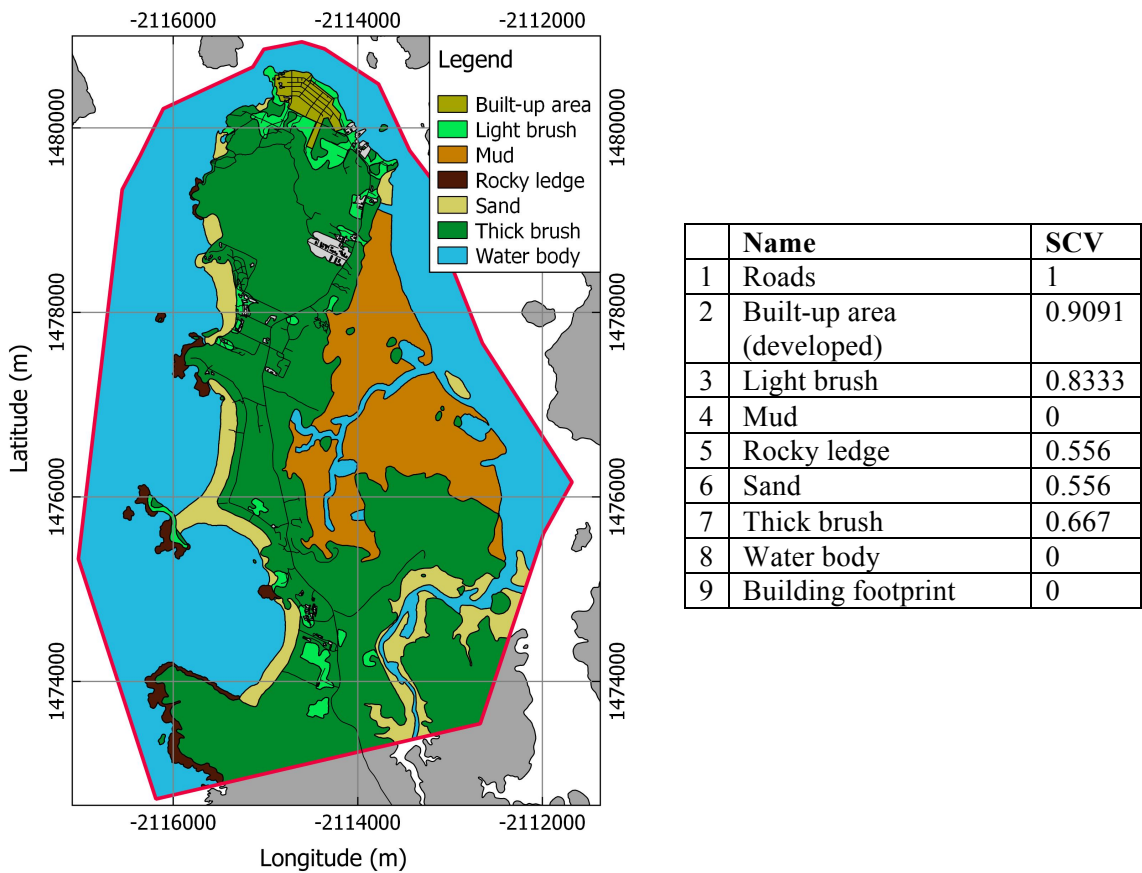


Figure 6.4 Land cover of Tofino used in the Pedestrian Evacuation Analyst and associated speed conservation value (SCV) table

### 6.3 Evacuation Capabilities

Tofino is located directly on the coast of Vancouver Island, within Zone C. The range of run-ups for this zone is between 7 m and 25 m. The current tsunami evacuation map of Tofino (Figure 6.5) uses a run-up of 20 m. However, this 20 m run-up correlates with the generated 23 m run-up of this study (Figure 6.6). The difference is likely due to the coarseness of the DEM used. The maximum run-up of 25 m is therefore likely not to be an overestimation. The evacuation procedures of Tofino do not specify whether individuals should evacuate by foot or vehicle, but the main evacuation route, by way of the Pacific Rim Highway, enables both as it is lined with a multi-use pathway. This route is the only one that spans the entire length of the community, and as such, is at risk of being congested if vehicle evacuation is used by a majority of the population.

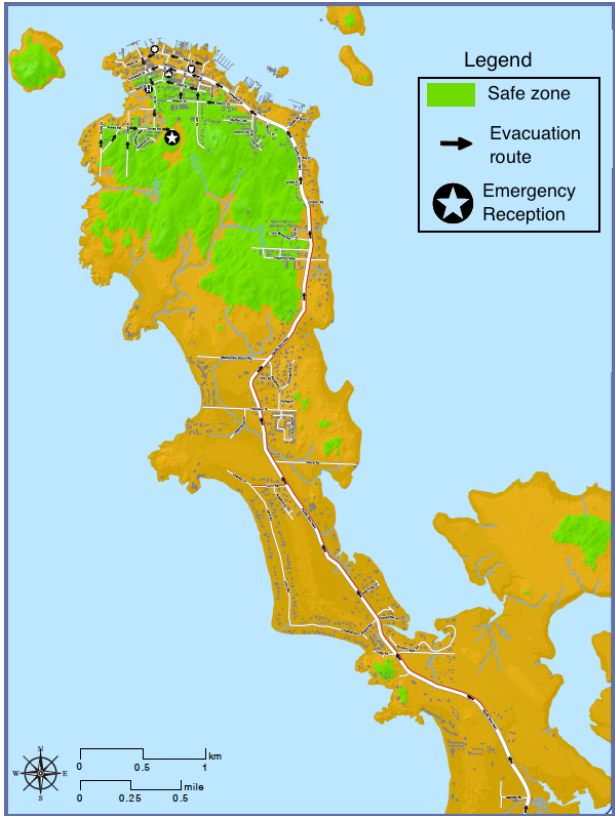


Figure 6.5 Tofino tsunami evacuation map, adapted from District of Tofino (2016)

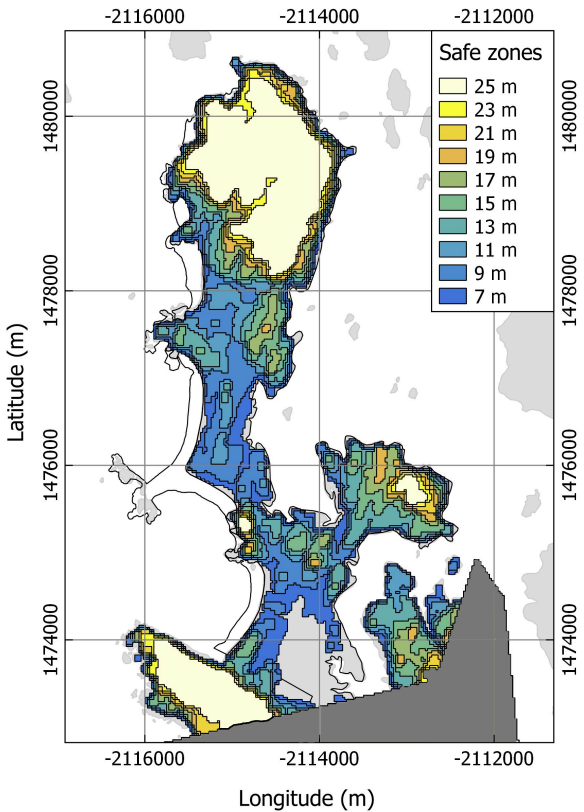


Figure 6.6 Tofino safe zones for run-ups between 7 m and 25 m

APD modeling produces more reliable time to safety results than distance-only approaches, like the Euclidean distance used in this study, as they consider not only the ground cover and slope and its effect on velocity, but obstacles are also considered. The results of the available time computed with the anisotropic path-distance model and population at-risk is presented in the following chapter.

### 6.3.1 Available Time

The minimum run-up to cause a HZ within the Tofino municipality boundary is 7 m (Figure 6.6). Most of the village is within the safe zones for run-ups up to 25 m. The HZ zone created in this area, for each run-up is also very small, as the northern part of the peninsula has steep hills. A second large SZ is located south of the community boundary. At run-ups of 15 m or greater, no natural SZ on the eastern side of the peninsula exists south of MacKenzie Beach until the smaller SZ north of Cox Bay Beach. In the West a portion of the SZ remains for all considered run-ups.

Table 6.2 Minimum available time within the municipal boundary of Tofino found with the anisotropic path-distance (APD) model and distance-only (DO) model for run-ups between 3 m and 25 at three pedestrian evacuation velocities: mobility impaired adult ambulatory speed (MI), average adult ambulatory speed (AW) and slow run (SR)

Run-up	MI			AW			SR		
	APD (min)	DO (min)	Δ (min)	APD (min)	DO (min)	Δ (min)	APD (min)	DO (min)	Δ (min)
3	19.4	25.8	-6.4	10.7	21.7	-11.0	23.8	27.0	-3.2
5	19.4	24.5	-5.2	10.7	21.7	-11.0	23.8	26.3	-2.6
7	13.9	21.9	-8.0	-2.4	17.7	-20.1	21.0	25.0	-4.0
9	9.47	19.9	-10.4	-3.0	14.5	-17.5	18.8	24.0	-5.2
11	-1.6	16.7	-18.4	-8.5	6.4	-14.9	13.3	22.4	-9.1
13	-5.0	13.3	-18.3	-16.5	4.0	-20.5	11.6	20.7	-9.1
15	-11.5	10.3	-21.9	-17.4	-0.8	-16.6	8.4	19.2	-10.9
17	-17.1	7.6	-24.8	-18.7	-4.9	-13.8	5.6	17.9	-12.3
19	-21.4	4.9	-26.3	-18.9	-8.0	-10.9	3.5	16.5	-13.0
21	-26.2	0.5	-26.8	-19.8	-11.5	-8.3	1.1	14.3	-13.3
23	-27.0	0.2	-27.3	-20.6	-12.1	-8.5	0.7	14.2	-13.5
25	-29.0	-0.1	-28.1	-21.6	-13.6	-8.1	-0.2	14.0	-14.4

The available time computed for Tofino using the distance-only approach, from the previous section, are overestimated compared to the available time found using the APD model. The absolute minimum available time, found at 25 m using the MI velocity, using the distance-only model is -0.1 min and -29.0 using the APD model, a difference of -28.1 min (Table 6.2). This is also the maximum difference observed for all run-ups and pedestrian evacuation velocity. A negative difference implies that the distance-only model overestimated, as the APD model is considered to be more correct because it is more precise. The minimum difference in available time is -5.2 min, -8.1 min, and -2.6 for the MI, AW and SR velocities and the maximum difference is -29.0 min, -20.1 and -14.4 min respectively. The minimum for the MI and SR occur at a 5 m run-up and at 25 m run-up for the AW. The maximum, on the other hand occurs at 25 m run-up for both MI and SR and 7 m run-up for AW. The differences in available time cause large discrepancies, between 26.6% and 4553.8%. The largest percentage stemmed from the error being calculated from the value near 0, for example SR 21 m to 25 m run-up. No trend could be identified in the difference in available time.

At the fastest evacuation time, SR, the minimum available time categorizes as high vulnerability from 11 m run-up and above. Using the distance-only model, the high vulnerability is only reached at 21 m run-up. It is not possible to make broad assumptions on the difference that the APD model would create in the available times of the communities, but an overestimation of 30 min could shift communities with low vulnerability into the high vulnerability category, and even below the life safety threshold.

Including the beaches in the analysis increases the maximum distance to safety and thus further decreases the minimum available time. The minimum MI available time found in Tofino, at 25 m run-up of -29.0, decreases to -40.1 min when including the beaches (Figure 6.7). This minimum is found in Chesterman Beach. As the beaches are a popular destination for both residents and tourists, it is important to consider them even if they are outside the legal municipal boundaries. Additionally, as they are directly on the coast, they are located in the most hazardous area.

Chesterman Beach has the lowest available times, followed by MacKenzie and MacKenzie Beach. The life safety is only threatened at a SR pace in Chesterman Beach and MacKenzie at 13 m and 25 m run-up respectively, with a minimum value of -5.8 min and -0.3 min. For AW velocity, life safety is threatened at in Chesterman Beach, Cox Bay, MacKenzie Beach, MacKenzie and West at minimal run-ups of 7 m, 15 m, 17 m, 17 m and 25 m. At 19 m run-up at the slowest pace, MI, the life safety threshold is reached in all zones, except for Village and Middle Beach. The life safety threshold is reached first in Chesterman Beach, followed by Cox Bay at 7 m and 11 m run-up respectively. A large decrease in available time occurs in MacKenzie and MacKenzie Beach at 17 m run-up as the natural SZ on the outcrop between MacKenzie Beach and Chesterman Beach disappears.

All zones, except for the Village, Middle Beach and Cox Beach have insufficient high grounds to maintain life safety at 25 m run-up. However, the minimum available time in West is just below the life safety threshold, -0.67 min. At a more conservative velocity, MI, only Village and Middle Beach can maintain life safety. This demonstrates a near universal need in Tofino for tsunami life safety mitigation.

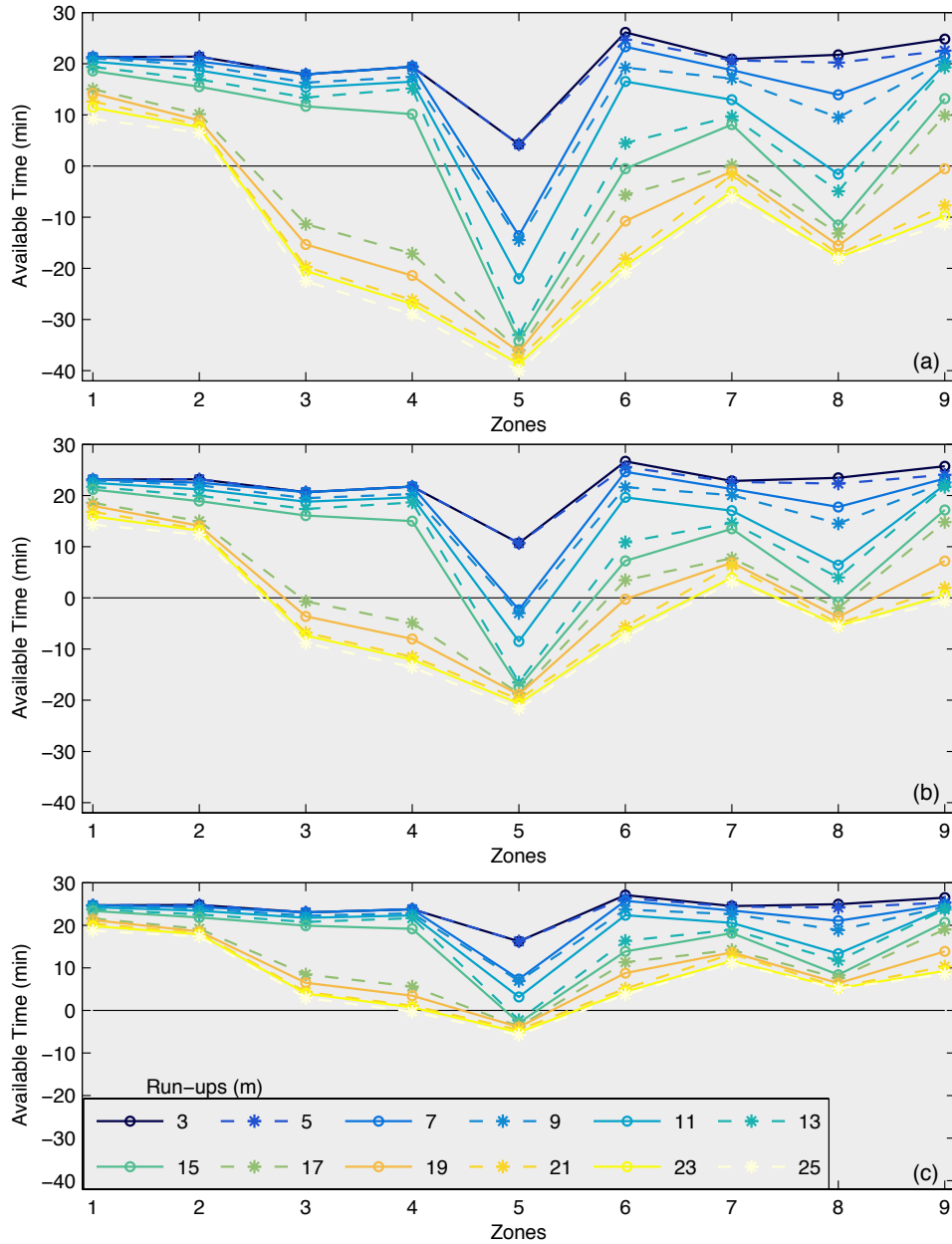


Figure 6.7 Minimum available time (min) by analysis zones for the municipality of Tofino found using the model tsunami arrival time at three evacuation velocities: (a) mobility impaired adult ambulatory speed (MI); (b) average adult ambulatory speed (AW) and, (c) slow run (SR)

### 6.3.2 Population At-Risk

Below a 13 m run-up, the only population within a HZ area that has an available time below the life safety threshold occurs on Frank Island within Chesterman Beach (5). The maximum number of tourists located within the two short-term rentals on Frank Island is 7. As this is a low number, the population at-risk, defined as the population within the HZ, is evaluated from 13 m and above. The population at-risk is presented in Figure 6.8.

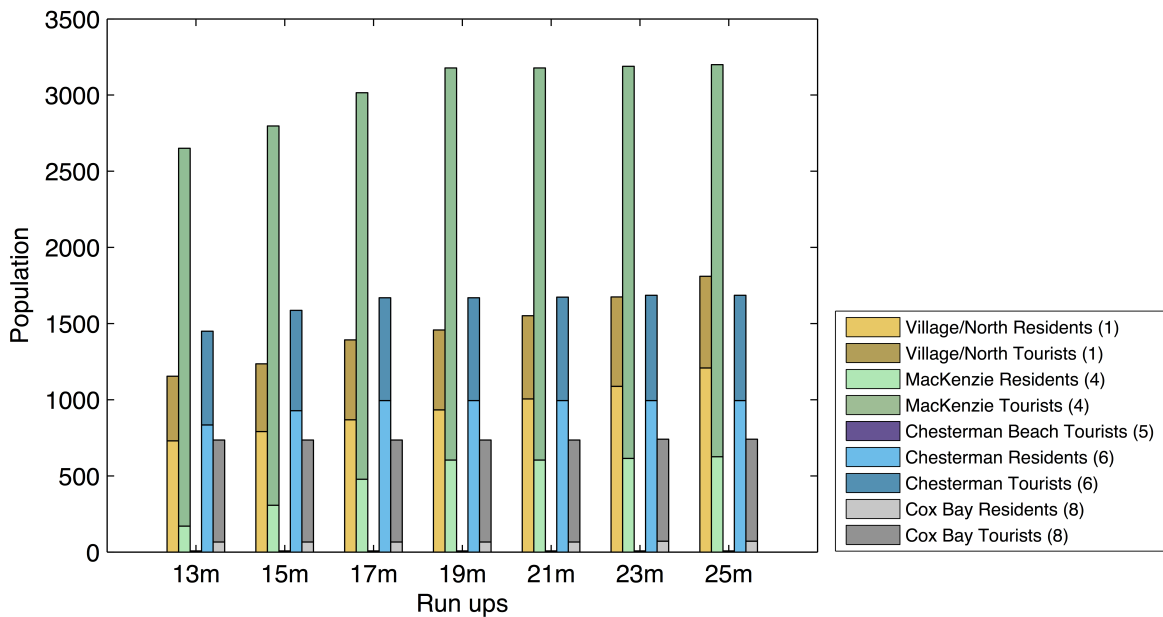


Figure 6.8 Cumulative resident and tourist population at-risk (located within the hazard zone) by analysis areas for the summer-night scenario

Although the life safety threshold is never reached in the Village, its maximum population at-risk during summer night scenario ranges from 1,154 to 1,810. MacKenzie has the largest population at-risk due to the large clusters of tourists (Figure 6.3) originating from 3 large resorts (Middle Beach Lodge, Best Western Tin Wis Resort and Crystal Cove Beach Resort and Campground). The tourist population at-risk in MacKenzie ranges from 2,481 to 2,575, significantly larger than the resident population, which ranges from 170 to 626. The Chesterman Beach tourist population at-risk remains at a constant 7. The resident and tourist population at-risk in Chesterman is almost equal, but with slightly less tourists, because this zone is mostly comprised of single family houses, with many being used for short-term rentals and bed and breakfasts, with its total population at-risk ranging from 1,450 to 1,686. The resident population at-risk within Cox Bay is very small, ranging between 66 and 74. However, a large tourist population is present (Figure 6.3) due to the Pacific Sand Beach Resort and Long Beach Lodge Resort, resulting in a constant 670 tourists at-risk. The total population at-risk for all zones within Tofino ranges from 5,998 to 7,444.

The daytime population was not estimated, but the beaches are a popular tourist attraction and a large number of tourists and residents can likely be found there during the day. As the available time is below the life safety threshold for Chesterman Beach, MacKenzie Beach and Cox Bay Beach at minimum run-ups of 7 m, 17 m and 19 m respectively, within probable run-ups it is certain that a large population would be at-risk in these areas during the day.

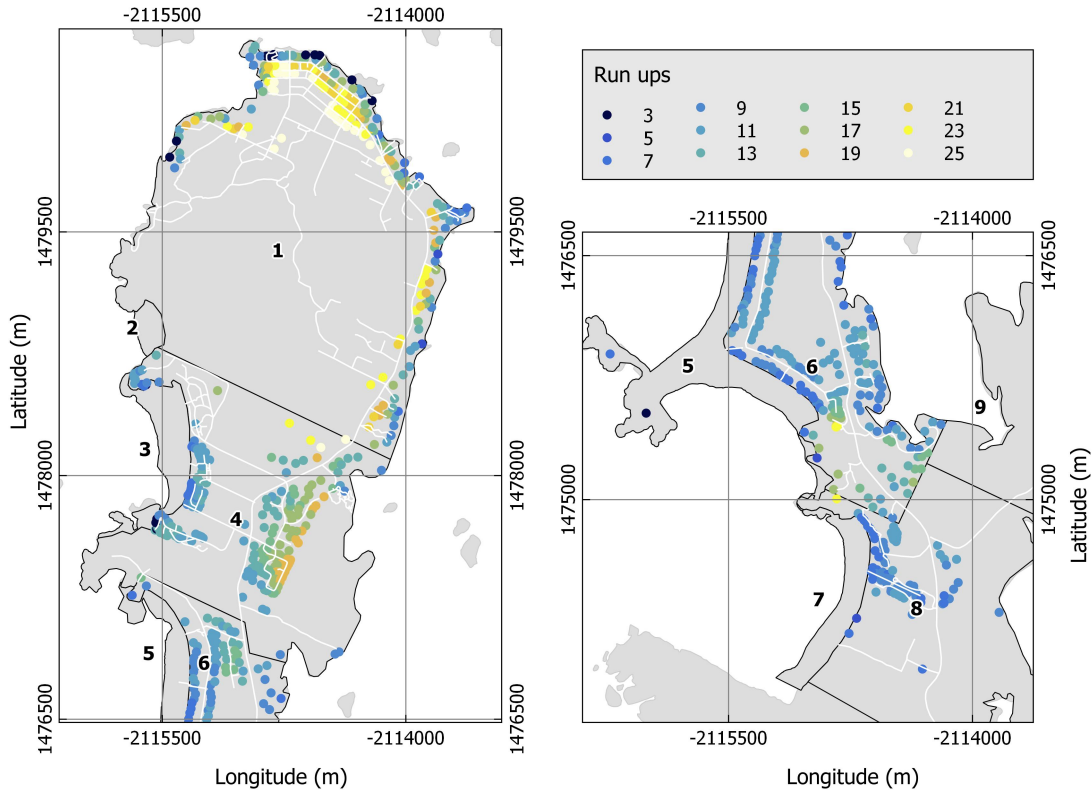


Figure 6.9 Buildings within the HZ for run-ups between 3 m and 25 m

Although the focus of the study is life safety, tsunamis can cause wide spread damage to structures as well. The buildings within the HZs are illustrated in Figure 6.9. Most buildings within Chesterman and Cox Bay are within the HZ at 11 m run-ups. The level of destruction endured is dependent on the construction type of the structure, the water level height and the flow velocities. Height restrictions exist in Tofino, meaning that there is no building taller than 5 storeys and existing buildings most likely cannot be used for vertical evacuation. The majority of residential buildings are simple wood construction single-family homes, based on previous tsunamis (Yeh, et al. 2005) certain level of damage, if not complete destruction is expected. While this is not the focus of the current research, it is important for municipalities to measure the potential economic impacts of a tsunami on their residents, and specifically the implications on future tourism due to the time needed to rebuild and the costs associated.

## 6.4 Life Safety Mitigation Measures

Life saving mitigation measures can take many forms. To reduce the run-up, dikes can be constructed but can be very expensive and are not aesthetically pleasing. Vertical evacuation buildings (VEBs) can also be used where run-up cannot be reduced and horizontal evacuation is not possible. VEBs can take the form of tsunami resistant buildings or engineered berms. This

tactic is implemented in Japan, where some VEBs are multi-purpose. For example, the roof of some residential apartment buildings in Kamaishi, Japan are designated VEBs and have stairwells open to the public at all times in case of a tsunami. VEBs must have enough height to be above the tsunami inundation level and large enough to accommodate all individuals who will be evacuating to that structure.

Dikes are not a feasible solution for Tofino as they would interfere with one of the primary tourism attractions, the beaches, and it would be very costly to build them to an appropriate height that would mitigate against tsunami waves. Therefore, optimal locations for VEBs to ensure life safety are examined in the following section.

#### **6.4.1 Vertical Evacuation Structures**

The locations for possible VEBs were limited to feasible locations where no other buildings were located. Three locations were found that ensured life safety for all tourist and resident populations for the night scenario (Figure 6.1, 6.13). The combination of VEB 1 and 2 is named VEB 3, and the combination of VEB1, VEB2 and VEB4 is named VEB5. The aim of the VEB location placement is to ensure universal life safety, thus the most conservative pedestrian evacuation velocity is used, MI. This velocity is also used for the analysis as time to safety calculated may be underestimated due to the large resolution of the DEM used, as demonstrated by Wood and Schmidlein (2012).

Time to safety is used in this section instead of the available time in order to better compare the decreasing effects of the VEB and to represent the range of tsunami arrival times between the calculated and BC EA value. The population at-life-safety-risk is henceforth defined as the population that has a time to safety equal or greater than the calculated arrival time of 28 min.

At a 13 m run-up the only population at-life-safety-risk is the tourist population on Frank Island (Table 6.3). VEB 1 is as close as physically possible to Frank Island, being on the eastern-most tip of Chesterman. However, this VEB did not reduce the entire population's time to safety below 28.1 min. VEBs cannot be located on the beach as they would not be structurally capable of withstanding a tsunami. Therefore, the Frank Island population, maximum of 7 and 4 during the summer and winter respectively, results in a minimum for the population at-life-safety-risk. Furthermore, the population at-life-safety-risk is further evaluated as the resident population at-risk (RAR) and the tourist population at-risk (TAR).

VEB 1 successfully reduces the population at-life-safety-risk in Chesterman at 15 m and 17 m run-up from 11 and 151, respectively, to 7. Most of the population has a time to safety below 20 min for 15 m run-up. At 17 m run-up the time to safety for the population is below 28.1 min but the large peak at 25 min of approximately 200 people remains. Adding a second VEB, VEB2,

attenuates the peak but a portion of the population with a time to safety above 20 min remains (Figure 6.10).

Table 6.3 Resident and tourist population within the hazard zone (HZ) with a travel time larger than the first wave tsunami arrival time of 28.1 min using a mobility impaired ambulatory speed (MI) for the summer and winter night scenario

Run-up		13m		15m		17m		19m		21m		23m		25m	
Season		Sum.	Win.	Sum.	Win.	Sum.	Win.	Sum.	Win.	Sum.	Win.	Sum.	Win.	Sum.	Win.
RAR	No VEB	0	0	11	4	99	39	220	87	384	152	445	176	478	189
	VE1	0	0	0	0	0	0	-	-	-	-	-	-	-	-
	VE3	-	-	-	-	0	0	0	0	11	4	27	11	33	13
	VE5	-	-	-	-	-	-	-	-	0	0	0	0	0	0
TAR	No VEB	7	4	7	4	59	34	429	244	703	400	721	410	732	417
	VE1	4	2	7	4	7	4	-	-	-	-	-	-	-	-
	VE3	-	-	-	-	7	4	7	4	7	4	19	11	19	11
	VE5	-	-	-	-	-	-	-	-	7	4	7	4	7	4
Total	No VEB	7	4	18	8	158	73	649	331	1087	553	1166	587	1210	606
	VE1	4	2	7	4	7	4	-	-	-	-	-	-	-	-
	VE3	-	-	-	-	7	4	7	4	18	8	46	22	52	24
	VE5	-	-	-	-	-	-	-	-	7	4	7	4	7	4

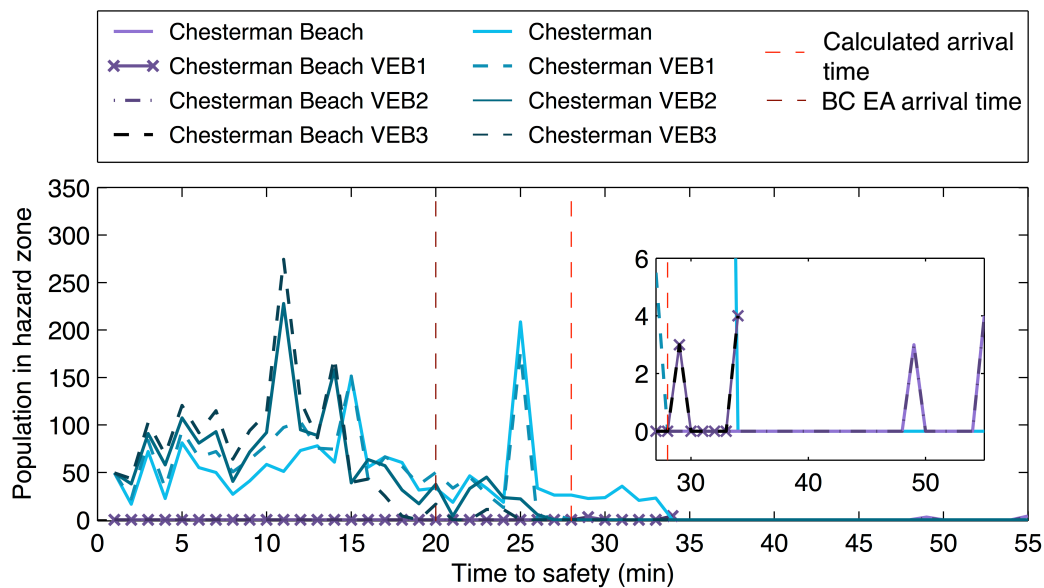


Figure 6.10 Population within the hazard zone for a run-up of 17 m using no VEB, VEB 1, VEB 2 and VEB 3 for Chesterman Beach and Chesterman for a mobility impaired adult ambulatory speed (MI)

The MacKenzie Zone first contributes to the population at-life-safety-risk at 19 m run-up. Two VEBs, as the configuration VEB3 are required to reduce the population at-life-safety-risk from 649 to 7 (Figure 6.11). The time to safety is reduced below 20 min in Chesterman but not in MacKenzie.

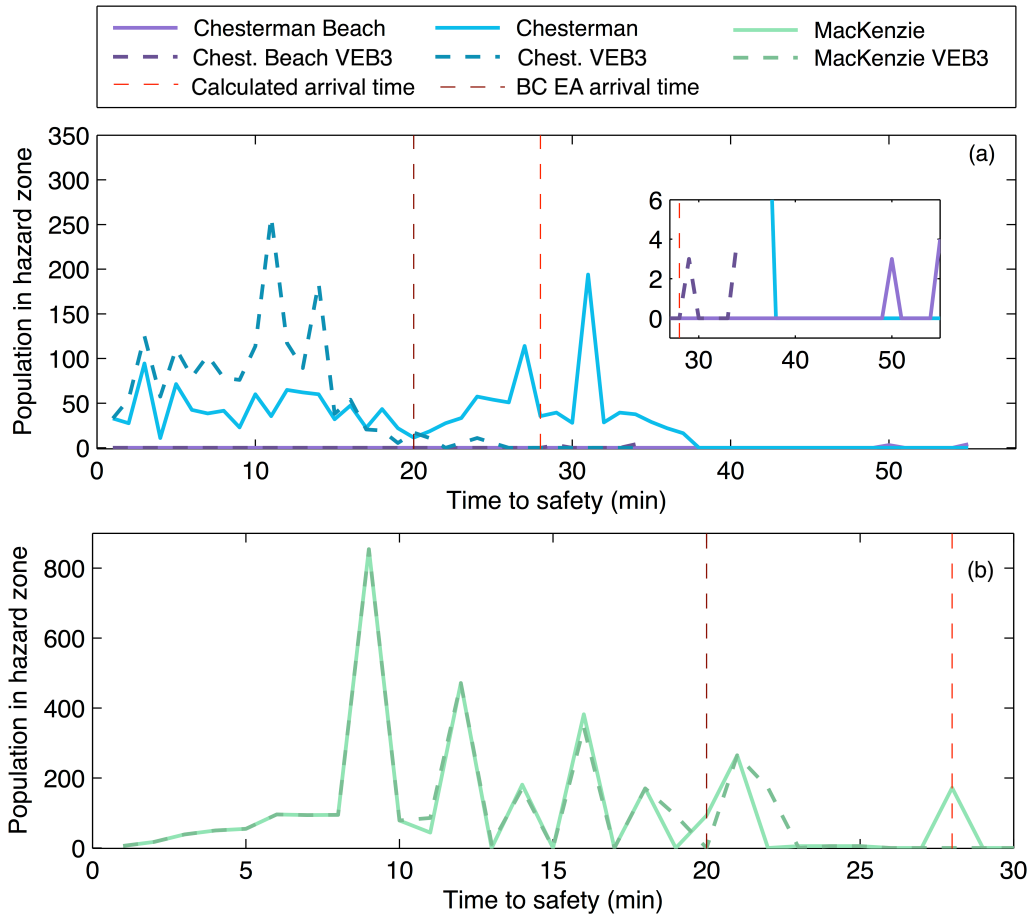


Figure 6.11 Population within the hazard zone for a run-up of 19 m using no VEB and VEB 3 for a mobility impaired adult ambulatory speed (MI), (a) Chesterman Beach and Chesterman; (b) MacKenzie

Three VEBs are necessary starting at 21 m run-up due to population at-life-safety-risk within Cox Bay. VEB1 and 2 do not reduce the population in Cox Bay as they are located too far north. The addition of VEB4 to form the VEB5 configuration is required. This configuration, due to VEB4, reduces the population at-life-safety-risk in Cox Bay from 11 for 21 m run-up and 39 for 23 m and 25 m run-up to 0 (Figure 6.12). The addition of VEB4 has no influence on the Chesterman and MacKenzie population. VEB 3 reduces the population at-life-safety-risk to 0 for 21 m to 25 m run-up in Chesterman and MacKenzie (Figure 6.13). However, 55, 65, and 85 individuals have a time to safety below 20 min in Chesterman at run-ups of 21 m, 23 and 25 m run-up. Similarly, 546, 1,084 and 1,095 individuals have a time to safety below 20 min in MacKenzie, of which 81.9 % to 87.9% are tourists. Resorts in the MacKenzie area should consider providing vertical refuge on their property as such a large number of tourists may need more than 20 min to reach safety to the proposed VEBs. Additionally, as the resorts are located along the beaches, in the most hazardous area, it would be an ideal location for vertical refuge.

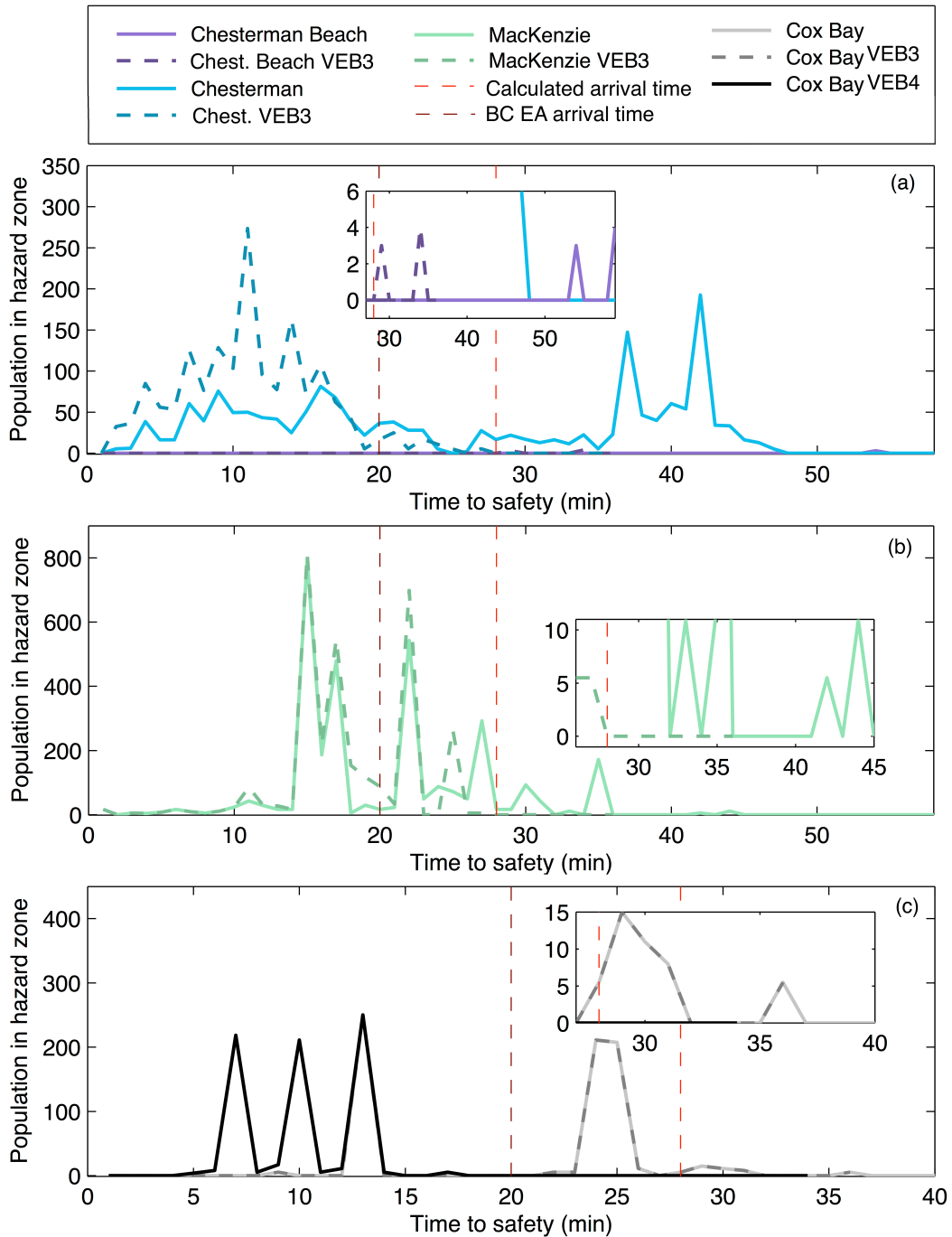


Figure 6.12 Population within the hazard zone for a run-up of 25m using no VEB, VEB3 and VEB4 for a mobility impaired adult ambulatory speed (MI), (a) Chesterman Beach and Chesterman; (b) MacKenzie; (c) Cox Bay

The VEB5 configuration of the three refuges at the maximum 25 m run-up decreases the time to safety below the tsunami arrival time of 28.1 min for all the beaches, not including Frank Island. The time to safety is below 20 min for most of Cox Bay Beach and Chesterman Beach, and below 28 min for MacKenzie Beach. The southwest portion of MacKenzie has a time to safety above 20 min, and mostly below 28 min. Fortunately those parts covered by forest do not include

many structures. Similarly, some parts of West have a time to safety above 20 min and 28.1 min, but are not areas that have any structures.

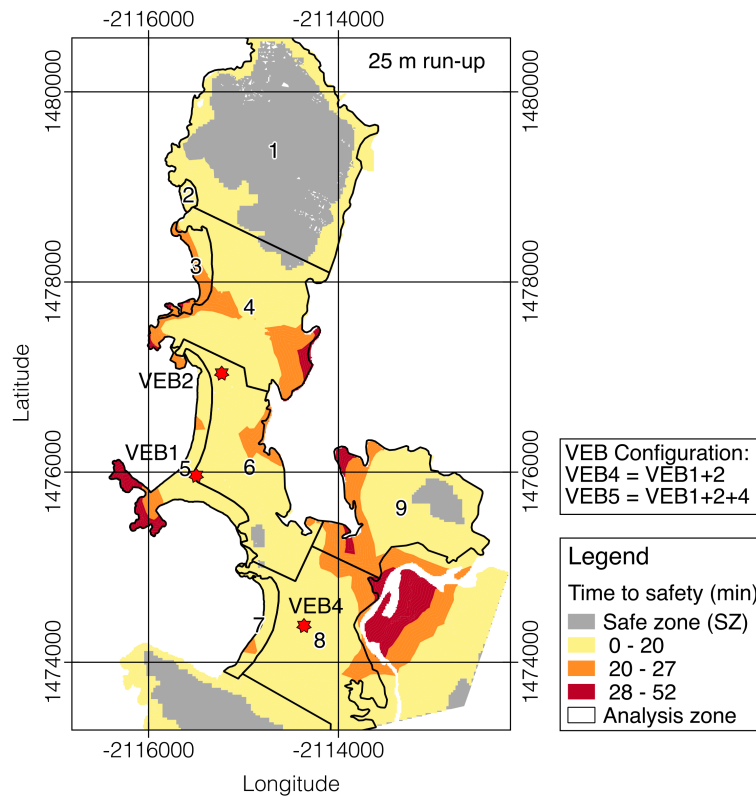


Figure 6.13 Time to safety (min) using with 3 vertical evacuation structures in the VEB5 configuration

## 6.2 Conclusions

Using a more precise anisotropic path-distance model, which considers the land cover and slope, results in much smaller available times in Tofino. The minimum available time decreases from -0.073 min, found with the distance-only approach, to -29.0 min within the Tofino municipality boundary. The minimum available time is even smaller, -40.1 min, when considering the beaches. Tofino has a need for tsunami life safety mitigation solutions South of the main village as the available time universally reaches the life safety threshold in the most conservative velocity, MI, at 19 m run-up. At the MI and AW velocity, the life safety threshold is reached at a minimum of 7 m run-up.

The path-only approach overestimates the available time by 14.4 min to 29.9 min for the three pedestrian evacuation velocities compared to the anisotropic path-distance model results. This results in errors between 26.6% and 4553.8%. No trend could be found in the differences in available time by run-up or evacuation velocities. It is likely that the available time in other communities in BC are also overestimated as they were found with the path-only approach.

However, no assumptions can be made about how much the available time is overestimated. The maximum difference observed in Tofino of -29.9 min is large enough that it can shift community's vulnerability category from low to high, and shift moderate vulnerability below the life safety threshold.

The population in Tofino was estimated for two scenarios: summer night and winter night. The winter population is much lower than in the summer and was estimated during the busiest winter month. The winter population was estimated at 4,506, which includes 2,630 tourists, more than the resident population from the census which represents 1,876 people. The summer population was found to be more than double the winter at 9,121 people. The summer population is very large due to the increase in residents from seasonal workers and the large tourist population of 4,621. The tourist population is an important subgroup to consider, as they may be more vulnerable to tsunami dangers due to a lack of education compared to the resident population.

The population was found to be in areas where available times are below the life-safety threshold at a minimum run-up of 13 m. The tourist population located in the two short-term rentals are an exception, as they are within life safety risk from 7 m run-up and above. The total population at-risk ranges between 5,998 and 7,444 for the summer night scenario. MacKenzie is the zone that has the largest population at-risk due to a large number of tourists from the 2 large resorts.

Three possible locations for vertical evacuation structures are suggested. Having the 3 structures, under the configuration VEB5, ensures a time to safety above the calculated tsunami arrival time of 28.1 min except for the Frank Island. No vertical evacuation structures can sufficiently reduce the time to safety below the tsunami arrival time there at mobility impaired ambulatory speed from 13 m run-up and above. VEB5 also reduces the time to safety below 28.1 min in all the beaches and populated areas. However, the time to safety could not be reduced below the BC EA arrival time value of 20 min. Large tourist populations are at-risk, mostly in MacKenzie. Therefore, locations for vertical evacuation structures should be considered on the resorts, as they are located on the coast in the most hazardous areas and to ensure safety of their clients.

# Chapter 7. Conclusions and Recommendations for Future Work

---

## 7.1 Conclusions

A life safety vulnerability assessment of the Canadian West Coast to a CSZ tsunami was performed in terms of evacuation capability for the five Tsunami Notification Zones with a distance-only approach. The evacuation capabilities are measured using the available time, where the life safety threshold is 0. The following conclusion can be drawn:

- The potential run-ups that can be expected from a Pacific subduction earthquake in each zone vary the most in Zone A, B and C as there is limited information regarding the tsunami hazard North of the Strait of Georgia. The largest run-ups are expected on the West of Vancouver, in Zone C, where the hazard is the greatest. The probable tsunami run-up ranges, including 50% for safety and 0.5 m allowance for sea level rise for each zone are 3.0 m to 11.0 m for Zone A and B, 5.0 m to 25 m for Zone C, 3.0 m to 7.0 for Zone D and 3.0 m to 5.0 m for Zone E.
- Although Zone E has the smallest probable run-up range, the surface area and population within the hazard zone is significantly larger than all other zone. The large inundated surface area is caused by the large number of communities in this zone and the large low-lying area of the Lower Mainland.
- Zone C has the highest vulnerability of all zones, agreeing with previous research that the outer Vancouver Island is the most at risk. It has the lowest available time median, with 25% of its communities within the moderate vulnerability threshold at 9 m run-up and above. Zone C also has the highest percentage, 39.7%, of its surface area inundated at its maximum probable run-up.
- All communities have an available time within the low vulnerability in Zone A, B, D and E at their maximum probable run-up. Landslides tsunami may pose a greater threat in these zones, especially in Delta and Richmond, as the tsunami arrival time would be shorter than one from a Cascadia tsunami.
- The available time life safety threshold is surpassed in 4 communities in Zone C, Barlett Island 32, Grassy Island 17, Hesquiat 1 and Tofino, at minimum run-ups of 19 m, 11 m, 21 m and 7 m. Winter Harbour, Ucluelet, Port Renfrew, Bamfield and 42 other First Nations communities were found to have an available time within the moderate of high vulnerability. Future study of the tsunami hazard should concentrate in these areas as the path-only approach has been found to underestimate the required time to safety, and therefore underestimate their vulnerability.

A more detailed vulnerability assessment using anisotropic path-distance modeling was performed in Tofino. The findings of this assessment are summarized below:

- The use of a more precise anisotropic path-distance model resulted in lower available times than the distance-only model. The distance-only model overestimated the available time by 14.4 min to 29.9 min in Tofino for the three pedestrian velocities considered.
- The minimum available time was found to be -29.0 min (below the life safety threshold) within the official municipality boundary. Adding the beaches to the analysis, which are popular tourist attractions, further reduced the available time to a minimum of -40.1 min.
- Two vertical evacuation structures were found to be necessary to reduce the time to safety below the tsunami arrival time of 28.1 min for run-ups between 13 m and 19 m. For run-ups of 21 m and greater, three vertical evacuation structures are required. No configuration could be found to reduce sufficiently the time to safety on Frank Island.

## **7.2 Recommendations for Future Work**

Based on the literature review and findings from this research the following suggestions for future work are recommended:

- A thorough investigation by numerical modeling following a similar probabilistic approach of ASCE 7-16 of the Canadian West Coast should be conducted to determine the tsunami inundation hazard in a uniform manner and more accurate minimum tsunami arrival times. Such models should include all possible tsunami sources, including the hazard from submarine and aerial landslides.
- Communities with the greatest life safety vulnerability that have been highlighted in this study should be further examined using more detailed evacuation models such as static anisotropic path-distance or dynamic agent-based models. Such models should include the built environment. Moreover, the merits of vehicle evacuation should be evaluated, mostly in communities with large distance to travel and time to safety.
- The available time results found should be replicated and compared with models using finer resolution elevation models and using more complex path-distance model to determine possible effects on the life safety vulnerability.
- Further vulnerability assessment should evaluate the short and long-term economic impacts of a tsunami on an individual, community and provincial level.

## References

---

- Abe, K. *Estimate of tsunami run-up heights from earthquake magnitudes*. Vol. 4, in *Tsunami: progress in prediction, disaster prevention and warning. Advances in technological hazards research*, by Y. Tsuchiya and N. Shuto, 21-25. Kluwer, 1995.
- Alerni Valley Museum. "The Great Tsunami of 1964." *Virtual Museum*. Alerni Valley Museum. 2016. [http://www.virtualmuseum.ca/sgc-cms/histoires\\_de\\_chez\\_nous-community\\_memories/pm\\_v2.php?id=record\\_detail&fl=0&lg=English&ex=00000820](http://www.virtualmuseum.ca/sgc-cms/histoires_de_chez_nous-community_memories/pm_v2.php?id=record_detail&fl=0&lg=English&ex=00000820) (accessed 08 16, 2016).
- American Society of Civil Engineers (ASCE). "Tsunami Loads and Effects." In *Minimum Design Loads for Buildings and Other Structures (7-16)*, by ASCE. 2016.
- Anderson, Peter. Improving End-To-End Tsunami Warning for Risk Reduction on Canada's West Coast. Contract Report, Simon Fraser University, Burnaby: Simon Fraser University, 2016.
- Anderson, Peter S., Stephen Braham, Olympia Koziatek, Amanda Oldring, Dawn Ursulak, and Marc d'Aquino. *British Columbia Tsunami Notification Methods*. Toolkit, Simon Fraser University, Telematics Research Lab, Burnaby: National Defence, 2016.
- Anguelova, Z., D. A. Stow, and J. Kaiser. "Integrating Fire Behavior and Pedestrian Mobility Models to Assess Potential Risk to Humans from Wildfires Within the U.S.–Mexico Border Zone." *The Professional Geographer* (Taylor and Francis Group) 62, no. 2 (2010): 230-247.
- Atwater, B. F., and D. K. Yamaguchi. "A Tsunami about 1000 Years Ago in Puget Sound, Washington." *Science* 258, no. 5088 (1992): 1614.
- Atwater, B.F. "Evidence of greate Holocene earthquake along the outer coast of Washington State." *Science* (Elsevier B.V.), 1987: 958-958.
- Atwater, Brian F., et al. "Summary of Coastal Geologic Evidence for Past Great Earthquakes in the Cascadia Subduction Zone." *Earthquake Spectra* 11, no. 1 (02 1995): 1-18.
- Ausenco Sandwell. *Climate Change Adaptation Guidelines for Sea Dikes and Coastal Flood Hazard Land Use*. Draft Policy Discussion Paper, BC Ministry of Environment, 2011.
- BC Earthquake Alliance Society. "Frequently Asked Questions (FAQs) for tsunami in British Columbia." *The Great British Columbia Shake Out*. 2016. [http://www.shakeoutbc.ca/downloads/Tsunami\\_FAQ.pdf](http://www.shakeoutbc.ca/downloads/Tsunami_FAQ.pdf) (accessed 08 15, 2016).
- Bodle, R. R. "Aleutian earthquake and sea wave of April 1, 1946." *Earthquake Notes* 17, no. 4 (1946): 6.
- Bretschneider, C. L., and P. G. Wybro. "Tsunami inundation prediction." *Proceedings of 15th Coastal Engineering conference*. Honolulu: ASCE, 1977. 1006-1024.
- Bryant, Edward. *Tsunami*. Kuala Lumpur: Springer, 2014.

- Burcharth, H. F., and S. Hughes. "Types and Functions of Coastal Structures." In *Coastal Engineering Manual*. Vicksburg: Coastal Engineering Research Center, 2003.
- Camfield, F. E. *Tsunami engineering*. Special Report 6, Coastal Engineering Research Centre, US Army Corps of Engineers, 1980.
- Canadian Hydrographic Service (CHS). "Data products and Surveys." *Fisheries and Oceans Canada*. 2016. <http://www.charts.gc.ca/data-gestion/index-eng.asp> (accessed 05 01, 2016).
- Canadian Hydrographic Service. "High-water Line for British Columbia." *Data Product and Survey*. 2016. <http://www.charts.gc.ca/data-gestion/index-eng.asp> (accessed 03 04, 2016).
- Centre for Sustainability Whistler. *Tofino Tourism Master Plan*. District Municipality of Tofino, 2014.
- Centre for Sustainability Whistler. *Tofino Vision to Action Sustainable*. Community Action Plan, Tofino: District of Tofino, 2014.
- Cherniawasky, Josef Y., Vasily V. Titov, Kelin Wang, and Jing-Wang Li. "Numerical Simulations of Tsunami Waves and Currents for Southern Vancouver Island from a Cascadia Megathrust Earthquake." *Pure and Applied Geophysics*, 2007: 465-492.
- Cheung, K., and Y. Yamazaki. "Validation of NEOWAVE with Measurements from the 2011 Tohoku Tsunami." *American Geophysical Union, Fall Meeting 2012*. American Geophysical Union, 2012.
- Church, R. L., and R. Sexton. *Modeling Small Area Evacuation: Can Existing Transportation Infrastructure Impede Public Safety?* Final Report, University of California, Santa Barbara and California Department of Transportation, 2002.
- Clague, J. J., I. Hutchinson, and J. L. Lesemann. "Tsunami hazard at the Fraser River Delta Columbia, Canada." Report for the Corporation of Delta and the City of Richmond, 2005, 27.
- Clague, J.J., and T.S. James. "History and isostatic effects of the last ice sheet in southern British Columbia." *Quaternary Science Review*, no. 21 (2002): 71-87.
- Clague, John J. "Evidence for Large Earthquake at the Cascadia Subduction Zone." *Review of Geophysics* (American Geophysical Union) 34, no. 4 (1997): 439-460.
- Clague, John J., Adam Munro, and Tad Murty. "Tsunami Hazard and Risk in Canada." *Natural Hazards* (Kluwer Academic Publishers) 28 (2003): 433-461.
- Clague, John J., and Peter T. Bobrosky. "The geological signature of great earthquake off Canada's west coast." *Geoscience Canada* 26, no. 2 (1999): 1-15.
- Clague, John J., and Peter T. Bobrowsky. "Evidence for a Large Earthquake and Tsunami 100-400 Years Ago on Western Vancouver Island, British Columbia." *Quaternary Research* 41, no. 2 (1994): 176-184.

- Clague, John J., Peter T. Bobrowsky, and Ian Hutchinson. "A review of geological records of large tsunamis at Vancouver Island, British Columbia, and implications for hazard." *Quaternary Science Reviews* (Pergamon) 19 (2000): 849-863.
- Cova, T. J., and R. L. Church. "Modeling community evacuation vulnerability using GIS." *Geographical Information Science* 11, no. 8 (1997): 763-784.
- Darienzo, Mark E., and Curt D. Peterson. "Episodic tectonic subsidence of Late Holocene salt marshes, northern Oregon Central Cascadia Margin." *Tectonics* (Elsevier B.V) 9, no. 1 (02 1990): 1-22.
- Digital Globe. "Tofino, British Columbia (49.1428, -125.9014)." *Google Maps*. 2016. <https://www.google.ca/maps/place/Tofino,+BC/@49.1289788,-125.9213324,8543m/data=!3m2!1e3!4b1!4m5!3m4!1s0x548990ccb0093843:0x331095695a741a35!8m2!3d49.1529842!4d-125.9066184> (accessed 07 05, 2016).
- District of Tofino. *Maps - Document Center*. Tofino, 2010.
- District of Tofino. *Maps - Document Center*. Tofino, 08 15, 2015.
- Dunbar, D., P. H. LeBlond, and T. S. Murty. "Maximum Tsunami Amplitude and Associated Currents on the Coast of British Columbia." *Science of Tsunami Hazards* (The Tsunami Society) 7, no. 1 (1989): 3-44.
- Environmental Systems Research Institute, Inc. (ESRI). *An overview of the Generalization toolset*. 2016. <http://desktop.arcgis.com/en/arcmap/10.3/tools/spatial-analyst-toolbox/an-overview-of-the-generalization-tools.htm> (accessed 08 25, 2016).
- Faupel, Charles E., Susan P. Kelley, and Thomas Petee. "The Impact of Disaster Education on Household Preparedness for Hurricane Hugo." *International Journal of Mass Emergencies and Disasters*, 1992: 5-24.
- Federal Emergency Management Agency (FEMA). *Guidelines for Design of Structures for Vertical Evacuation from Tsunamis (FEMA P-646)*. Guidelines, U.S. Department of Homeland Security, 2012.
- Fine, I. V., J. Y. Cherniawsky, A. B. Rabinovich, and F. Stephenson. "Numerical modeling and observations of tsunami waves in Alberni Inlet and Barkley Sound, British Columbia ." *Pure and Applied Geophysics* 165, no. 11-12 (2008): 2019-2044.
- Fujima, K. "Friction laws for long waves on dry bed." *Proceedings of the IUGG/IOC International Tsunami Symposium*. Novosibirsk: IUGG/IOC, 1980. 115-119.
- Geist, E. L. "Local Tsunamis and Earthquake Parameters." *Advances in Geophysics* 39 (1998): 117-209.
- GeoBC. "Digital Elevation Model for British Columbia - CDED - 1:250,000." *GeoBC*. Lands and Natural Resource Operations Ministry of Forests. 02 20, 2012. <https://catalogue.data.gov.bc.ca/dataset/digital-elevation-model-for-british-columbia-cded-1-250-000> (accessed 01 25, 2015).

- Geological Survey of Canada. "GeoGratis." *Natural Resources Canada*. Geofacts Natural Resources Canada. 01 01, 2011. <http://geogratings.gc.ca/api/en/nrcan-rncan/ess-sst/3e11b6eb-5b15-504e-88d2-4de05c5f1f56.html> (accessed 08 04, 2015).
- Get Prepared. *Tsunamis*. 2016. <http://www.getprepared.gc.ca/cnt/hzd/tsnms-en.aspx> (accessed 08 15, 2016).
- Gonzales, F. I., R. J. LeVeque, and L. M. Adams. *Tsunami Hazard Assessment of the Ocosta School Site in Westport, WA*. Technical Report, University of Washington, 2013.
- Gonzalez, F.I., H.B. Milbirn, E.N. Bernard, and J. Newman. *Deep-ocean Assessment and Reporting of Tsunami (DART)*. Status Report, National Oceanic and Atmospheric Administration, National Data Buoy Center, Seattle: National Data Buoy Center, 1998.
- Hasegawa, H. S., and G. C. Rogers. "Quantification of the Magnitude 7.3 British Columbia Earthquake of June 23, 1846." *Tectonophysics* (Elsevier) 49 (1978): 185-188.
- Hebenstreit, G. T., and T. S. Murty. "Tsunami Amplitude from Local Earthquakes in the Pacific Northwest Region of North America Part 1: The Outer Coast." *Marine Geodesy* 13 (1989): 101-146.
- Henry, R. F., and T. S. Murty. *Resonance periods of multi-branched inlets with tsunami amplification*. 28, Ottawa: Department of Environment, Marine Sciences Directorate, 1972, 47-79.
- Hensen, W. R., et al. *The Alaska Earthquake of March 27, 1964; field investigations and reconstruction effort*. Professional Paper 541, U.S. Geological Survey, 1966.
- Houston, J. R., and A. W. Garcia. *Type 16 Flood Insurance Study: tsunami predictions for the West Coast of the continental United States*. Technical Report H-78-26, Vicksburg: U.S. Army Engineer Waterways Experiment Station, 1978.
- Intergovernmental Panel on Climate Change (IPCC). *Managing the Risks of Extreme Events and Disasters to Advance Climate Change Adaptation*. Special Report, New York: Cambridge University Press, 2012.
- IPCC. *Fourth Assessment Report: Climate Change 2007*. Intergovernmental Panel on Climate Change, Cambridge University Press, 2007.
- Italian Ministry for the Environment, Land and Sea (IM-ELS). *Reduce tsunami risk: strategies for urban planning and guidelines for construction design*. Department for Environmental Research and Development, in collaboration with the Asian Disaster Preparedness Center, 2006.
- Jobe, R., and P. White. "A new cost-distance model for human accessibility and an evaluation of accessibility bias in permanent vegetation plots in Great Smoky Mountains National Park, USA." *Journal of Vegetation Science* 20 (2009): 1099-1109.
- Johnstone, W. M., and B. J. Lence. "Assessing the value of mitigation strategies in reducing the impacts of rapid onset, catastrophic floods." *Journal of Flood Risk Management* (Blackwell Publishing Ltd), 2009: 1-13.

- Johnstone, W. M., and B. J. Lence. "Use of Flood, Loss, and Evacuation Models to Assess Exposure and Improve a Community Tsunami Response Plan: Vancouver Island." *Natural Hazards Review* 13, no. 2 (2012): 162-171.
- Johnstone, W. M., and B. J. Lence. "Use of Flood, Loss, and Evacuation Models to Assess Exposure and Improve a Community Tsunami Response Plan: Vancouver Island." *Natural Hazard Review*, 2012: 162-171.
- Jones, Robert L. "Canadian Disasters: An Historical Survey." *Natural Hazards* (Kluwer Academic Publishers) 5 (1992): 43-51.
- Jonkman, S. N., vanGelder, P. H. A. J. M. and Vrijling, H. "An overview of quantitative risk measures and their application for calculation of flood risk." *ESREL 2002 European Conference*. Châtenay-Malabry Cedex: European Safety and Reliability Association, 2002.
- Kanoglu, U. *The runup of long waves around pievewice linear bathymetries*. PhD thesis, Los Angeles: University of Southern California, 1997.
- Katada, Toshitaka, Noriyuki Kuwasawa, Harry Yeh, and Cherri Pancake. "Intergrated simulation of tsunami hazards." *EERI's Eighth U.S. National Conference on Earthquake Engineering (8NCEE)*. 2006.
- Kelman, I., and R. Spence. "An overview of flood actions on buildings." *Engineering Geology* 73, no. 3-4 (2004): 297-309.
- Klinkenberg, Brian. *BC Environment Standard Projection*. 1995.  
<http://ibis.geog.ubc.ca/~brian/Course.Notes/bceprojection.html> (accessed 08 29, 2016).
- Komar, P. D. *Beach Processes and Sedimentation*. Upper Saddle River, N.J.: Prentice Hall, 1998.
- Kowalik, Z., and P. M. Whitmore. "An investigation of two tsunamis recorded at Adak, Alaska." *Science of Tsunami Hazards* 9 (1991): 67-83.
- Laghi, M., A. Cavelletti, and P. Polo. *Evacuation route tools ArcGIS toolbox user's manual*. User's Manual, Italian Ministry for the Environment and the Territory and Asian Disaster Preparedness Center, 2006.
- Lander, J. F. *Tsunamis Affecting Alaska, 1737–1996*. U.S. Department of Commerce, Boulder: National Geophysical Data Center, 1996.
- Langmuir, Eric. *Mountaintcraft and Leadership. Official Handbook of the Mountain Leader Training Boards of Great Britain and Northern Ireland*. Edinburgh, Scotland: Britain & Scottish Sports Council, 1984.
- Leon, J., and A. March. "An urban form response to disaster vulnerability: Improving tsunami evacuation in Iquique, Chile." *Environment and Planning B: Planning and Design* 43, no. 5 (2016): 826-847.

- Leonard, G. S., et al. "Interim tsunami evacuation planning zone boundary mapping for the Wellington and Horizons regions defined by a GIS-calculated attenuation rule." *GNS Science*, 2009.
- Leonard, L. J., and J. M. Bednarski. "Field Survey Following the 28 October 2012 Haida Gwaii Tsunami." *Pure and Applied Geophysics* (Birkhäuser ) 171 (2014): 3467-3482.
- Leonard, L. J., Garry C. Rogers, and Stephane Mazzotti. "Tsunami hazard assessment of Canada." *Natural Hazard* 70 (2013): 237-274.
- Leonard, Lucinda J., Roy D. Hyndman, and Stephane Mazzotti. "Coseismic subsidence in the 1700 great Cascadia earthquake: Coastal estimates versus elastic dislocation models." *The Geological Society of America Bulletin* 116, no. 5-6 (2003): 655-670.
- Li, Y. *Tsunamis: Non-Breaking Solitary Wave Run-up*. Report KH-R-60, Caltech, 2000.
- Li, Y., and F. Raichlen. "Energy Balance Model for Breaking Solitary Wave Runup." *Journal of Waterway, Port, Coastal, and Ocean Engineering* 129, no. 2 (2003): 47-59.
- Li, Y., and F. Raichlen. "Solitary Wave Run-up on Plane Slopes." *Journal of Waterway, Port, Coastal, and Ocean Engineering* 127, no. 1 (2001): 33-44.
- Liu, P. L-F., and Yong-Sik Cho Seung-Buhm Woo. *Computer Program for Tsunami Propagation and Inundation*. Ithaca, NY: School of Civil and Environmental Engineering, Cornell University, 1998.
- May, A. D. *Traffic Flow Fundamentals*. Upper Saddle, NJ: Prentice Hall, 1990.
- McCaffrey, Robert, and Chris Goldfinger. "Forarc deformation and great subduction Earthquakes: implications for Cascadia offshore earthquake potential." *Science* 267 (02 1995): 856-859.
- McMillan, Alan D., and Ian Hutchinson. "When the Mountain Dwarfs Danced: Aboriginal Traditions of Paleoseismic Events along the Cascadia Subduction Zone of Western North America." *Ethnohistory* 49, no. 1 (2002): 41-68.
- McMurty, Gary M., et al. "Stratigraphic constraints on the timing and emplacement of the Alika 2 giant Hawaiiin submarine landslide." *Journal of volcanology and geothermal research* (Elsevier), no. 94 (1999): 35-58.
- McSaveney, M., and M. Rattenbury. *Tsunami impact in Hawke's Bay*. In Client Report 2000/77, Institute of Geological and Nuclear Sciences, 2000.
- Mikami, T., M. Kinoshita, S. Matsuba, S. Watanabe, and T. Shibayama. "Detached Breakwaters Effects on Tsunamis around Coastal Dyke." *8th International Conference on Asian and Pacific Coasts* . Procedia Engineering, 2015. 422-427.
- Ministry of Education. *Emergency Management Planning Guide for Schools, Districts and Authorities*. Guide, British Columbia: British Columbia, 2015.
- Moneo, Shannon. "Signs warning of tsunami seen as blight." *The Globe and Mail*, 04 17, 2007.

- Mosher, D. C., H. A. Christian, J. A. Hunter, and J. L. Luternauer. "Onshore and offshore geohazards of the Fraser River delta." In *Fraser River Delta, British Columbia: Issues of an Urban Estuary*, Geological Survey of Canada, Bulletin no. 567, by B. J. Groulx, D. C. Mosher, J. L. Luternauer and D. E. Bilderback, 67-79. Natural Resources Canada, 2004.
- Murata, S. *Tsunami: To survive from Tsunami. Advance Series on Ocean Engineering 32*. World Scientific, 2009.
- Murty, T. S. *Seismic Sea Waves: Tsunamis*. Bulletin of the Fisheries Research Board of Canada, 198, Fisheries Research Board of Canada; Canada. Fisheries and Marine Service, 1977, 377.
- Murty, T.S., and R.E. Brown. *The submarine slide of 27 April, 1975 in Kitimat inlet and the water waves that accompanied the slides*. Pacific Marine Science Report 79-11, Institute of Ocean Sciences, Sidney: Institute of Ocean Sciences, 1975.
- Nader, Charles. *Numerical modeling of water waves*. 2nd Edition. London: London CRC Press, 2004.
- Naito, Clay, H. R. Riggs, Young Wei, and Christina Cercone. "Shipping-Container Impact Assessment for Tsunamis." *Waterway, Port, Coastal Engineering*, 2016.
- National Oceanic and Atmospheric Administration (NOAA). *How does the Tsunami Warning System Work?* 2016a. [http://www.tsunami.noaa.gov/warning\\_system\\_works.html](http://www.tsunami.noaa.gov/warning_system_works.html) (accessed 09 24, 2016).
- National Oceanic and Atmospheric Administration (NOAA) Center for Tsunami Research. *Tsunami Modeling and Research*. 2016b. <http://nctr.pmel.noaa.gov/model.html> (accessed 08 15, 2016).
- National Oceanic and Atmospheric Administration (NOAA). *National Data Buoy Center*. 06 21, 2016c. <http://www.ndbc.noaa.gov/dart.shtml> (accessed 08 12, 2016).
- National Oceanic and Atmospheric Administration (NOAA). *Ocean facts*. 08 27, 2015. <http://oceanservice.noaa.gov/facts/oceandepth.html> (accessed 08 23, 2016).
- National Oceanic and Atmospheric Administration (NOAA). *Tsunamis*. 2016d. <http://wcatwc.arh.noaa.gov/?page=tsunamiFAQ> (accessed 08 12, 2016).
- National Oceanic and Atmospheric Administration (NOAA) – National Centers for Environmental Information (NGDC). *NGDC/WDS Global Historical Tsunami Database*. 2011. [https://www.ngdc.noaa.gov/hazard/tsu\\_db.shtml](https://www.ngdc.noaa.gov/hazard/tsu_db.shtml) (accessed 08 12, 2016).
- National Research Council (NRC). *The National Building Code of Canada (NBCC)*. 2015.
- Natural Resources Canada (NRCan). *Aboriginal Lands - British Columbia*. 06 01, 2016.
- Natural Resources Canada (NRCan). *CanVec Features*. 2016.
- Nelson, A. R., H. M. Kelsey, E. Hemphill-Haley, and R. C. Witter. "OxCal analyses and varve-based sedimentation rates constrain the times of 14C-date tsunamis in southern Oregon." *Geological Society of America*. U.S. Geological Survey, 2002. 547-548.

- Ng, M.K.-F., P.H. LeBlond, and T.S. Murty. "Simulation of tsunamis from great earthquakes on the Cascadia subduction zone ." *Science* 250, no. 4985 (1990a): 1248-1251.
- Ng, Max, Paul H. LeBlond, and Tad S. Murty. "Numerical Simulation of Tsunami Amplitudes on the Coast of British Columbia Due to Local Earthquakes." *Science of Tsunami Hazards* (Tsunami Society) 8, no. 2 (1990b): 87-127.
- Northwest Hydraulic Consultants. *Lower Mainland Dike Assessment*. Final Report GS15LMN-054, Ministry of Forests, Lands and Natural Resource Operations, 2015.
- Ollerhead, J., D. J. Huntley, A. R. Nelson, R. Alan, H. M. Kelsey, and M. Harvey. "Optical dating of tsunami-laid sand from an Oregon coastal lake." *Quaternary Science Reviews* 20, no. 18 (2001): 1915-1926.
- Open Navigation Surface Working Group (ONSWG). *Description of Bathymetric Attributed Grid Object (BAG)*. Format Specification Document, Open Navigation Surgence, 2013.
- OpenStreetMap. *Road Network*. Tofino, 2016.
- Plafker, G. *Tectonics of the March 27, 1964 Alaska earthquake*. Professional Paper 543-I, U.S. Geological Survey, 1969.
- Post, J., et al. "Assessment of human immediate response capability related to tsunami threats in Indonesia at a sub-national scale." *Natural Hazards and Earth System Science* 9, no. 4 (2009): 1075-1086.
- Power, W. "Review of Tsunami Hazard in New Zealand." *GNS Science*, 2013: Wellington.
- PreparedBC. *Tsunamis*. 2016. <http://www2.gov.bc.ca/gov/content/safety/emergency-preparedness-response-recovery/preparedbc/know-the-risks/tsunamis> (accessed 08 11, 2016).
- Province of British Columbia. *Tsunami Notification Process Plan*. Province of British Columbia, 2013.
- Rabinovich, A. B., R. E. Thomson, B. D. Bornhold, I. V. Fine, and E. A. Kulikov. "Numerical modeling of tsunamis generated by hypothetical landslides in the Strait of Georgia, British Columbia." *Pure and Applied Geophysics* 160 (2003): 1273-1313.
- Reese, S., B. A. Bradley, J. Bind, G. Smart, W. Power, and J. Sturnman. "Empirical building fragilities from observed damage in the 2009 South Pacific tsunami." *Earth Science Review* 107 (2011): 157-173.
- Santos, Angela, A. Oliveira Tavares, and M. Queiros. "Numerical modeling and evacuation strategies for tsunami awareness: lessons from the 2012 Haida Gwaii Tsunami." *Geomatics Natural Hazards and Risk*, 2016: 1442-1459.
- Satake, K., and Y. Tanioka. "Tsunami generation of the 1993 Hokkaido Nansei-Oki earthquake." *Pure and Applied Geophysics* 144 (1995): 803-821.
- Satake, K., K. Shimazaki, Y. Tsuji, and K. Ueda. "Time and site of a giant earthquake in Cascadia inferred from Japanese tsunami records of January 1700." *Nature* 379, no. 6562 (1996): 246-249.

- Satake, K., K. Wang, and B. Atwater. "Fault slip and seismic moment of the 1700 Cascadia earthquake inferred from Japanese tsunami descriptions." *Journal of Geophysical Research* 108, no. B11 (2003).
- Satake, K., K. Wang, and B. F. Atwater. "Fault slip and seismic moment of the 1700 Cascadia earthquake inferred from Japanese tsunami description." *Journal of Geophysical Research: Solid Earth* 108, no. B11 (2003).
- Schmidtlein, M. C., and N. J. Wood. "Sensitivity of tsunami evacuation modeling to direction and land cover assumptions." *Applied Geography* 56 (2015): 154-163.
- Sinvhal, Amita. *Understanding Earthquake Disaster*. McGraw Hill Professional, 2010.
- Smart, G. M., M.H. M. Crowley, and E. M. Lane. "Estimating tsunami run-up." *Natural Hazard*, 2015: 1933-1947.
- Soloviev, S. L., and Ch, N. Go. *Catalogue of Tsunamis on the Eastern Shore of the Pacific Ocean (1513-1968)*. Canadian Translation of Fisheries and Aquatic Sciences, 5078, Moscow: Original: Nauka Publishing House, 1984.
- Sorensen, J. H. "Hazard Warning Systems: Review of 20 Years of Progress." *Natural Hazard Review* 1, no. 2 (2000): 119-124.
- Statistics Canada. *2011 Census collection*. 12 30, 2015. <https://www12.statcan.gc.ca/census-recensement/2011/ref/about-a-propos/col-eng.cfm> (accessed 09 29, 2016).
- Statistics Canada Catalogue no. 92-163-x. *Designated Place Boundary File, 2011 Census*. Statistics Canada Catalogue no. 92-163-x, 2011.
- Statistics Canada Catalogue no. 92-166-X. "Population Centre Boundary File." 2011.
- Statistics Canada Catalogue no.92-160-X. "Boundary Files." 2011.
- Statistics Canada. *Data Quality and Confidentiality Standards and Guidelines (Public), 2011 Census Dissemination*. Guidelines, Statistics Canada, 2011.
- Stephenson, F. E., A. B. Rabinovich, O. N. Soloviev, O. I. Yakovenko, and E. A. Kulikov. "Tsunamis on the Pacific coast of Canada recorded in 1700-2005." *Advances in Natural and Technological Hazards Research* (Springer) 24 (2010): 225.
- Stephenson, F., and A. Rabinovich. "Tsunamis on the Pacific Coast of Canada Recorded in 1994–2007." *Pure and Applied Geophysics* 166, no. 1-2 (2009): 177-210.
- Synolakis, C. E. *The runup of long waves*. PhD Thesis, Pasadena, CA: California Institute of Technology, 1986.
- Synolakis, C. E. *The Runup of Long Waves*. Report KH-R-61, Caltech, 1986.
- Synolakis, C. E. "The runup of solitary waves." *Journal of Fluid Mechanics* 185 (1987): 523-545.
- Tadepalli, S., and C. E. Synolakis. "The run-up of N-waves on sloping beaches." *Proceedings of the Royal Society A: Mathematical, Physical & Engineering Sciences* (Royal Society of London) 445 (1994): 99-112.

- Tanaka, Kazuko. "The impact of disaster education on public preparation and mitigation for earthquakes: a cross-country comparison between Fukui, Japan and the San Francisco Bay Area, California, USA." *Applied Geography*, 2005: 201-225.
- The Arlington Group Planning + Architecture Inc.; EBA, a Tetra Tech Company; DE Jardine Consulting; Sustainability Solutions Group;. *Sea level rise adaptation primer: A toolkit to build adaptive capacity on Canada's south coasts*. Primer, British Columbia Ministry of Environment, 2013.
- Thomson, R.E., B.D. Bornhold, and S. Mazzotti. *An Examination of the Factors Affecting Relative and Absolute Sea Level in British Columbia*. Technical, Fisheries and Oceans Canada, Institute of Ocean Sciences, Sidney: Fisheries and Oceans Canada, 2008.
- Thomson, R. E. *Oceanography of the British Columbia Coast*. Canadian Special Publications of Fisheries and Aquatic Sciences 56, Department of Fisheries and Oceans, Institute of Ocean Sciences, Ottawa: Department of Fisheries and Oceans, 1981.
- Titov, V. V. *Numerical modeling of long wave runup*. PhD thesis, Los Angeles, CA: University of Southern California, 1997, 144.
- Titov, V. V., and C. E. Synolakis. "Extreme inundation flows during the Hokkaido–Nansei–Oki tsunami." *Geophysical Research Letters* 24, no. 11 (1997): 1215-1318.
- Titov, V. V., and C. E. Synolakis. "Numerical modeling of tidal wave run-up." *Journal of Waterway, Port, Coastal, and Ocean Engineering* (ASCE) 124, no. 4 (1998): 157-171.
- Titov, V. V., et al. "Real-time tsunami forecasting: Challenges and solutions." *Natural Hazard* 35 (2005): 41-58.
- Titov, V., and F.I. Gonzalez. *Implementation and testing of the Method of Splitting Tsunami (MOST) mode*. NOAA Tech. Memo. ERL PMEL-112 (PB98-122773), Seattle: NOAA/Pacific Marine Environmental Laboratory, 1997.
- Tobler, W. *Three presentations on geographical analysis and modeling: Non-isotropic geographic modeling speculations on the geometry of geography global spatial analysis*. Technical Report 93, National Center for Geographic Information and Analysis, 1993.
- UMA Engineering LTD. "City of Port Alberni Tsunami Inundation Zone Study." File #: 6337-005-00-01, Port Alberni, 1992.
- Vaugeois, Nicole, Patrick Maher, Erin Heeney, Blake Rowsell, Shannon Bence, and Micki McCartney. *BC Resort Community Labour Market Strategic Analysis*. Final Report, go2, 2013.
- von Baeyer, H.C. "Catch the Wave." *The Sciences* 39, no. 3 (1999): 10.
- Whitmore "Expected Tsunami Amplitudes and Currents Along the North American Coast for Cascadia Subduction Zone Earthquakes." *Natural Hazard* 8 (1993): 59-73.
- Whitmore, P., et al. "NOAA/West Coast and Alaska tsunami warning center Pacific Ocean response criteria." *Science of Tsunami Hazard* 27, no. 2 (2008): 1-21.

- Wigen, S. O., and W.R. H. White. *Tsunami of March 27-29, 1964 West Coast of Canada*. 1964: Department of Mines and Technical Surveys, 1964.
- Wigen, S.O. *Tsunami of May 22, 1960, west coast of Canada* . Technical Report, Marine Sciences Brang, 1960, 6 p.
- Witter, R. C., et al. *Simulating tsunami inundation at Bandon, Coos County, Oregon, using hypothetical Cascadia and Alaska earthquake scenarios*. Special Paper 43, Oregon Department of Geology and Mineral Industries, 2011, 63 pages.
- Wood, N. J., and M. C. Schmidlein. "Anisotropic path modeling to assess pedestrian-evacuation potential from Cascadia-related tsunamis in the US Pacific Northwest." *Natural Hazard*, 2012: 275-300.
- Wood, N. J., and M. C. Schmidlein. "Community variation in population exposure to near-field tsunami hazards as a function of pedestrian travel time to safety." *Natural Hazards*, 2013: 1603-1628.
- Xie, Jinsong, Ioan Nistor, and Tad Murty. "Tsunami risk for Western Canada and numerical modeling of the Cascadia fault tsunami." *Natural Hazard*, 2012: 149-159.
- Yeh, H., I. Robertson, and J. Preuss. *Development of Design Guidelines for Structures that Serve as Tsunami Vertical Evacuation Sites*. Open File Report 2005-4, Olympia: Washington Division of Geology and Earth Resources, State of Washington, 2005.

## **Appendix A: List of Suppressed Communities**

---

## A.1 Tsunami Notification Zones

Each Tsunami Notification Zone (TNZ) maps include a list of communities at-risk within each respective zone (PreparedBC 2016). Some communities were not included as they are not populated areas or were not present in any of the communities GIS feature class files. The identified communities at-risk from the TNZ lists are presented by zone in Table A.1 to A.5 with their status (included or not) and the reason for not being included if that is the case. Also included are the alternative names used for some First Nation communities.

Table A.1 List of communities not included and alternative names in Zone A of the Tsunami Notification Zone

<b>Communities</b>	<b>Included (Yes/No)</b>	<b>Reason for not being included</b>
Alice Arm	No	Not populated
Gingolx	Yes	
Gitxaala (Dolphin Island 2)	Yes	
Hunts Inlet	No	Not populated
Kitsault	No	Missing
Lawnhill	No	Missing
Lax Kw'alaams Port Simpson	Yes	
Masset	Yes	
Metlakatla (S1/2 Tsimpsean 2)	Yes	
Old Masset Village Council	Yes	
Oona River	No	Not populated
Port Clements	Yes	
Port Edward	Yes	
Prince Rupert	Yes	
Queen Charlotte	Yes	
Sandspit	Yes	
Skidegate	Yes	
Stewart	Yes	
Tlell	Yes	
Tow Hill	No	Not populated

Table A.2 List of communities not included and alternative names in Zone B of the Tsunami Notification Zone

<b>Communities</b>	<b>Included (Yes/No)</b>	<b>Reason for not being included</b>
Alert Bay (Da'naxda'xm)	Yes	
Bella Bella	Yes	
Bella Coola	Yes	
Bull Harbour	No	Not populated
Butedale	No	Not populated
Dawnsons Landing	No	Not populated
Duncanby Landing	No	Not populated
Dzawada'enuxw (Kingcome)	Yes	
Tsulquate 4 (Gwa'sala-'Nakwaxda'xw)	Yes	
Gwanaenuk (Kwa-wa-aineuk)	Yes	
Hartley Bay	Yes	
Heitsuk	No	Missing
Hyde Creek	Yes	
Kimsquit	Yes	
Kingcome	Yes	
Kitimat	Yes	
Kitamaat (Haisla Natin)	Yes	
Kitasoo (Klemtu)	Yes	
Fort Rupert (Kwakiutl)	Yes	
(Gwayasdums 1) Kwicksuteaineuk-ah-kwaw-ah-mish	Yes	
Mamalilikulla-Qwe'Qwe'Sot'Em	Yes	
Mitchell Bay	No	Missing
Namgis (Alert Bay)	Yes	
Namu	No	Missing
Bella Coola (Nuxalk Nation)	Yes	
Ocean Falls (Katit 1)	No	Missing
Oweekeno Wuikinuxv	Yes	
Port Hardy	Yes	
Port McNeul	Yes	
Rivers Inlet (Katit 1)	Yes	
Shearwater	Yes	
Sointula	Yes	
Sullivan Bay	No	Not populated
Telegraph Cove	No	Missing
Tlatlasikwala	Yes	
Warner Bay	No	Not populated

Table A.3 List of communities not included and alternative names in Zone C of the Tsunami Notification Zone

<b>Communities</b>	<b>Included (Yes/No)</b>	<b>Reason for not being included</b>
Ahousaht (Marktosis 15)	Yes	
Bamfield	Yes	
Boat Basin	No	Missing
Cape Scott	No	Not populated
Ceepeecee	No	Not populated
Chamiss Bay	No	Missing
Chetarpe	No	Missing
Clo-oose (Malachan 11)	No	Missing
Coal Harbour	Yes	
Ditidaht	No	Missing
Ecoole	No	Missing
Ehattesah (Ehatis 11)	Yes	
Fair Harbour	No	Missing
Green Cove Landing (Elhlateese 2)	Yes	
Haggard Cove	No	Missing
Hecate	No	Missing
Hesquiat	Yes	
Holberg	Yes	
Hot Springs Cove	No	Missing
Hupacasath	Yes	
Huu-ay-aht	Yes	
Kootwowis	No	Missing
Ka:’yu:’k’t’h’/Che:k:’tles7et’h (formely Kyuqout) (Houpsitas 6)	Yes	
Mahatta River	Yes	
Marktosis	Yes	
Mohachaht/Muchalaht	Yes	
Nahmint (Chuchakacook 4)	Yes	
Nitnat Lake	No	Not populated
Nootka	No	Not populated
Nuchalitz (Ehatis 11)	Yes	
Nuchatlaht	Yes	
Oinimitis	Yes	
Opitsat	Yes	
Pacheedaht (Pacheena 1)	Yes	
Port Alberni	Yes	
Port Alice	Yes	
Port Renfrew	Yes	
Quatsino	Yes	

Table A.3 (continued) List of communities not included and alternative names in Zone C of the Tsunami Notification Zone

<b>Communities</b>	<b>Included (Yes/No)</b>	<b>Reason for not being included</b>
Quinaquilth	No	Missing
Quisitis	No	Missing
Quortsowe	Yes	
Sechart	No	Not populated
Tahsis	Yes	
Tla-o-qui-aht (Opitsat 1)	Yes	
Tofino	Yes	
Toquaht	Yes	
Tseshah	Yes	
Uchucklesaht	No	Missing
Ucluelet	Yes	
Winter Harbour	Yes	
Whyae	No	Missing
Yuquot	Yes	
Zeballos	Yes	

Table A.4 List of communities not included and alternative names in Zone D of the Tsunami Notification Zone

<b>Zone D – Communities</b>	<b>Included (Yes/No)</b>	<b>Reason for not being included</b>
Beecher Bay	Yes	
Central Saanich	Yes	
Colwood	Yes	
Equimalt	Yes	
Jordan River	No	Missing
Metchosin	Yes	
North Saanich	Yes	
Oak Bay	Yes	
Saanich	Yes	
Shirley	Yes	Missing
Sidney	No	
Songhees (Esquimalt)	Yes	
Sooke	Yes	
Tsawout (East Saanich 2)	Yes	
T'Souke	Yes	
Victoria	Yes	
View Royal	Yes	

Table A.5 List of communities not included and alternative names in Zone E of the Tsunami Notification Zone

<b>Communities</b>	<b>Included (Yes/No)</b>	<b>Reason for not being included</b>
Big Bay	No	Not populated
Bones Bay	No	Not populated
Brittania Beach	Yes	
Bowen Island	Yes	
Buckley Bay	Yes	
Burnaby	Yes	
Campbell River	Yes	
Cedar	Yes	
Central Saanich	Yes	
Chemainus	Yes	
Comox	Yes	
Cortez Island	No	Not populated
Courtenay	Yes	
Cowichan	Yes	
Cowichan Bay	Yes	
Cracroft	No	Missing
Crofton	Yes	
Cumberland	Yes	
Delta	Yes	
Denman Island	Yes	
District of Highlands	Yes	
Duncan	Yes	
Earls Cove	Yes	
East Thurlow Island	No	Not populated
Echo Bay	No	Missing
Edgmont (Edgmont No. 26)	Yes	
Fanny Bay	Yes	
Gabriola Island	Yes	
Galiano Island	Yes	
Gambier Island	Yes	
Garden Bay	Yes	
Gibsons	Yes	
Halalt	Yes	
Hardwicke Islands	No	Missing
Horny Island	Yes	
K'omoks (Comox)	Yes	
Karlukwees	Yes	
Klahoose	Yes	
Kwiakah (Saaiyouck 6)	Yes	

Table A.5 (continued) List of communities not included and alternative names in Zone E of the Tsunami Notification Zone

<b>Zone E – Communities</b>	<b>Included (Yes/No)</b>	<b>Reason for not being included</b>
Ladner	Yes	
Ladysmith	Yes	
Lang Bay	Yes	
Langford	Yes	
Lantzville	Yes	
Lasqueti Island	Yes	
Lyackson	Yes	
Lions Bay	Yes	
Lund	Yes	
Madeira Park (South Pender Harbour)	Yes	
Malahat	Yes	
Mayne Island	Yes	
McNab Creek	Yes	
Mill Bay	Yes	
Ministrel Island	Yes	
Musqueam	Yes	
Nanaimo	Yes	
Nanoose Bay	Yes	
Nelson Island	No	Not populated
New Westminster	Yes	
North Saanich	Yes	
North Vancouver City	Yes	
North Vancouver DM	Yes	
Oyster River	No	Missing
Parksville	Yes	
Pauquachin	Yes	
Penelakut	Yes	
Pender Island	Yes	
Port Melton (Kaikalahun 25)	No	Missing
Port Moody	Yes	
Port Neville	Yes	
Powell River	Yes	
Quadra Island	No	Not populated
Qualicum	Yes	
Qualicum Beach	Yes	
Richmond	Yes	
Roberts Creek	Yes	
Royston	Yes	
Saltair	Yes	

Table A.5 (continued) List of communities not included and alternative names in Zone E of the Tsunami Notification Zone

<b>Zone E – Communities</b>	<b>Included (Yes/No)</b>	<b>Reason for not being included</b>
Saltery Bay	Yes	
Saltspring Island	Yes	
Saturna Island	Yes	
Savary Island	No	Missing
Sayward	Yes	
Sechelt	Yes	
Secret Cove	No	Missing
Semiahmoo	Yes	
Shelter Point	No	Not populated
Sliammon	Yes	
Snueymuxvw (Chemainus 13)	Yes	
Squamish	Yes	
Squamish DM	Yes	
Surrey	Yes	
Stz'uminus (Oyster Bay 12)	Yes	
Texada Island	No	Not populated
Thompsonn Sound	No	Not populated
Thormanby Island	No	Not populated
Tlowitsis (Homalco 9)	Yes	
Tsarlip (South Saanich 1)	Yes	
Tsawwaassen	Yes	
Tsell-Waututh (Burrard Inlet 3)	Yes	
Tseycum (Union Bay 4)	Yes	
Union Bay	Yes	
Vancouver	Yes	
We Wai Kai Nation (Cape Mudge)	Yes	
West Thrurlow Island	No	Not populated
West Vancouver	Yes	
White Rock	Yes	
Woodfiber	Yes	
Xemalhkwa - Homalco	Yes	

## A.2 Census Supressed Communities

The following table presents the list of communities where their population data was completely or partly suppressed to meet confidentiality agreements from the 2011 Census.

Table A.6 List of communities where their population were suppressed by the census for confidentiality

<b>Name</b>	<b>Type</b>	<b>Zone</b>
Aiyansh (Kitladas) 1	NVL	A
Dodge Cove	UNP	A
Gitwinksihlkw	NVL	A
Lax Kw'alaams 1	IRI	A
Laxgalts'ap	NVL	A
New Aiyansh	NVL	A
Nisga'a	NVL	A
Port Clements	VL	A
S1/2 Tsimpsean 2	IRI	A
Dead Point 5	IRI	B
Gwayasdums 1	IRI	B
Hope Island 1	IRI	B
Hopetown 10A	IRI	B
Kulkayu (Hartley Bay) 4	IRI	B
Port Hardy	DM	B
Port McNeill	T	B
Thomas Point 5	IRI	B
Ahaminaquus 12	IRI	C
Alberni 2	IRI	C
Clakamucus 2	IRI	C
Elhlateese 2, IRI (5923805)	IRI	C
Hesquiat 1	IRI	C
Klehkoot 2	IRI	C
Numukamis 1	IRI	C
Sachsa 4	IRI	C
Tin Wis 11	IRI	C
Victoria	CY	C
Village Island 1	IRI	C
Winter Harbour	UNP	C
Yuquot 1	IRI	C
Zacht 5	IRI	C
Esquimalt	IRI	D
Chekwelp 26	IRI	E
Coquitlam 1	IRI	E

Table A.6 (continued) List of communities where their population were suppressed by the census for confidentiality

<b>Name</b>	<b>Type</b>	<b>Zone</b>
Coquitlam 2	IRI	E
Cowichan 9	IRI	E
Cowichan Lake	IRI	E
Cowichan	IRI	E
Gabriola Island Trust Area part B	IST	E
Gabriola Island Trust Area part C	IST	E
Galiano Island 9	IRI	E
Gambier Island Trust Area part B	IST	E
Gambier Island Trust Area part C	IST	E
Gambier Island Trust Area part D	IST	E
Kil-pah-las 3	IRI	E
Kowtain 17	IRI	E
Langley	DM	E
Musqueam 4	IRI	E
Nanaimo River 2	IRI	E
Nanaimo	CY	E
Pentledge 2	IRI	E
Port Coquitlam	CY	E
Porteau Cove	UNP	E
Portier Pass 5	IRI	E
Richmond	CY	E
Saltspring Island Trust Area part F	IST	E
Saltspring Island Trust Area part H	IST	E
Sechelt (Part)	IGD	E
Sechelt	DM	E
Seymour Creek 2	IRI	E
Shingle Point 4	IRI	E
South Wellington part B	IST	E
Squirrel Cove 8	IRI	E
Surrey	CY	E
Theik 2	IRI	E
Thetis Island Trust Area part B	IST	E
Tzart-Lam 5	IRI	E
Vancouver	CY	E
West Vancouver	DM	E
Yawaucht 11	IRI	E
Yekwaupsum 18	IRI	E

## **Appendix B: Arrival Time Validation Data**

---

The following table presents a comparison of the arrival time data between the tsunami first wave arrival time and the BC Earthquake Alliance Society (2016) data.

Table A.7 First tsunami wave arrival time result comparison: column [2] are the calculated values from the Arrival Time process and column [3] are the estimated values from BC Earthquake Alliance Society (2016). Calculated values greater than the estimated values are in red.

Zone	Location [1]	Arrival time (min)		Difference [3]-[2]	Error (%)
		Calculated [2]	Estimate [3]		
A	Prince Rupert	169.7	170	0.3	0.2
B	Bella Bella	104.6	40	-64.6	-161.5
C	Tofino	28.1	20	-8.1	-40.5
C	Ucluelet	27.1	25	-2.1	-8.4
C	Port Alberni	68.3	65	-3.3	-5.1
C	Winter Harbour	42.3	30	-12.3	-41.0
C	Port Renfrew	32.7	35	2.3	6.6
D	Sooke Harbour	49.6	55	5.4	9.8
D	Esquimalt	66.0	70	4.0	5.7
D	Victoria	66.0	75	9.0	12.0
D	Sidney	94.7	120	25.3	21.1
E	Delta	105	135	30.0	22.2
E	Richmond	120.1	135	14.9	11.0
E	Nanaimo	127.4	155	27.6	17.8

## **Appendix C: Example of Evacuation Maps**

---





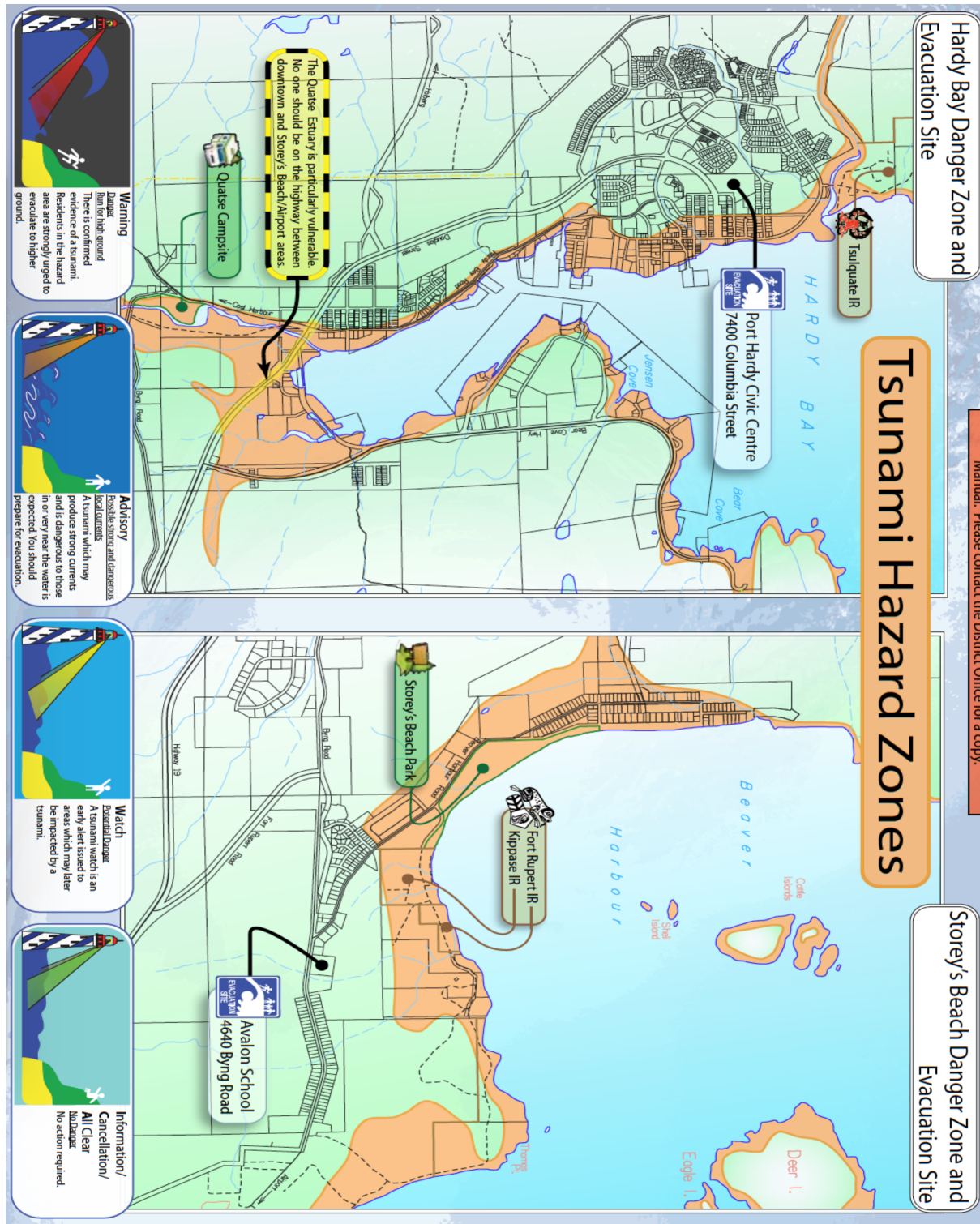


Figure A.3 Port Hardy tsunami evacuation zone, Zone C (District of Port Hardy 2016)